Leukocyte HMGB1 Guides Neoangiogenesis in Regenerating Skeletal Muscle

Thesis

Lara Campana, M.Sc.

Leukocyte HMGB1 guides neoangiogenesis in regenerating skeletal muscle

A thesis submitted in fulfilment of the
requirements of the Open University for the
Degree of Doctor of Philosophy

April 2012

DSS Med/04 – General Pathology

Director of study: Prof. Patrizia Rovere-Querini

DiBiT

Department of Biological and Technical Research

PhD Program in Cellular and Molecular Biology

Vita-Salute San Raffaele University

Date of Submission : 5 April 2012
Date of Award: 14 June 2012

ProQuest LLC.
789 East Eisenhower Parkway
P.O. Box 1346
Ann Arbor, MI 48106 – 1346

LIST OF CONTENTS

LIST OF CONTENTS 2

ABSTRACT 4

INTRODUCTION 5

1. THE HOMEOSTATIC RESPONSE OF TISSUES TO INJURIES 5
   - *1.1 Inflammation controls tissue healing* 5
   - *1.2 Angiogenesis and vessel remodelling, indispensable steps for tissue healing* 9
   - *1.3 Inflammation influences the activation of endogenous stem/progenitor cells in injured tissues* 15
2. SKELETAL MUSCLE DAMAGE AND REPAIR AS A PARADIGM OF STERILE INJURIES 16
   - *2.1 The ABC of muscle* 17
   - *2.2 Accessory, non-muscle derived cells actively participate to muscle regeneration* 20
3. HMGB1 IN HOMEOSTATIC RESPONSES TO TISSUE INJURY 25
   - *3.1 The ABC of HMGB1* 26
   - *3.2 Necrotic cells releases HMGB1* 27
   - *3.3 Inflammatory cells actively secrete Hmgb1* 29
4. FUNCTIONAL EFFECT OF HMGB1 33
   - *4.1 RAGE and TLRs are HMGB1 receptors* 33
   - *4.2 HMGB1 effect on cell migration* 36
   - *4.3 HMGB1 effect on inflammatory responses in health and disease* 38
   - *4.4 HMGB1 promotes wound healing* 44
5. PUTTING THE PUZZLE TOGETHER: WHAT IS THE CONTRIBUTION OF DISTINCT SOURCES OF HMGB1 TO TISSUE REPAIR? THE NEED FOR A NEW ANIMAL MODEL 47
   - *5.1 HMGB1 and muscle repair* 47
   - *5.2 Limitations in HMGB1 study* 48
   - *5.3 An original mouse model to address HMGB1 dynamics in vivo* 49
   - *5.4 The choice of an appropriate acute damage model* 50

MATERIALS AND METHODS 55

1. MUSCLE DAMAGE INDUCTION AND REPAIR EVALUATION 55
2. BOXA TREATMENT 55
3. MAGNETIC RESONANCE IMAGING (MRI) 55
   - *3.1 MRI acquisition* 55
   - *3.2 Data processing* 56
4. FOETAL LIVER TRANSPLANTATION AND CHIMERISM ASSESSMENT 57
5. FLOW CYTOMETRY ON TOTAL MUSCLE 57
6. MRNA ANALYSIS 58
7. WESTERN BLOT ANALYSIS ON $CD45^+$ CELLS AND TOTAL MUSCLE LYSATES 59
8. ELISAS 60
9. IMMUNOHISTOCHEMISTRY 60
10. IMMUNOFLUORESCENCE 61
    - *10.1 Pax7 and MyoD staining* 61
    - *10.2 Hmgb1 staining* 62
    - *10.3 Myosin Heavy Chain (MyHC) and CD11b staining on cell culture* 62
11. MURINE MACROPHAGE DIFFERENTIATION AND POLARIZATION 63
    - *11.1 Murine macrophage differentiation* 63
    - *11.2 Murine macrophage polarization* 63
12. SATELLITE CELL ISOLATION, EXPANSION AND CO-COLTURE WITH MURINE MACROPHAGES 63
    - *12.1 Satellite cells isolation and expansion* 63
    - *12.2 Satellite cells differentiation* 64
    - *12.3 Satellite cells – Macrophages co-colture* 64
    - *12.4 Differentiation assessment and quantification* 65
13. STATISTICAL ANALYSIS 65
    - *13.1 General* 65
    - *13.2 MRI statistics* 65

RESULTS - 1 66

1. CHARACTERISTICS OF CTX-INDUCED ACUTE DAMAGE MODEL 66
   - *1.1 Kinetic of repair of CTX injected muscle* 66

1.2 Immunological characterization of CTX injected muscle *67*
1.3 Hmgb1 expression during damage and repair after CTX injection *69*
2. MRI AS A TOOL TO STUDY ACUTE MUSCLE DAMAGE 71
2.1 Introduction to MRI *71*
2.2 Analysis of TA muscle by MRI *72*
2.3 MRI as a tool to assess muscle oedema and inflammation *74*
2.4 MRI is a valuable tool to study tissue architecture during muscle damage *76*

DISCUSSION – 1 ..... **78**

RESULTS – 2 ..... **82**

1. HMGB1 ACTION IN INJURED/REGENERATING MUSCLE 82
1.1 Schedule for pharmacological blockade of extracellular HMGB1 ..... *82*
1.2 Hmgb1 controls inflammation in muscle damage *84*
2. OPTIMIZATION OF THE PROCEDURE FOR TRANSPLANTATION OF HAEMATOPOIETIC PRECURSORS FROM FOETAL LIVER 92
2.1 Chimerism assessment *93*
2.2 Muscle regeneration after transplantation with foetal liver precursor cells *95*
3. LEUKOCYTE HMGB1 CONTROLS MUSCLE REPAIR THROUGH REGULATION OF ANGIOGENESIS 98
3.1 Effective chimerism in lethally irradiated WT mice transplanted with Hmgb1$^{-/-}$ foetal liver cells (FLT) *98*
3.2 Hmgb1$^{-/-}$ FLT mice have normal PB and BM populations of white blood cells *99*
3.3 Leukocyte Hmgb1 controls muscle repair *101*
3.4 Leukocyte Hmgb1 controls neither inflammation nor macrophage polarization *105*
3.5 Leukocyte Hmgb1 barely influences satellite cell biology *113*
3.6 Leukocyte Hmgb1 controls angiogenesis in repairing muscle *119*

DISCUSSION-2 ..... **124**

BIBLIOGRAPHY **132**

LIST OF FIGURES **151**

RESULTS – 1 151
RESULTS – 2 151

LIST OF TABLES **154**

ACKNOWLEDGEMENTS **155**

ABSTRACT

HMGB1 is ubiquitously present in the cell nucleus and highly conserved among species. It is released by necrotic cells and actively secreted by immune cells in the extracellular environment, where it behaves as a DAMP (Damage-Associate Molecular Pattern). Up to now all studies addressing the role of HMGB1 in wound healing have been carried out either *in vitro* or using pharmacological inhibitors. To assess the relative contribution of leukocyte HMGB1 and of passively released HMGB1 we have set up an *ad hoc* animal model. In this system, haematopoietic cells selectively lack HMGB1 by transplanting *Hmgb1*$^{+/+}$ or *Hmgb1*$^{-/-}$ foetal livers into WT recipients. The role of leukocyte HMGB1 in tissue repair has been analyzed after skeletal muscle damage. I have used histological and magnetic resonance imaging (MRI) to non-invasively evaluate muscle inflammation and tissue architecture. In the absence of Hmgb1, there is a lower number of regenerating fibres at day7 after injury and an aberrant repair with smaller fibres at day15. *In vitro* no differential effects of *Hmgb1*$^{-/-}$ and *Hmgb1*$^{+/+}$ macrophages are detected on satellite cells differentiation/fusion, suggesting that events taking place *in vivo* are independent of the direct macrophage/satellite cell cross talk. No obvious differences are observed in the extent of leukocyte infiltration, as assessed both by cytofluorimetric and MRI analysis, suggesting that leukocyte Hmgb1 is not required for the attraction of inflammatory cells. qPCR unveils a role for leukocyte Hmgb1 in the production of angiogenic stimuli such as Ang2 and TNFα, probably in a hypoxia-dependent manner. Accordingly, the number of CD31 cells is dramatically reduced in the absence of leukocyte Hmgb1. Collectively our data suggest that HMGB1 secreted by leukocytes guides muscle regeneration through a paracrine role on vascular bed reconstitution.

[282 words]

INTRODUCTION

1. The homeostatic response of tissues to injuries

Injured tissues are generally able to heal (1, 2). Wound healing is a complex process that requires the interaction between multiple cell types and involves panoply of distinct molecules (3). Within minutes from tissue injury endogenous "danger" signals, cytokines and chemokines are released from parenchymal and incoming inflammatory cells. A regulated interplay between immune cells, endothelial cells and stem cells is needed to complete heal tissue (4).

1.1 Inflammation controls tissue healing

The first line of defence after injury or infections is polymorphonuclear cells (PMNs), the most abundant being neutrophils (4). They arrive within minutes from tissue damage. The primary role of these phagocytic cells is to recognize, eat and kill invading microbes and/or to remove damaged cells and debris in preparation for tissue repair. They efficiently kill microbes thanks to specific metabolic enzymes such as the phagocyte NADPH oxidase (NOXs) and nitric oxide synthases (NOSI and NOSIII). Moreover they encapsulate an impressive number of proteases in defined intracellular compartments named granules (5). The major antimicrobial strategies used by neutrophils are:

- Phagocytosis, which comprises confining microbes in specialized phagosome compartments and their elimination
- Degranulation, which releases antimicrobial molecules at the site of infection/injury
- Neutrophil Extracellular Traps (NETs) formation. NETs are composed of decondensed chromatin decorated with granular and cytoplasmic proteins. NETs prevent microbe spreading out of the site

of entry, while apparently limiting the collateral tissue damage from granular contents and promoting synergy between granular and cytoplasmic proteins (6)

Macrophages, either resident in the tissue or recruited from circulating monocytes, are the second in line of defence against invading microorganisms and injuries (4). Progressively the number of neutrophils decreases and macrophages become the predominant infiltrating cells (7). Macrophages and neutrophils cooperate at the site of tissue injury or infection. The two cell types have both overlapping and complementary functions. Both are professional phagocytes even if macrophages have a limited anti-microbial potential. Macrophages have a longer lifespan and distinct tissue localization. However macrophages and neutrophils cluster at the site of inflammation/injury following networks of chemotactic stimuli. These networks are initiated by resident macrophages together with epithelial and endothelial cells. Neutrophils, which are recruited first, prompt macrophage recruitment. Neutrophil secrete molecules, such as intra-granular proteins, that foster macrophage pro-inflammatory function (8). Macrophages eat dead neutrophils at the site of damage, thus suppressing the production of pro-inflammatory mediators and facilitating the resolution of inflammation and tissue healing (7). The first evidence for a pivotal role of macrophages in wound healing has been reported in guinea pigs. Treatment with macrophage antiserum and glucocorticoids slowed cutaneous wound healing (9-11). More recent reports have confirmed the observation in mice in which macrophages are ablated using genetic tools. In those mice skin wounds fail to repair when macrophages are ablated at early time points after damage induction (Figure 1). The wound heals correctly when macrophages are depleted during terminal phase of tissue healing (9, 11). The phenomenon has been confirmed also in other pathophysiological settings, like acute muscle repair (2).

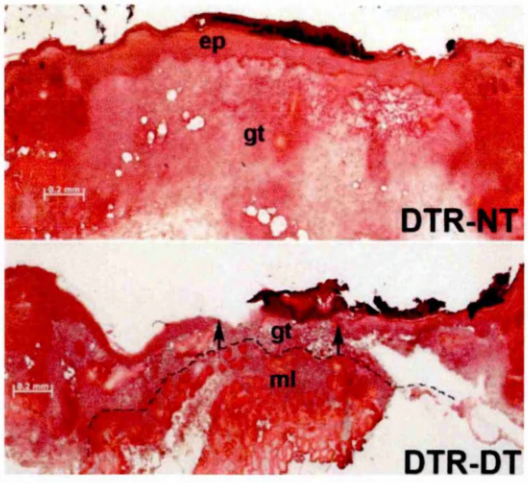

Figure 1 – Mice depleted of macrophages (DTR-DT) display a defect of re-epithelialization at day5 after wound (11).

Most wound macrophages derive from circulating monocytes. Upon arrival at the injured site monocytes rapidly acquire macrophage features, expressing CD206 (mannose receptor 1), while maintaining some monocyte features (Ly6C and dectin-1). At least two monocyte subsets have been described in mice. Inflammatory macrophages are characterized by $Ly6C^{high}$, $CCR2^{high}$, CX_3CR1^{low} and migrate into wounds during early phase of inflammation. A second population is characterized by $Ly6C^{low}$, $CCR2^{low}$, CX_3CR1^{high} expression and seems to egress later from circulation. In humans distinct populations are distinguished on the basis of the expression of CD16. $CD14^{+}CD16^{+}$ cells express high levels of CX_3CR1 and may be orthologs of $Ly6C^{low}$ population in mice. The most abundant population is composed of $CD14^{+}CD16^{-}$ monocytes that express low levels of CX_3CR1 (12).

Macrophages resulting from the extravasating monocytes are known to be plastic cells. The current paradigm distinguishes classical and alternative activated macrophages. The former are endowed with pro-inflammatory and antimicrobial capacities, the latter cooperate in tissue healing and parasitic infection clearance (7). However these extreme phenotypes are not found *in vivo* where they show remarkable plasticity and apparently continuously modulate and adapt their functions according to

environmental cues. Thus the best way to describe macrophage phenotypes *in vivo* is a continuous spectrum of characteristics. Wound healing macrophages are considered as a population with unique characteristics, some peculiar of classically activated and some of alternatively activated macrophages (Figure 2, panel B). Similarly to classical activated macrophages they react promptly to environmental cues, such as danger signals or microbial products. One of the first innate signals generally released by granulocytes after tissue injury is IL4. The early exposure to IL4 prompts wound healing macrophages to upregulate arginase-I expression, a feature typical of alternative activated macrophages. The maintenance of a macrophage phenotype useful to tissue repair is strictly linked to generation of adaptive immune responses that in wound healing are instrumental for limiting inflammatory responses (8). T_H2-type immune responses are able to produce IL4 too and this is thought to be one of the main mechanisms for keeping macrophages in their pro-healing phenotype. For instance cells stimulated *in vitro* with IL4 are able to produce components of extracellular matrix. Also they secrete polyamines that suppress the clonal expansion of neighbouring lymphocytes (13).

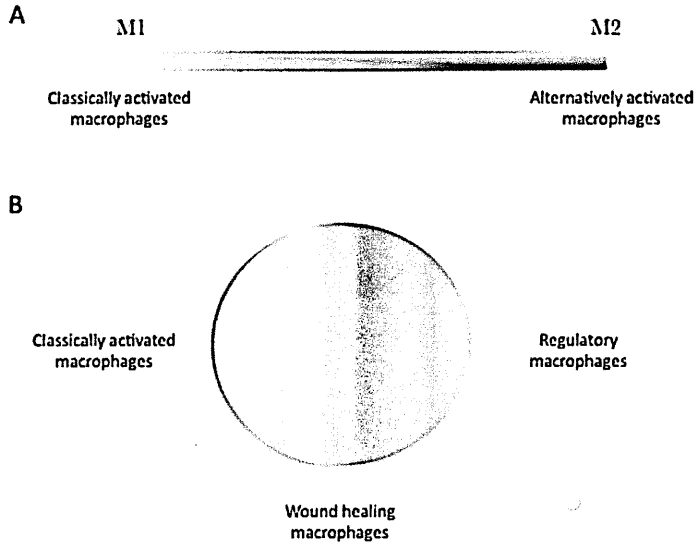

Figure 2 - Colour wheel of macrophage activation. A. A monochromatic depiction of the previous nomenclature showing the linear scale of the two macrophage designations, M1 and M2. B. The three main populations of macrophages are arranged according to the three primary colours, with red

designating classically activated macrophages, yellow designating wound-healing macrophages and blue designating regulatory macrophages. Secondary colours, such as green, may represent tumour-associated macrophages, which have many characteristics of regulatory macrophages but also share some characteristics of wound-healing macrophages (8).

Macrophage polarization is crucial: a hyperactive matrix deposition activity results in fibrosis, while dystregulated pro-inflammatory activity may result in chronic inflammation and possibly autoimmunity. Several *in vivo* studies have demonstrated that macrophage phenotype in healing tissue can change over time. Regulatory macrophages can arise following distinct stimuli (8). For instance macrophages acquire the ability to secrete TGFβ after phagocytosis of apoptotic cells (14), while stimulation of macrophages with immune complexes results in IL10 production. IL10 produced by T regulatory lymphocytes (Treg) is another trigger for the generation of regulatory macrophages (8).

1.2 Angiogenesis and vessel remodelling, indispensable steps for tissue healing

Macrophages in wound healing control the correct balance between pro- and anti-angiogenic factors (7). Accordingly, in mice depleted of macrophages vascularization is reduced and abnormal (Figure 3). Defective angiogenesis frequently associates to a jeopardized healing (11, 15).

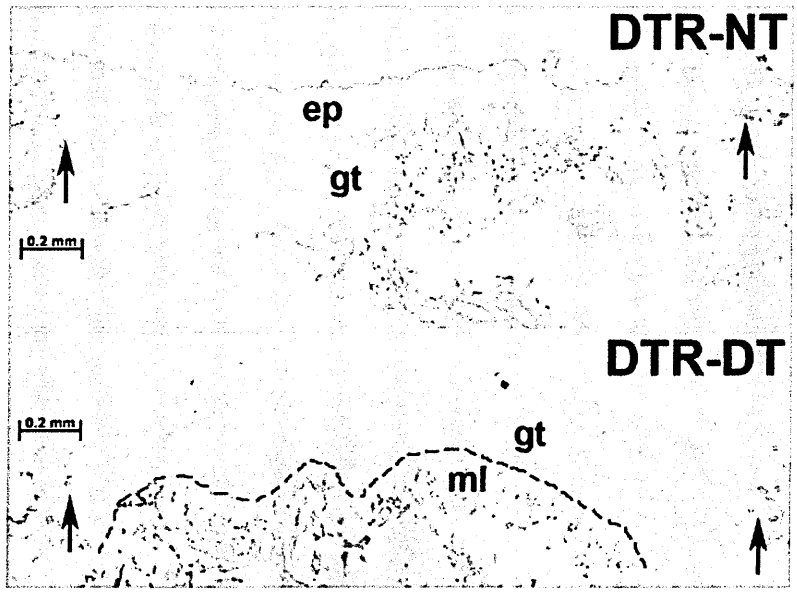

Figure 3 – Angiogenesis is impaired in the absence of macrophages. DTR transgenic mice were subjected to excisional wounding and either left untreated (NT) or treated with DT (macrophage-depleted mice). Representative sections of wounds on day 5 post-injury showing impaired vessel formation in macrophage-depleted mice (bottom) compared with untreated mice (top). Arrows indicate the wound edges. ep, epithelium, gt, granulation tissue, ml, muscle layer. Dashed line indicates border between granulation tissue and subcutaneous muscle layer. Scale bar = 0.2 mm (11).

Also the endothelium is a plastic compartment that reacts to tissue needs in response to physiological and pathological environmental cues. Inflammatory events and extracellular matrix remodelling almost always accompany extensive reshaping of the vascular bed. Early after tissue injury, vascular permeability increases, driven by nitric oxide (NO), excess of Vascular Endothelial Growth Factor (VEGF) and an array of other mediators still not completely elucidated. The increased permeability allows inflammatory cells and plasma components to exit the bloodstream. Subsequently a vascular expansion occurs within adjacent avascular areas, possibly supporting the enhanced need of oxygen and nutrients associated to repair. Expansion of vascular bed is due to endothelial cell (EC) proliferation and migration (16). A nascent sprout from a pre-existing vessel comprises three EC types: tip, stalk and phalanx. Tip cell specification is essential for sprouting and is controlled both by inflammatory and extracellular matrix (ECM) molecules. Thus the tip EC is characterized by a unique

expression profile: it expresses molecules able to digest ECM (e.g. metalloproteinase 1) and receptors able to sense angiogenic factors (e.g. VEGF receptor 2 and 3) (17). Tip cells proliferate poorly and are highly specialized. Tip cells sense Tumour Necrosis Factor α (TNFα) or bradykinin that induce lamellipodia and filopodia formation, typical of invading tip cells. Stalk and phalanx compartments are able to proliferate and they sense distinct stimuli to allow new vessel tube formation. Some of the factors involved in the process are known, such as Fibroblast Growth Factor-2, prostaglandin E2 and the chemokines CCL2 (Figure 4) (16).

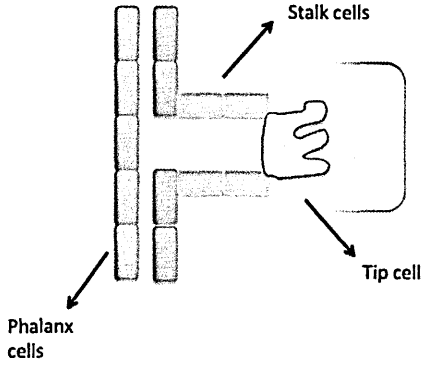

Figure 4 – Cartoon representing a growing vessel. Schematic representation of a tip cell (green) extending filopodia toward an angiogenic stimulus (red gradient), followed by stalk cells (pink), while phalanx cells (light blue) remain quiescent (17).

Hypoxia is one of the main stimuli for angiogenesis. Three hypoxia-inducible factor-α proteins (HIF-1α, HIF-2α, HIF-3α) senses oxygen availability. If a hypoxic environment is present those short-living proteins are stabilized and translocate into the nucleus, where they associate with β-subunits to activate target genes, binding to hypoxia responsive elements on DNA (Figure 5).

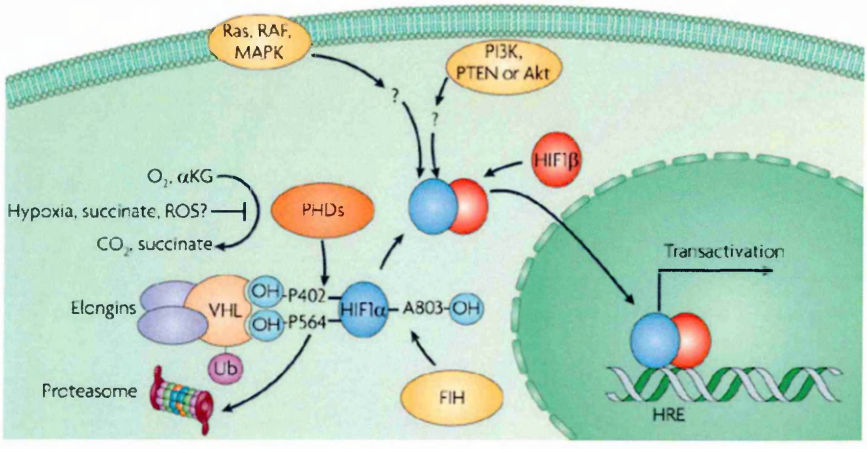

Figure 5 - The classical O_2 sensing pathway. HIF1α is hydroxylated through O_2-dependent enzymes at P402 and/or P564. This modification is due to one of the three prolyl hydroxylase (PHD) enzymes, which mediate recognition of the VHL–elongins complex and ubiquitination (Ub) of HIF1α and hence targeting for proteasomal degradation. Tricarboxylic acid cycle intermediates such as succinate and fumarate, or perhaps mitochondrial reactive oxygen species (ROS), can inhibit the activity of PHDs, also stabilizing HIF1α. Stabilized HIF1α associates with HIF1β, which binds to cognate hypoxia-responsive elements (HREs) in target genes (18).

Hypoxia is crucial for endothelial tip cell specification. VEGF and hypoxia promote Delta-like 4 (Dll4) expression in endothelial tip cells, which suppress endothelial cell fate into adjacent stalk cells by activating Notch signalling. Stalk cells are in charge of carrying oxygenated blood, leading to downregulation of VEGF and thus promoting negative feedback loop to stabilize vessels and ensure oxygen supply to regenerating tissue (19). Cytokines, such as IL6 and TGFβ have been involved in angiogenesis. In tumour models of glioblastoma IL6 seems to increase cell invasion through angiogenesis promotion (20). Moreover the action of IL6 has been related to the efficacy of some anti-angiogenic therapies in patients with ovarian clear cancer cells; its action may be related to the hypoxic status of the tumour and to HIF pathway activation (21). *In vitro,* TGFβ promotes the organization of EC in tube-like structure in three-dimensional collagen gel culture. Moreover TGFβ *in vivo* stimulates angiogenesis at local sites of injection. TGFβ also regulates the synthesis of other pro-angiogenic factors such as Platelet-Derived Growth Factor (PDGF) (22).

Anti-angiogenic factors are also needed to ensure correct tissue vascularization and repair. Thrombospondins (TSPs) are a family of five matricellular proteins able to guide ECM synthesis and remodelling. TSPs have been associated with ECM organization and modulation of bioavailability of growth factors implied in angiogenesis, such as basic Fibroblast Growth Factor (bFGF), TGFβ and VEGF (19).

To sense the surrounding microenvironment ECs rely on the angiopoietins system (23). Angiopoietins are vascular morphogenesis related proteins that play a pivotal role in controlling vessel homeostatic functions. The ligand-receptor system comprises two receptors (Tie1 and Tie2) and four ligands (Ang1, Ang2, Ang3 and Ang4). Tie receptors are expressed mainly by ECs, haematopoietic stem cells and a sub-population of pro-angiogenic tumour-associated macrophages. Angiopoietins have been originally identified as Tie2 ligands. So far no specific Tie1 ligand is known. Several cell types constitutively express Ang1, including pericytes, fibroblast and smooth muscle cells. In contrast Ang2 is expressed almost selectively by ECs. It is barely expressed by quiescent ECs, while it is rapidly upregulated upon EC activation. Both FGF2 and VEGF are potent inducer of Ang2 expression (24).

Ang1 and Ang2 bind to the same extracellular domain of the Tie2 receptor. Upon engagement of Tie2, Ang1 is able to trigger receptor autophosphorylation. This is followed by PI3 Kinase activation that results in phosphorylation and activation of Akt. Akt in turn blocks the activity of the forkhead transcription factor FKHR-1. This cascade of events leads to the stabilization of the endothelium, with survival of quiescent ECs and consequent block of Ang2 production. It seems that the Ang1-Tie2 interaction is constitutively required to control vascular quiescence and to maintain endothelium. Ang2 expression is tightly regulated. mRNA encoding for Ang2 is virtually absent in quiescent endothelial cells. Its expression is under the control of several endotheliotropic factors (e.g. FGF2, VEGF and TNFα) but also of environmental cues (e.g. hypoxia or superoxides). Ang2 protein is contained in

endothelial cell Weibel-Palade bodies, ready for release in the extracellular space. Stimuli for Ang2 secretion are for example thrombin and histamine. Released Ang2 is a potent signal to activate endothelium and it primes ECs to be responsive to cytokines, thus further enhancing ongoing inflammatory response (Figure 6) (24).

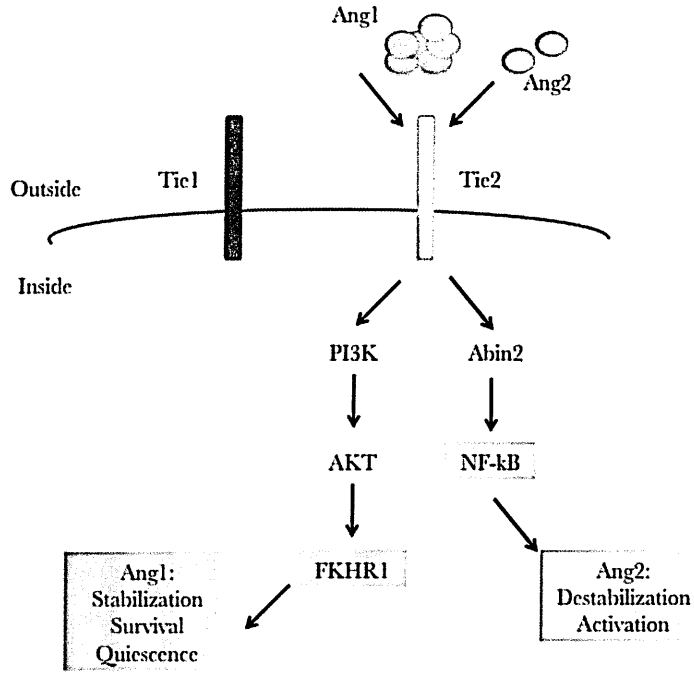

Figure 6 - Angiopoietins signalling regulates quiescent and activated endothelial-cell phenotype. Ang1 signalling is constitutively required for endothelial cell survival and quiescence. Ang2 antagonism destabilizes the endothelial cell (yellow box) thereby rendering it responsive to stimulation by inflammatory and angiogenic cytokines (24).

Ang2 has also other effects on ECs that are context-dependent. In the presence of VEGF it facilitates angiogenesis, while its absence promotes vessel regression. Ang2 overexpression *in vivo* also promotes wound healing (24).

Angiogenesis is essential for the synthesis, deposition and organization of a new ECM. ECM components in turn guide fibroblast migration. Infiltrating macrophages secrete molecules such as FGF and TGFβ that also favour conversion of fibroblasts to myofibroblasts, the cell type apparently needed for wound closure (25). Thus inflammation, angiogenesis and re-epithelialization are strictly interconnected.

1.3 Inflammation influences the activation of endogenous stem/progenitor cells in injured tissues

Skin wound healing is the general paradigm used to described molecules and event involved in tissue healing, including activation of local regenerative response in parenchymal cells. However the study of other tissues may be informative.

Following injury an acute inflammatory response arises in the lung. To repair the tissue epithelial cell spreading and migration is needed (Figure 7). Inflammation produces several molecules involved in this process:

- Members of the epithelial growth factor and fibroblast growth factor families (e.g. TGFβ, Hepatocyte Growth Factor - HGF, Epidermal Growth Factor - EGF and Insulin-like Growth Factor – IGF1)
- Chemokines (e.g. CCL2)
- Interleukins (e.g. IL2, IL4, IL13)
- Prostaglandins (e.g. PGE_2)

These factors controls processes involving ECM remodelling and chemoattraction of resident and distant stem cells to the site of injury (26).

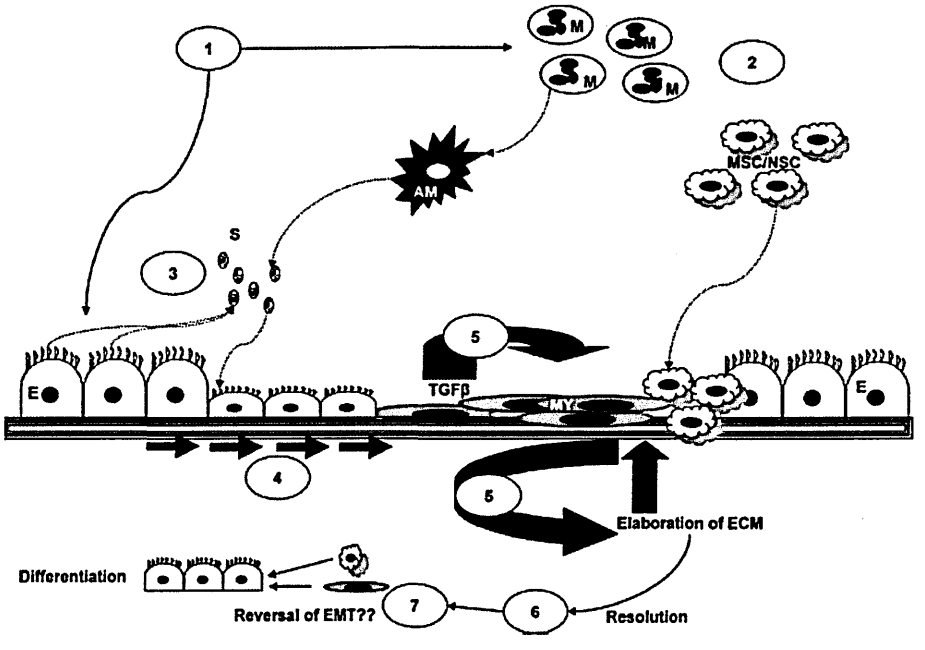

Figure 7 - Processes involved in epithelial repair in the airways. Injury (1) initiates activation of macrophages (M) to activated macrophages (AM) and the recruitment of immune cells, (2), mesenchymal stem cells (MSC), or niche stem cells (NSC). Soluble factors (S) (3) act on epithelial cells and fibroblasts, which spread and migrate (4) closing the wound and establishing intact barrier function. TGF-β signalling results in trans-differentiation of epithelial cells to myofibroblasts (MY), and in a further elaboration of ECM. During resolution (6), immune cells disappear from the site of injury, macrophages are deactivated and epithelial cells terminally differentiate (7) (26).

Also upon renal injury a robust and productive acute inflammation is elicited. Inflammation stimulates resident progenitor cells to proliferate (27). Skin, lung and kidney share the signalling pathways through which progenitor cells are able to exit G_0 phase of cell cycle to enter into G_1 and then into S and G_2 phase, the Rho GTPases, the MAP kinase and the Wnt/β-catenin (25-27).

In tissues of different origin like the myocardium IGF1, EGF and HGF are the main effector molecules on progenitor cells. Also in cardiac tissue they act in combination with cytokines such as IL6 and TNFα (28).

Even if the effector molecules are conserved among tissues of distinct origin, the induction of the inflammatory response is different. In the case of epithelia the disruption of the barrier allows microbes to enter the body (25-27). In the case of heart damage inflammation is normally sterile (28). What can be a good model to investigate the role of immuno-derived molecules in condition of sterile injury?

2. Skeletal muscle damage and repair as a paradigm of sterile injuries

To define the dynamics of tissue repair *in vivo* we need an appropriate model. Skeletal muscle damage is a very interesting and potentially useful pathophysiological sterile condition for the study of immuno-derived molecules in tissue repair.

2.1 The ABC of muscle

Adult skeletal muscle is composed by myofibres, long, cylindrical cells containing multiple nuclei that are typically located in the periphery of the fibre. To generate the *syncitium* monucleated myoblasts fuse together and organize their cytoplasm to generate sarcomeres, the contractile functional unit of muscle. Ancestors of myoblasts are satellite cells, resident muscle stem cells typically located in the subsarcolemma, between the fibres and the basement membrane (Figure 8) (29).

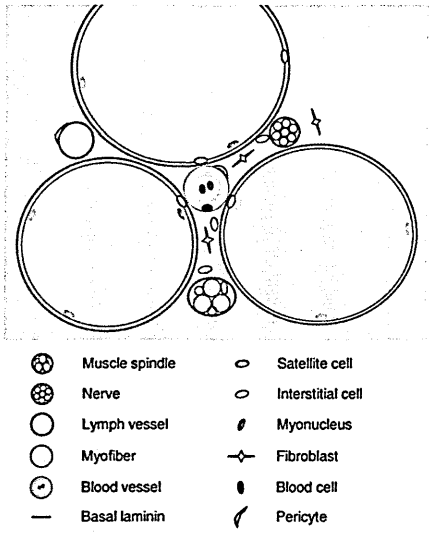

Figure 8 – Anatomical location of satellite cells and relationship with other muscle resident cell types (30).

A sheath of connective tissue, the epimisium surrounds the whole muscle. It extends inside the muscle to form septi around multiple fibres and it is called perymisium. Finally, each single muscle fibre has around its own connective tissue sheath, the endomisium. Connective tissue allows the blood and lymphatic vessels to come in and out from the tissue. Each muscle fibre contains myofibrils with a diameter of around 0,5-2 μm. In each myofibrils contractile units called sarcomers are present. In normal muscle inflammatory cells are completely absent, making inflammatory infiltrate a hallmark of muscle damage (Figure 9) (31).

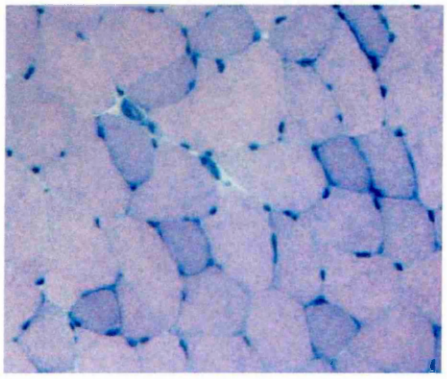

Figure 9 – Hematoxylin and eosin staining of the healthy skeletal muscle of a C57Bl/6 mouse (see methods).

Skeletal muscle effectively regenerates after an acute damage. The regenerative ability of skeletal muscle has long been known, as well as the presence of inflammatory cell infiltration in damaged muscle (32, 33). It is interesting to understand how the muscle enacts an efficient repair process. An early hypothesis has been that new myofibres are generated via budding of myotubes from existing, injured fibres (32). Following studies demonstrated that this rapid repair occurs through the differentiation and subsequent cell fusion of myogenically specified mononuclear precursor cells contained within the population of satellite cells described above. Alexander Mauro in 1961 proposed that satellite cells could represent a population of "dormant myoblasts" left over from embryonic muscle development and capable of recapitulating the developmental program of skeletal myogenesis in response to muscle injury (34). Subsequent studies in both chicken and mouse demonstrate that multinucleated myotubes could indeed be generated *in vitro* from single myogenic precursor cells: *in vivo*-labelled and cultured *in vitro*-labelled satellite cells have been shown to participate in the regeneration of damaged muscle, contributing almost exclusively *via* fusion with pre-existing myofibres (35). Pulse-chase experiments using tritiated thymidine to label dividing cells indicate that DNA synthesis among sublaminar nuclei is limited to satellite cell nuclei, and that "true" muscle nuclei do not undergo mitosis. These approaches result in the labelling of a relative low number of satellite cells, indicating

their general quiescence in a physiological condition. However, even in the absence of muscle injury, some DNA labelled in the pulse phase eventually appears in myofibres in the chase phase, indicating a basal capacity of these cells to incorporate into adult muscle fibres (36). These studies are the basis of our current view of satellite cells as the primary mediators of postnatal muscle growth and repair. These cells respond to regenerative cues, such as injury or exercise, by proliferating to form myoblasts, that can undergo a limited number of cell cycles before terminally differentiating and fusing to form multinucleated myotubes (Figure 10) (35).

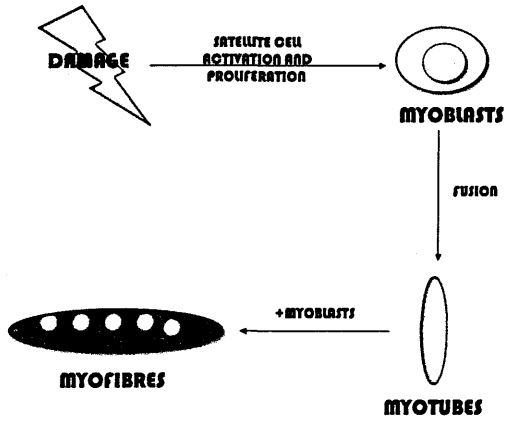

Figure 10 - Muscle regeneration *via* satellite cell fusion process (Adapted from (35)).

Satellite cell behaviour following tissue damage is quite well defined. The response to damage is orchestrated by transcription factors of the basic helix-loop-helix family. The process of regeneration can be dived into three stages, each of which is defined by the expression of specific factors. The first is the proliferative stage, in which satellite cell population expands. Quiescent and early-activated satellite cells express Pax7. During the first phase, satellite cells start expressing MyoD and Myf5. The second phase is the differentiation, in which the transcription factors MRF4 and myogenin are activated and Pax7, MyoD and Myf5 expression persist. MRF4 and myogenin drives

the expression of muscle specific genes that are required to enter the last phase, the fusion, in which the mature myofibre is formed (Figure 11) (30).

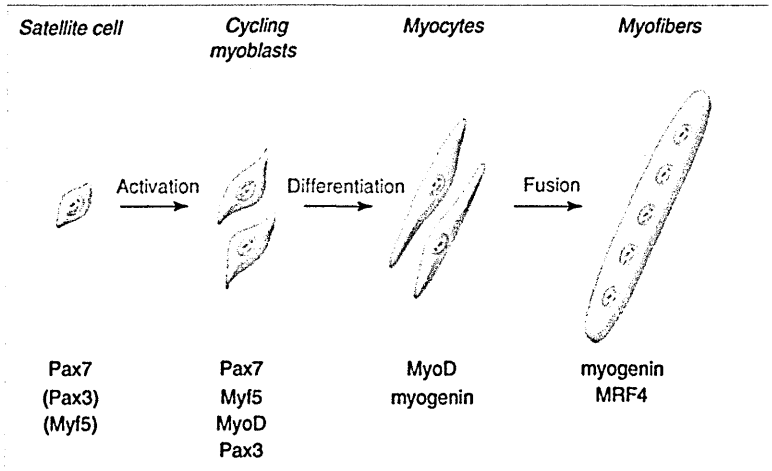

Figure 11 - Satellite cell differentiation genetic program (30).

2.2 Accessory, non-muscle derived cells actively participate to muscle regeneration

The view that satellite cells proliferate, differentiate and fuse to regenerate muscle has been challenged in the past few years. It has become clear that most progenitors in distinct tissues rely on microenvironmental cues generated by accessory cells, local signals and stromal structures. The regulatory effects of such cell populations mainly influence satellite cell proliferation and differentiation. For instance it has been discovered that inflammatory cells are not merely phagocytes that remove damaged fibres, but represent active and necessary players that generates signals that acts at distinct stages of satellite cells life cycle (29). Tissue resident progenitors with localization similar to satellite cells are endowed both with fibrogenic and adipogenic potential. They proliferate upon injury and secrete a number of trophic factors (37).

Acute muscle damage is a model of sterile injury with prototypic inflammatory responses composed by neutrophils, macrophages and T lymphocytes. Fine tuning of such an effective immune response and molecules involved in the cross-talk with

muscle cells are still poorly defined (29). Neutrophils appear in damaged muscle within few hours from damage, peak at 24 hours post-injury and then rapidly decline. Macrophages appear later, peak at day3 after damage and persist for several days after which they gradually disappear (38). Myeloid cells are likely to influence muscle repair both in a direct and in an indirect way. In fact they can perturb the proliferation, differentiation and fusion of satellite cells or they can act on third parties, such as mesenchymal cells or endothelial cells (29).

Neutrophils play a controversial role. They have two major pro-regenerative functions. They degranulate and secrete proteases that digest the extracellular matrix (ECM) and secrete pro-inflammatory cytokines that recruit macrophages, the main actors in muscle repair. ECM remodelling is crucial step to set the stage for subsequent repair. Moreover neutrophils have a high phagocytic ability. Depletion of neutrophils in a mouse model of acute damage results in accumulation of tissue debris and slower muscle regeneration (39). However neutrophil infiltration is followed by a marked respiratory burst and free radicals release, that may cause additional damage to fibres (40).

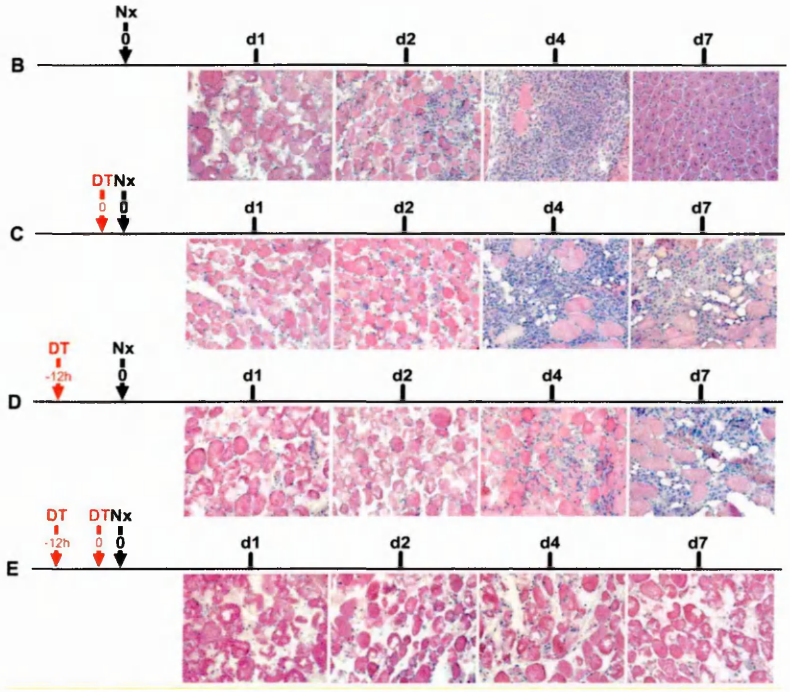

Figure 12 - Delayed repair in skeletal muscle is induced in macrophage-depleted mice. Nx = noxetin, a toxin used to induce acute muscle damage, as well as cardiotoxin. DT = Diphtheria Toxin, used to induce macrophage depletion. d = day post injury. Mice used here are genetically engineered to have the Diphtheria Toxin Receptor (DTR) under the control of CD11b promoter. When administered, DT kills specifically $CD11b^{+}$ cells, so macrophages (2).

Macrophages are key players in muscle regeneration. Depletion of monocyte/macrophages using CD11b-DTR genetic system results in failure of healing of acutely damaged muscles (Figure 12) (2).

Part of the contribution of macrophages to the repair of damaged muscle may rely on their ability to remove all debris. In 1990 it was demonstrated in a rat model that macrophages modulate immunological and inflammatory responses rather than only acting as scavenger cells and that they display different characteristics in the various phases of muscle repair (41). As mentioned, macrophage heterogeneity is dictated by environmental stimuli. The pro-/anti-inflammatory macrophage paradigm is sound and generally well accepted. However *in vivo* study only partially recapitulates *in vitro* characteristics of polarized macrophages (8). In our laboratory we have characterized the phenotype of infiltrating macrophages at distinct time points after muscle injury, in a model of cardiotoxin induced local and sterile damage. Early- and late-phase macrophages in healing skeletal muscle display features of both pro- and anti-inflammatory macrophages. As pro-inflammatory macrophages they phagocytose tissue debris and dead fibres and they secrete pro-inflammatory cytokines such as TNFα in early phase after tissue injury. However they also express scavenger receptor molecules, such as CD163 and CD206, typical of anti-inflammatory cells (Figure 13).

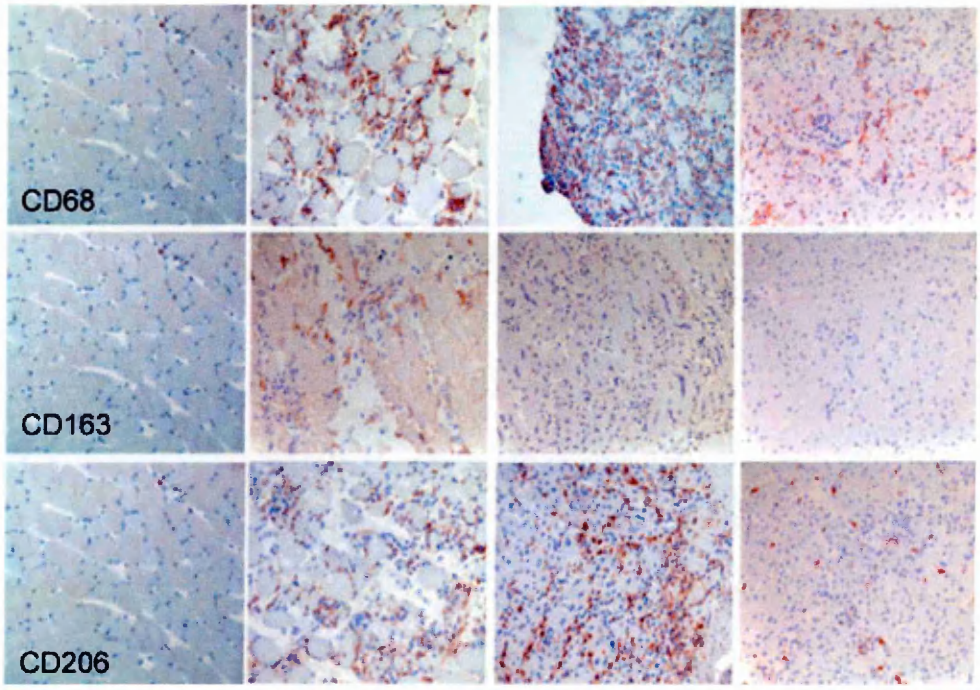

Figure 13 - Macrophage characteristics in injured and regenerating muscles (42). In the first column untreated muscles are shown. Day3, 7 and 10 after cardiotoxin injection are shown in the subsequent columns.

Phagocytosis possibly contributes to switch macrophages into fully anti-inflammatory cells, able to secrete anti-inflammatory cytokine (e.g. IL10), pro-myogenic (e.g. IGF1) and pro-angiogenic factors (e.g. VEGF). Those macrophages can sustain proliferation, differentiation and fusion of satellite cells (29, 42, 43). All factors secreted by macrophages should be tightly regulated according to their function. For example early-phase macrophages release factors mainly involved in satellite cells activation and proliferation, while late-phase macrophages sustain fusion and differentiation (43). A clear example is Platelet Derived Growth Factor (PDGF). In muscle it is secreted early after injury by endothelial cells and platelets and by macrophages late after injury. In early phases of muscle injury PDGF promotes satellite cell activation, migration and proliferation, while limiting differentiation. In late phase of tissue repair it sustains angiogenesis, thus promoting healing. Degranulating platelets release TGFβ just after injury and it recruits monocyte/macrophages (44) and inhibits satellite cell differentiation to allow the correct expansion of the regenerative population

(45, 46). Later in repair TGFβ is secreted by late-phase macrophages and orchestrates the ECM remodelling and angiogenesis. Finally it acts in an autocrine-paracrine manner to promote PDGF secretion by macrophages. Excess of TGFβ causes fibrosis and loss of function of the repairing muscle (43). The last factor described is IGF1. IGF1 receptors are abundantly expressed in skeletal muscle (44). IGF1 is both a circulating hormone released by liver and a local autocrine/paracrine factor secreted by muscle cells and macrophages. In the latter case it is highly expressed throughout the regenerative process and it promotes proliferation, differentiation and fusion of satellite cells (47). Local IGF1 has hypertrophic and hyperplasic effects, since it increases both the number of myonuclei per fibre and the protein synthesis inside the fibre. IGF1 engages IGF1 receptor type I on satellite cells and on regenerating fibres activating at least three intracellular signalling pathways: (i) the MAPK pathway; (ii) the PI3K pathway; (iii) the calcium-clamodulin dependent kinase pathway (48). Local IGF1 is released both by early-and late-phase macrophages, and thus is active all throughout the repair phase (43). The proliferative effect is evident early after damage. This is likely to happen since IGF-1 has a negative effect on myoblast differentiation when in combination with TNFα, typically secreted by early-phase macrophages (49). A plethora of factors released both by early- and/or late-phase macrophages are active in a similar manner during muscle regeneration such as Hepatocyte Growth Factor (HGF), Fibroblast Growth Factor 2 (FGF2), IL6 and IL10 (44).

Interestingly not only macrophages act on muscle, but the muscle also influences macrophages, for example by releasing molecules that promote macrophages invasion. Chemoattractiveness of myogenic cells is highest immediately after they are activated to proliferate and declines as the muscle begins to differentiate. Among the molecules that could account for this attraction effect MCP1/CCL2 is one of the most studied. The elevated expression of MCP1/CCL2 soon after injury and its ability to serve as a muscle-derived chemoattractant for macrophages *in vitro* have contributed to growing

interest in chemokines in regulating communication between muscle and macrophages after injury (50).

In skeletal muscle damage, i.e. in condition of sterile injury, the homeostatic response of tissue to injury is surprisingly similar to that of an infected tissue to microbe invasion. How is the inflammatory response elicited in sterile condition and why the resulting response is so similar to the microbial-induced one?

3. Hmgb1 in homeostatic responses to tissue injury

Inflammation is classically conceived as response to infections that represent a threat for body/tissue homeostasis (51). In the self-non-self model, foreign (non-self) molecules foster innate as well as adaptive immunity. Innate immunity in this scenario is then viewed as a controller and regulator of adaptive immune responses (52). In such a model the recognition of foreign signals is entrusted to Pathogen Recognition Receptor (PRRs) that distinguish among distinct Pathogen Associated Molecular Patterns (PAMPs). Innate immune cells exploit this pattern recognition system to trigger or select specific T and B cells responses. However empirical evidence indicate that trauma, cancers, radiation or chemical injuries elicit sterile inflammation even in the absence of microbial components (51). The "danger" model assumes that the immune responses are governed from within, responding to endogenous danger signals released by distressed cells. Embracing the danger model view, what really matters is not whether the signal is from exogenous (non-self) or endogenous (self) origin, but whether the signal is dangerous or not (52). By analogy with PAMPs the endogenous danger signals are referred to as DAMPs (Danger Associated Molecular Patterns). Danger signals are also referred to as alarmins to indicate their role in alerting immune system after tissue damage (51). PAMPs and DAMPs induce similar responses (1). Several danger signals have been described so far, such as Heat Shock proteins, S100 proteins and HMGB1 (see Table 1). They all share some features:

- They are rapidly released by necrotic cells

- Cells of the immune system can secrete these signals without dying, often using specialized secretion systems
- They recruit and activate innate immune cells by interaction with specific receptors on these cells (e.g. Toll-like Receptors, TLRs)
- They cooperate to restore tissue homeostasis (51)

3.1 The ABC of HMGB1

HMGB1 is a small protein (215 amino acids long) that has been initially identified as a nuclear factor. It is composed by two L-shaped domains, named HMG boxes A and B and by a 30 residues long acidic tail (Figure 14). The three domains are connected by short linker peptides. HMGB1 is ubiquitously expressed in virtually all cell types and tissues, albeit at distinct levels (53) and it is highly conserved among species (99% identity in mammals). The BoxA and BoxB share a limited amino acid identity but have some similarity in the structure (54).

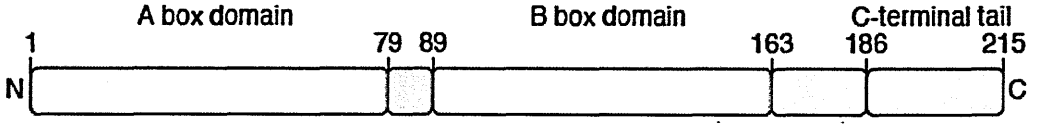

Figure 14 – Schematic view of HMGB1 structure (54).

HMGB1 binds to DNA without sequence specificity in the minor groove and facilitates a number of nuclear transaction, such as transcription, replication and V(D)J recombination. It interacts with a number of nuclear proteins, such as p53 and NF-kB and TBP (TATA Binding Protein). Once bound to DNA, HMGB1 bends it with angles of 90° or more. This activity facilitates the assembly of protein complexes onto DNA. HMGB1 also binds DNA at the site of entry or exit of nucleosomes, thus allowing DNA sliding on nucleosomes (53). HMGB1 is highly mobile within the nucleus and binds both to euchromatic and heterochromatic DNA domains (55).

3.2 Necrotic cells releases HMGB1

Necrotic cells releases HMGB1, which elicits inflammatory responses both *in vitro* and *in vivo* (54). When cells undergo apoptotic cell death HMGB1 remains strictly associated to the apoptotic chromatin, at least during the first phase of the process (Figure 15) (55).

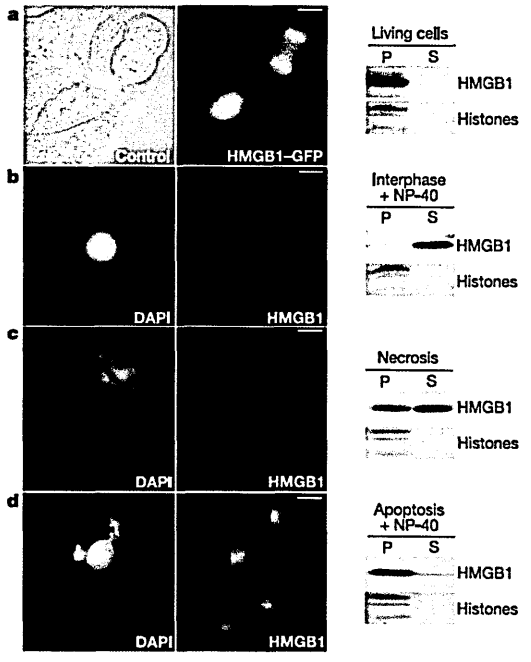

Figure 15 - Chromatin association of HMGB1 in living and dead HeLa cells. Both the cell culture supernatant (S) and the cells (P) have been analyzed by SDS–gel electrophoresis. Histones have been visualized by Coomassie blue, HMGB1 by immunoblotting or immunostaining with antibody to HMGB1, DNA by DAPI. Scale bars, 7.5 μm. A. Living cells expressing HMGB1–GFP, imaged by differential interference contrast and in green fluorescence. B. Interphase cells after permeabilization. C. Necrotic cells without permeabilization. D. Apoptotic cells with permeabilization (55).

HMGB1 is indeed a highly motile molecule inside the nucleus of living cells. In contrast HMGB1 mobility in apoptotic cells is near to zero. The link between dying cell DNA and HMGB1 is not required for apoptosis, since $Hmgb1^{-/-}$ embryonic fibroblast has similar susceptibility to apoptosis respect to $Hmgb1^{-/-}$ cells. Moreover apoptotic DNA has been demonstrated to be a sort of "sink" for HMGB1. In fact recombinant HMGB1-Cy5 relocated into the apoptotic nucleus of $Hmgb1^{-/-}$ fibroblast. The

interaction between HMGB1 and apoptotic DNA seems to be dependent on post-translational modification of hystones and chromatin modification, while it is independent of DNA fragmentation, typical event of apoptotic cell death (55).

Later reports however have clearly demonstrated that during late phase of apoptosis and in particular during post-apoptotic necrosis, a fraction of HMGB1 is released possibly in association with nucleosomes derived by caspase-dependent nuclease activation (56). These HMGB1-nucleosomes complexes may represent a preferential substrate for autoimmunity (57). Of importance, released HMGB1 directly elicits TNFα release from monocytes (55) and in a model of massive acetaminophen-induced liver necrosis HMGB1 neutralization strikingly reduced the extent of liver inflammation. Thus HMGB1 has been identified as one of the main diffusible signals for necrosis (55).

The HMGB1 released by necrotic cells is an endogenous immune adjuvant that elicits antigen-presenting cells (APCs) maturation. Maturation of APCs in case of microbial infection is regulated by TLRs. They recognize microbial patterns and induce the overexpression on APCs of MHC class I and class II antigen and co-stimulatory molecules. In sterile injuries, however, endogenous adjuvant might exist to induce immune responses. HMGB1 when released by necrotic cells has been demonstrated to be an endogenous immune adjuvant. *In vitro* human dendritic cells (DCs) have been exposed to supernatants from either wt or $Hmgb1^{-/-}$ embryonic fibroblasts. The latter fails to upregulation of co-stimulatory molecules on DCs (58).

In vivo the adjuvant role has been verified on lymphoma (RMA cell line) tumour model. RMA necrotic cells are poorly immunogenic and fail to vaccinate animals to react against subsequent tumour challenges. When RMA necrotic cells have been injected alone, in fact, most of the mice challenged with live RMA cells developed lymphoma. However mice are protected from tumour development when vaccinated with both wt necrotic fibroblast supernatant and apoptotic RMA. The protection has

been less effective when apoptotic RMA are co-injected with supernatants from necrotic Hmgb1$^{-/-}$ fibroblasts (58).

3.3 Inflammatory cells actively secrete Hmgb1

HMGB1 has been previously implied in inflammatory response to septic shock and lung inflammation (59-61). Serum HMGB1 levels peak 16-32h after treatment with LPS (Figure 16, left panel). Consistently, *in vitro* LPS induces TNFα and IL-1 secretion by monocyte/macrophages within minutes from stimulation, while the production of HMGB1 is delayed at 18-24h after stimulation. Treatment *in vivo* with blocking antibodies for HMGB1 dramatically reduces the mortality of LPS challenged mice (Figure 16, right panel). HMGB1 levels in sera of patients with severe infections correlate with poor survival (59).

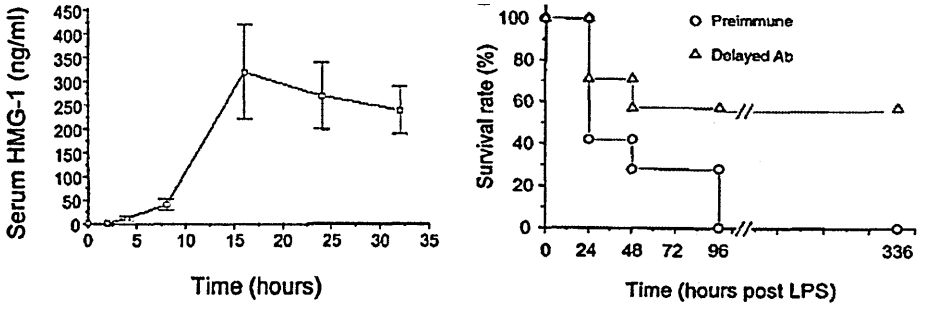

Figure 16 – On left panel accumulation of HMG-1 in serum of LPS-treated mice is shown. Male Balb/C mice (20 to 23 g) have been treated with LPS [10 mg/kg, intraperitoneally]. Serum has been assayed for HMG-1 by immunoblotting; the detection limit is 50 pg. On right panel survival curve of mice treated with anti-HMGB1 antibodies is shown. Delayed administration of anti-HMGB-1 protects against LPS lethality in mice. Male Balb/C mice (20 to 23 g) have been randomly grouped and treated with an LD100 of LPS. AntiÐHMG-1 or pre-immune serum (0.4 ml per mouse) has been administered at 2, 24, and 36 hours after LPS (59).

The release of HMGB1 by LPS-stimulated macrophages is calcium dependent and regulated by calcium/calmodulin-dependent protein kinase Iα (CaMK Iα) (62). Results

obtained in sepsis models have been confirmed in a model of endotoxin-induced acute lung injury. Subsequently to LPS intratracheal administration massive neutrophil recruitment and TNFα and IL1β production occur. The treatment with anti-HMGB1 antibodies reduced the oedema and the neutrophil recruitment while do not affect the early production of TNFα and IL1β (60). Moreover TNFα itself triggers HMGB1 secretion by monocytes (59).

HMGB1 is now well accepted as a late-mediator of local and systemic sepsis. Further highlighting its extracellular role two questions arise:

i) how is it relocated from the nucleus to the cytosol?

ii) how is it secreted?

Cytokines are normally externalized through the endoplasmatic reticulum-Golgi route. Some of them, however, lack a signal peptide and are processed in a non-canonical pathway. The prototypic leaderless cytokine is IL1β that translocates into secretory lysosomes and is secreted upon exocytosis. Secretory lysosomes are defined as calcium-regulated secretory organelles that share features of both secretory granules and lysosomes. Leukocytes and platelets are particularly enriched in these organelles. HMGB1 is a leaderless protein; therefore it was hypothesized that it could follow the secretory granule pathway as IL1β. This has been actually demonstrated in monocytes stimulated with LPS: HMGB1 translocates from the nucleus to the cytoplasm, where it is observed as punctuate staining at the periphery of cells (Figure 17). Biochemical approaches have helped in defining those compartments as organelles belonging to the endolysosomal compartment. No HMGB1 has been observed in early endosomes. In the secretory lysosomes it has been observed a partial co-localization of HMGB1 with IL1β (63).

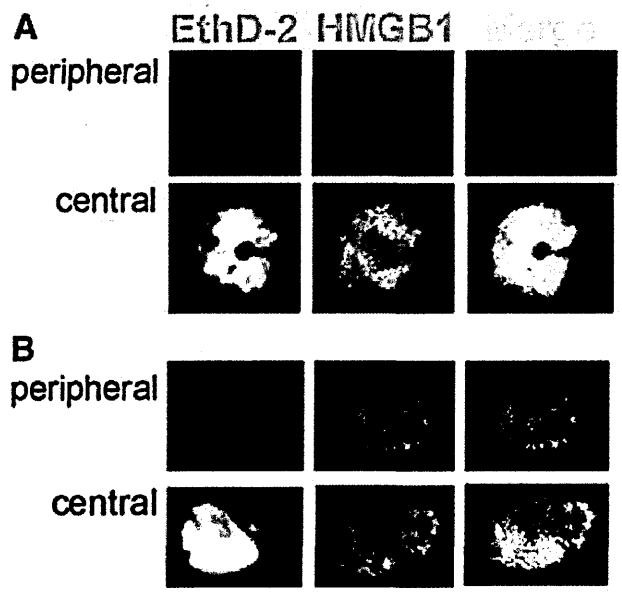

Figure 17 - Immunofluorescence analysis of HMGB1 in resting and LPS-activated monocytes. Monocytes, freshly isolated (A) or cultured for 18 h with LPS (B), have been stained with ethidium homodimer-2 (nucleus) and anti-HMGB1 antibody (HMGB1, green channel) and analyzed by confocal microscopy. Two sections of the same cells (peripheral and central) are shown, which allows the nuclear (central) and cytoplasmic (peripheral, absent at time 0, and evident after 18 h of activation) staining to be appreciated. The merged images verify the almost complete co-localization of HMGB1 and nucleus at time 0 (A, yellow), which decreases after LPS activation (B) (63).

Actively secreted HMGB1 is molecularly distinct from HMGB1 active in the nucleus. Using proteomic and bioinformatic tools it was demonstrated that secreted HMGB1 is hyperacetylated into two critical clusters of lysines. Moreover two cryptic nuclear export signals were identified in the protein. The acetylation at the C-terminal is necessary and sufficient for HMGB1 export from the nucleus but it is dispensable for localization in secretory granules that are released upon specific stimuli (64).

A second pathway of HMGB1 export exists. Pro- IL1β is cleaved in the cytoplasm by caspase 1. Caspase 1, in turn, is produced by cleavage of pro-caspase 1. Pro-caspase 1 processing takes place in large protein complexes named inflammasome. They are organized on nucleotide-binding oligomerization domain-like receptor (NLR) protein scaffolds. NLRs probably sense microbial components (PAMPs) as well as endogenous danger signals (DAMPs). The related NLR family member Nalp3 mediates pro-caspase

1 processing upon contact with PAMPs. It has been hypothesize that HMGB1 could be processed into Nalp3 inflammasome upon monocyte/macrophage activation. In macrophages primed with LPS and stimulated with uric acid Nalp3 inflammasome is activated and promote caspase 1 activation. Mice lacking caspase 1 are resistant to endotoxemia, as well as wt mice treated with anti-HMGB1 antibodies. In wt mice injected with LPS a peak of serum HMGB1 is reported; on the contrary in caspase 1 deficient mice no increase in circulating HMGB1 was observed (Figure 18) (65).

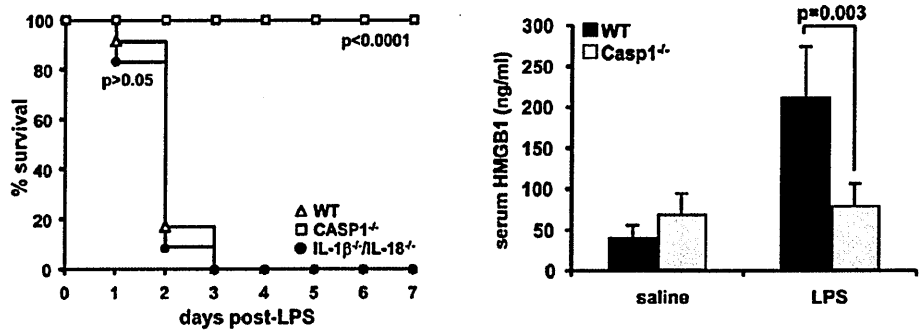

Figure 18 - LPS-induced endotoxemia requires caspase 1-dependent HMGB1 release, but not the caspase 1 substrates IL-1β and IL-18. A, WT, caspase $1^{-/-}$, and IL-$1b^{-/-}$/IL-$18^{-/-}$ mice have been injected i.p. with 40 mg/kg LPS and their survival has been monitored (left panel). Caspase 1 absence causes a decrease in circulating HMGB1 levels during endotoxemia. WT and caspase 12/2 mice have been injected i.p. with either saline or 40 mg/kg LPS, 24 h before serum was collected to measure secreted HMGB1 (65).

When murine bone marrow derived macrophage (BMDM) of murine origin are primed with LPS and then given a second stimulus to activate inflammasome they activate a Nalp3 and caspase 1 dependent HMGB1 secretion. Upon S. typhimurium infection, BMDMs activate Ipaf inflammasome. Ultimately also Ipaf inflammasome leads to caspase 1 activation. It has been demonstrated that upon contact with the bacterium BMDMs secrete HMGB1 in an inflammasome and caspase 1 dependent manner. Caspase 1 inhibitors block both Nalp3- and Ipaf-dependent HMGB1 secretion, thus demonstrating that caspase 1 is required for HMGB1 secretion upon

inflammasome activation. The secretion of HMGB1 is not dependent on the cleavage activity of caspase 1 on HMGB1, as it is for IL1β (65).

It has been recently been proposed that an autophagy-based unconventional secretion of substrates exists. Whereas basal autophagy blocks inflammasome and IL1β secretion, induced autophagy acts in the opposite way. IL1β co-localizes with LC3 in the cytoplasm of cells with autophagy induced by starvation. On the contrary inhibition of autophagic flux leads to block of IL1β secretion in BMDM. Starvation also induces HMGB1 secretion in an Atg5 (i.e. autophagy) -dependent manner. Interestingly some stimuli that induce inflammasome, such as nigericin, also induces autophagy and autophagy-related HMGB1 secretion, pointing out a strict cooperation between distinct non-canonical secretory pathways (66).

4. Functional effect of Hmgb1

The logical questions that follow are: (i) are there specific receptors for extracellular HMGB1? (ii) what is the role of extracellular HMGB1?

4.1 RAGE and TLRs are HMGB1 receptors

Before the discovery of HMGB1 as a late mediator of sepsis another protein, amphoterin, was known to bind the surface of embryonic rat neurons to enhance neurite outgrowth. HMGB1 and amphoterin turned out to be the same protein. Amphoterin, i.e. HMGB1, binds to the Receptor for Advanced Glycation End products (RAGE) to exert its action on neurons (67). RAGE is a member of the immunoglobulin superfamily and it is expressed on endothelium, vascular smooth muscle cells, mononuclear phagocytes and the central nervous system. The extracellular domain is composed by one "V" type and two "C" type domains and is very similar to neural cell adhesion molecules. The RAGE binding site of HMGB1 resides in the BoxB domain and the interaction is mediated by the V1 domain of the receptor. RAGE is a multi-ligand receptor that can

bind also advanced glycation end products (AGEs), S100 proteins, heparin and β-amyloid protein (Figure 19) (68).

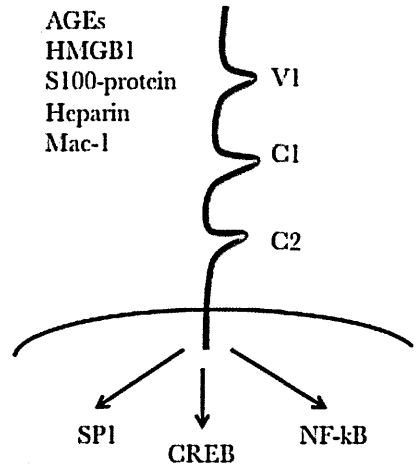

Figure 19 – Structure of RAGE and signalling pathways induced by HMGB1 binding to RAGE. The cytosolic tail is required for RAGE-mediated intracellular signalling. The distal Ig domain (V1) binds HMGB1 and other RAGE ligands. Ligand binding to RAGE regulates gene expression through the transcription factors NF-κB, CREB and SP1 (68).

The affinity of HMGB1 for RAGE can be modulated by other HMGB1 ligands. HMGB1 has a heparin-binding site at the N-terminus of the BoxA domain. Heparin binding causes a conformational change in HMGB1 and decreases the affinity of the protein for RAGE (69). NF-kB is activated downstream RAGE engagement by HMGB1. The activation of NF-kB depends both on Ras activation and p38 MAP kinase (MAPK)-Erk1/2 signalling. Activation of the MAPK pathway ultimately leads to phosphorylation and degradation of inhibitor of NF-kB (IkB). Interestingly, a NF-kB binding site has been described in the RAGE promoter, thus creating a possible positive-feedback loop (70). Rac and Cdc42 are activated in consequence of HMGB1/RAGE engagement by HMGB1 to favour neurite outgrowth and several migratory mechanisms (67). RAGE *in vitro* caused NF-kB translocation into the nucleus.

HMGB1 enhances NF-kB nuclear translocation in a TLR4 dependent manner, and both TLR2 and TLR4 are required to activate transcription of NF-kB target genes (71). A physical interaction of HMGB1 with TLR2 and 4 has been demonstrated using fluorescence resonance energy transfer (FRET) (72). Both receptors are present on endothelial cells and on innate immune cells. After HMGB1 interaction, adaptor proteins such as myeloid differentiation primary response protein 88 (MyD88) and TIR-domain containing adaptor protein (TIRAP) bind to TLR2 and TLR4. MyD88 recruits members of the IRAK family that activate downstream TRAF6 kinase. The signalling pathways culminated in NF-kB activation through phosphorylation and degradation of its inhibitor IkB. TLR2/4 engagement also causes p38 MAPK pathway activation. Therefore there may be intersections between RAGE and TLRs signalling (Figure 20).

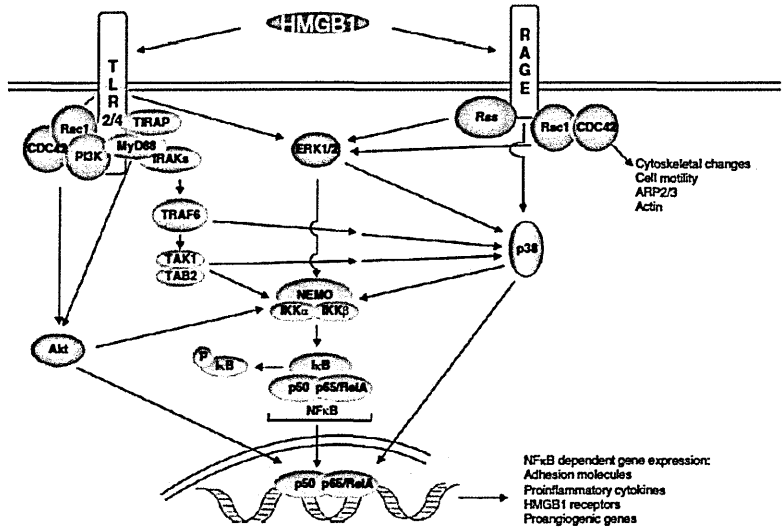

Figure 20 - Convergence of TLR and RAGE signalling. Schematic representation of signalling events mediated by TLR and RAGE receptor activation is reported. The outcome of the interplay between TLR2/4 and RAGE is likely to differ between cell types (70).

HMGB1/TLRs interaction have been proposed to control HMGB1 inflammatory activity, while RAGE signalling could be mainly related to HMGB1 migratory activity. However, this may be an oversimplification (70).

HMGB1 also binds to the carbohydrate chains of syndecans, particularly it has been demonstrated for syndecan-1. Syndecans are able both to transduce intracellular signal as independent membrane receptors and to act as co-receptors for integrins or growth factors. The HMGB1/proteoglycans interaction has been proposed to be involved in the pro-migratory action of HMGB1 (68).

4.2 HMGB1 effect on cell migration

Pro-migratory ability of extracellular HMGB1 has been one the first effects to be described (68).

HMGB1 favours the migration of vascular smooth muscle cells: *in vitro,* cells have been treated with small interfering RNA for TLR4 and in the absence of TLR4 no migration has been observed, indicating that the migration is TLR4 dependent. It has been also established that the effect passes through the signalling of PI3K and Akt (73). The same pro-migratory effect has been observed with rat smooth muscle cells and the effect is MAPK dependent (74).

HMGB1 triggers the migration of stem and precursor cells as well. For instance recombinant HMGB1 induces vessel-associated stem cells migration (75). In our lab we have demonstrated that HMGB1 produced by human inflammatory macrophages induces vessel-associated stem cell migration and that BoxA, the antagonist of HMGB1 for RAGE binding, reduced the effect (Figure 21) (76). When injected into the muscles of dystrophic mice, HMGB1 triggers vessel-associated stem cell migration *in vivo* in a RAGE dependent manner (77). HMGB1 also triggers migration of rat myoblasts *in vitro* in a RAGE-dependent and p38 MAPK-dependent fashion (78).

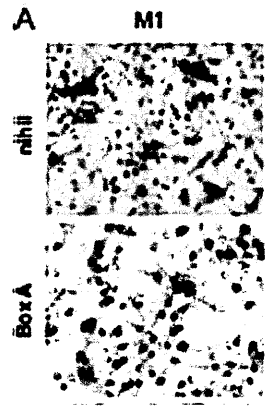

Figure 21 – Human mesoangioblast migrate in response to pro-inflammatory macrophage conditioned media (M1) in a Boyden chamber assay. When media are supplemented with the HMGB1 antagonist BoxA mesoangioblast migration is dramatically reduced (76).

Other progenitors that rely on HMGB1 for their migration are endothelial precursor cells. Endothelial precursor cells express RAGE and TLR2 but not TLR4 and HMGB1 increases their migration onto fibronectin and fibrinogen. Cells respond to HMGB1 with a bell-shaped dose-response curve; anti-RAGE but not anti-TLR2 and 4, blocking antibodies inhibit migration. Thus HMGB1 induces endothelial precursor cell migration on matrix protein in a RAGE-dependent manner (79).

HMGB1 modulates the response to chemoattractants of several innate immune cells. For example freshly isolated adherent monocytes express HMGB1 and RAGE. Although a direct chemotactic role of HMGB1 on monocytes has been excluded, HMGB1 increases trans-endothelial migration of monocytes. Experiments performed in the presence of anti-RAGE antibodies have identified an autocrine and paracrine role of HMGB1/RAGE interaction in trans-endothelial migration of human monocytes (80).

In vitro experiments I have performed before starting my PhD project indicate that murine monocytes migrating to a known chemotactic stimulus, such as CXCL12/SDF1, secrete HMGB1 and that the secreted HMGB1 acts in an autocrine/paracrine manner to facilitate migration. A similar effect has been observed in dendritic cells (Figure 22). In supernatants of migrating monocytes CXCL12 elutes in the same fraction of HMGB1, indicating a possible physical interaction of the two

proteins (81). These results have been recently confirmed and expanded in an elegant studies by Schiraldi et al. (82). Previous data from my lab have linked the facilitating role of HMGB1 on dendritic cell migration with the RAGE-mediate upregulation of chemokines receptor for homing at lymphoid organs, such as CCR7 and CXCR4 (83).

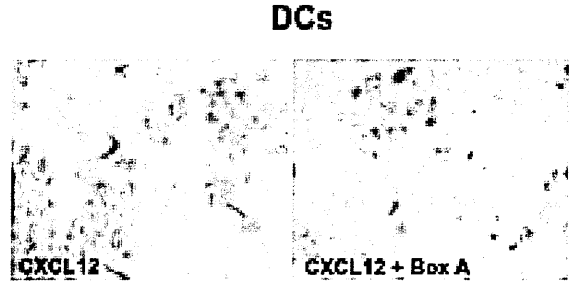

Figure 22 – HMGB1 is required for murine dendritic cell migration in response to a chemoattractant (CXCL12). Boyden chamber assay is performed in the presence or in the absence of HMGB1 antagonist BoxA (81).

There is a single report indicating an anti-migratory effect of HMGB1. This seems to be peculiar of enterocytes in inflammatory situations. In this paper the authors demonstrate that HMGB1 expression is increased in necrotizing enterocolitis both in human and mice. They have cultured human enterocyte cell lines on a monolayer and scratched the plate. Enterocytes are left closing the wound in the presence or in the absence of HMGB1 inhibitor. When HMGB1 is blocked enterocyte migration is reduced and the scratch fails to close. Therefore HMGB1 is necessary for enterocyte migration in a 2D model. On enterocyte TLR4 expression is upregulated in condition of damage. The expression in human enterocytes of a dominant negative form of TLR4 demonstrates that HMGB1/TLR4 interaction functions to inhibit enterocyte migration (84).

4.3 HMGB1 effect on inflammatory responses in health and disease

HMGB1 is required for the development and progression of inflammation in a number of disease conditions (85). HMGB1 senses intracellular nucleic acids and elicits primary response thus defending the host genomic integrity from pathogen invasion. This is a general mechanism of innate immunity present in all cells and is mediating a type I interferon mediated responses (86, 87).

HMGB1 is important in the pathogenesis of diseases such as systemic lupus erythematosus (SLE) and epilepsy. Pathogenetic factors for SLE are increased cell death with defect of apoptotic bodies clearance that in turn trigger breaking of immune tolerance to nuclear antigens. In such processes HMGB1 binds the "eat me" signal phospatidylserine impairing clearance of apoptotic cells. Moreover it inhibits integrin-dependent recognition of apoptotic material by macrophages (85). Finally HMGB1-nucleosomes complexes are recognized by TLR2 eliciting pro-inflammatory cytokine production. Those complexes inhibit immune tolerance to nuclear components such as double strand DNA even in non-SLE prone mice (57). In epilepsy inflammation is one of the worsening factor in several types of seizures. HMGB1 increases and anticipates the seizures induced by a chemoconvulsant in a TLR4 dependent manner. Epileptic events promote HMGB1 release, creating a dangerous vicious cycle (88).

There are several mechanisms by which HMGB1 accomplishes its immune-regulating functions in health and disease. It targets both innate and adaptive immune cells and I am going to briefly review the effects of HMGB1 on monocyte-macrophages, antigen presenting cells and T lymphocytes. Human peripheral blood mononuclear cells have been exposed to HMGB1 and it stimulated the release of TNFα, IL6, IL8, MIP1α, MIP1β but not IL10 or IL12. Also LPS is able to induce the same molecules on human molecules. However, while LPS is active in 1h after stimulation, the HMGB1 effect is delayed, accordingly to its role as late-mediator of sepsis (61).

The demonstration that HMGB1 physically interacts with microbial moieties and modifies its function should be taken into account interpreting these results.

HMGB1-TLR4 interaction is anyway able to induce inflammation *per se*. The minimal portion of HMGB1 required to induce pro-inflammatory cytokine release is located in the B box (position 89-108) (89). Specifically cysteine in position 106 (C106) is required to have HMGB1/TLR4 binding and induction of TNFα release by macrophages.

The interaction occurs between HMGB1 B Box and the TLR4/MD2 complex. After binding HMGB1 is internalized with the complex itself. The redox state is a possible regulator of HMGB1 extracellular activity. The critical role of C106 has been discovered using mutagenesis approach in all the residues within the B box (90). Very recently other critical residues have emerged as crucial regulators of HMGB1/TLR4 binding. Other two cysteines are highly conserved in HMGB1, C23 and C45. They can form a disulfide bond in recombinant HMGB1 (rHMGB1) able to induce the release of inflammatory cytokines from human macrophages (i.e. TNFα) and NF-kB nuclear translocation (see molecule in line 1 of Table 1). Up to now these modifications have not been described for the native molecule. When rHMGB1 is exposed to reducing agents no pro-inflammatory activity is detected (molecule in line 3 of Table 1). The same outcome is observed when the protein is oxidized and terminal oxidation modifications are present either on C23, C45 or C106 (molecule in lines 2 and 4 in Table 1). It is now clear that the a specific redox state of the three cysteines is required for the TNF-stimulating activity of HMGB1 (see Table 1, line 1) (89).

In the extracellular environment HMGB1 forms complexes with exogenous and endogenous molecules to enhance their activity on immune system (1). For example if rHMGB1 without inflammatory activity forms complexes with LPS it increases by 100-fold the magnitude of cell response to LPS itself. A similar potentiating effect is described when HMGB1 binds to TLR2 or TLR9 ligands, such as in the case of nucleic acid mentioned before (91). HMGB1 can bind also endogenous molecules such as IL1α, IL1β (92), CXCL12 (81) and nucleosomes (57). A better understanding of the

biology of HMGB1 interactions with other molecules is of pivotal importance to understand which receptor is used by which complex to enhance cytokine effect. In general HMGB1/molecule X complexes signal mainly through molecule X receptor, meaning that the synergistic effect of HMGB1 results from quantitative rather than qualitative changes in intracellular signalling pathways (91).

Schematic molecular overview	Cytokine inducing capacity and NF-KB nuclear translocation
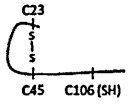	Yes
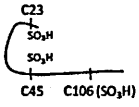	No
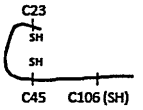	No
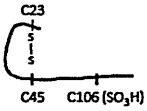	No
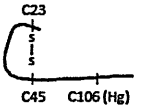	No
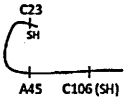	No

Table 1 – Distinct redox state of HMGB1 have distinct outcomes on its pro-inflammatory activity (89).

HMGB1 is a key molecule in the cross-talk between professional antigen presenting cells such as dendritic cells (DCs) and T cells (93). To initiate T cell-dependent immune responses immature DCs internalize antigens by phagocytosis, macropinocytosis or endocytosis and upregulate the expression of co-stimulatory molecules (e.g. CD80, CD83, CD40). DCs process ingested antigens and present them in association with major histocompatibility complex molecules (MHC) class I and

class II. Finally DCs secrete signals useful for T cell proliferation and polarization. HMGB1 has been proposed to affect all of these steps (94). HMGB1 released by necrotic cells has been demonstrated to participate to DC maturation, by enhancing co-stimulatory but not MHC expression in a RAGE dependent manner (58). Maturing DCs are in turn able to secrete HMGB1 (95).

Secreted HMGB1 interacts with RAGE and activates p38 MAPK and NF-kB pathways. This leads to proliferation and survival of naïve $CD4^+$ T cells. Moreover maturing DCs start secreting IL12, thus promoting Th1 polarization on naïve $CD4^+$ T cells. The ability of DCs to secrete HMGB1 is acquired after starting of the maturation process by either PAMPs or cytokines. Immature DCs do not secrete HMGB1 (95).

HMGB1 also exerts a direct pro-proliferative effect also on $CD8^+$ T cells (94-96). To activate adaptive immune responses maturing DCs must reach the T cell zone of lymph nodes. Our group have demonstrated that maturing DCs depend on RAGE for homing to draining lymph nodes. Bone marrow-derived DCs from RAGE-/- mice failed to reach draining lymph nodes when co-injected with complete Freund adjuvant in the footpad of wt mice. On the other hand wt DCs perfectly reach the lymph nodes both of wt and RAGE -/- mice, thus confirming that integrity of RAGE signalling, and possibly of HMGB1/RAGE interaction is required for maturing DCs homing to lymph nodes (Figure 23) (97).

NK interaction also regulates DC maturation and function. NK cells trigger immature DCs to secrete IL18 in the synaptic cleft between the two cells. DC activated NK cells are able to secrete HMGB1 in the surrounding environment. Secreted HMGB1 participate, as mentioned, to DC maturation but also it protects DC from lysis by activated NK cells (98).

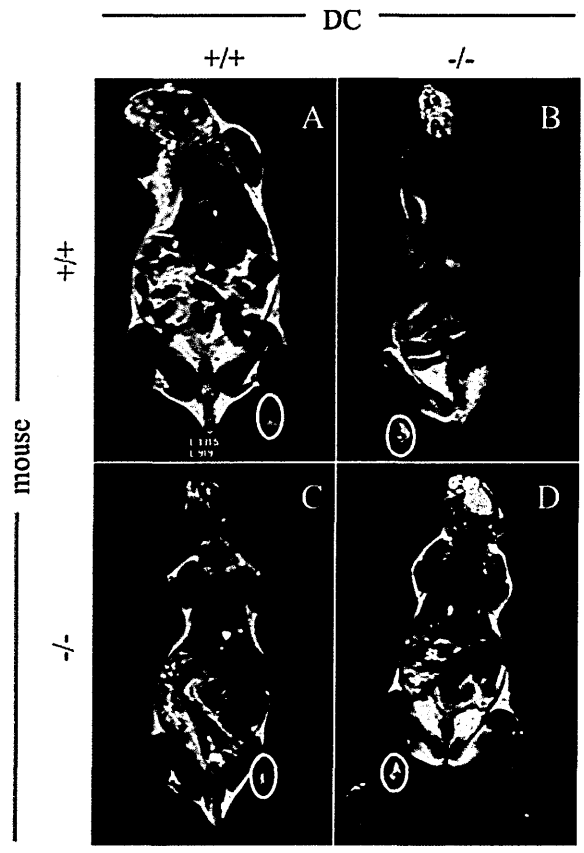

Figure 23 - Selective migration of RAGE$^{-/-}$ DCs to draining lymph nodes. MRIs of wild-type (bottom panel) or RAGE$^{-/-}$ mice 48 h after injection into the footpads of DCs labe-led with SPIO. DCs have been either wild type (right panels) or RAGE$^{-/-}$ (left panels). The black spot (i.e. migrating DC) is highlighted by the white circle and is lacking only in DC RAGE$^{-/-}$ transfer into either wt or RAGE $^{-/-}$ mice (97).

HMGB1 satisfies three key requirements for a DAMP. In fact HMGB1 is:

(i) readily secreted upon necrosis or cell stress;

(ii) segregating in apoptotic cells, at least during early-apoptosis;

(iii) important for DC maturation and T cell activation (94).

A further feature of a DAMP is to favour tissue repair. To prompt tissue healing, HMGB1 should be involved in the termination of the inflammatory response. In CD24$^{-/-}$ mice the acetaminophen-induced liver necrosis results in the death of animals because of excessive inflammatory response to injury. The increased susceptibility has not been observed in a model of sepsis, indicating that CD24 distinguishes among PAMPs and DAMPs. CD24 binds to HMGB1 and other DAMPs, such as heat shock protein 70 and

90. The interaction between DAMPs and CD24 negatively regulates their stimulatory activity on immune response by inhibiting NF-kB activation (99).

A recent report has pointed out that treating mice with HMGB1 reduces the percentage of CD25+FoxP3+ regulatory T cells in the spleen and this seems to be a TLR4 dependent mechanism (100). The actual relevance of these event remains to be established.

4.4 HMGB1 promotes wound healing

HMGB1 involvement in wound healing has been first investigated in the skin. In an excisional wound on the back of mice HMGB1 blockade with BoxA impaired healing (Figure 24). *In vitro* studies confirmed that HMGB1 has a positive role on migration but not proliferation of keratinocytes. Conversely treating diabetic ulcer with HMGB1 ameliorates repair, while no effect of BoxA has been observed on the repair kinetics of diabetic mice. This is not contradictory since the effect of BoxA blockade depends on the local availability of native HMGB1 that in diabetic mice is greatly reduced (3).

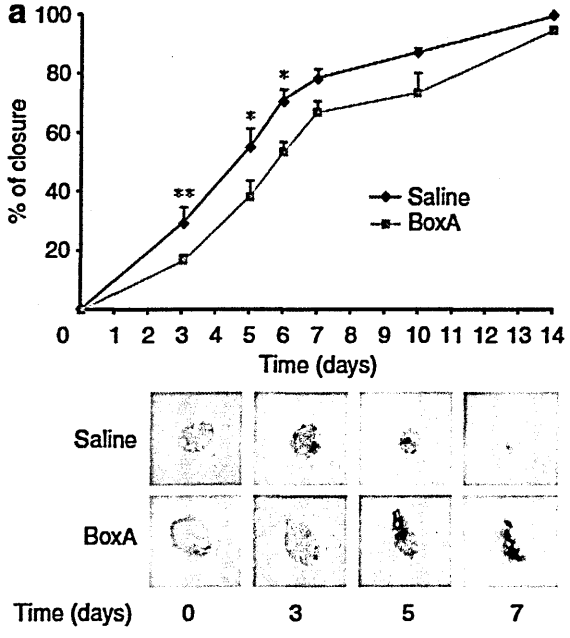

Figure 24 – Treatment of skin wound with BoxA results in delayed wound healing (3).

HMGB1 is able to induce fibroblast collagen deposition inside the wound in a RAGE dependent fashion. The contribution to matrix remodelling could be one of the mechanisms involved in the pro-healing function of HMGB1 (101).

HMGB1 has been implied also in cardiac repair after myocardial infarction (102). In a model of total heart ischemia post-ischemic treatment with HMGB1 improves the cardiac function, diminishes the infracted area and reduces pro-inflammatory cytokines (e.g. IL1β and IL6) levels in the infracted hearts (103).

HMGB1 also facilitates repair in myocardial infarction. HMGB1 acts directly on cardiac c-kit$^+$ stem cells, which express RAGE. In mice subjected to myocardial infarction proliferation of c-kit$^+$ cells increases *in vivo*. Moreover scar is virtually absent in hearts treated with HMGB1 as compared to untreated ones since the infracted area is almost completely regenerated, with a general amelioration of the cardiac function. HMGB1 promotes c-kit$^+$ cells differentiation towards cardiomyocytes. However while HMGB1 is migratory *in vitro, ex-vivo* no migratory effect is observed (104). The indirect effect of HMGB1 on migration of c-kit$^+$ cells can pass through fibroblasts. Human cardiac fibroblasts express RAGE. They have been stimulated *in vitro* with HMGB1: released soluble factors induce cardiac stem cells proliferation and migration *in vitro*. HMGB1 pro-healing function is exerted through conditioning of microenvironment cell components (105).

HMGB1 plays a role also in post-ischemic wound healing, as indicated by studies in a peripheral ischemia model on both normal and diabetic mice. Normal mice have been subjected to ischemia of hind limbs and muscles have then been treated with BoxA to block HMGB1. HMGB1 blockade reduces reperfusion of the ischemic limb and a worse repair (Figure 25). It has been observed that the number of CD31$^+$ cells (i.e. vessels) is reduced in BoxA-treated limbs. A similar effect has been obtained with injection of anti-VEGF antibodies. In diabetic mice HMGB1 levels in the ischemic limb

are reduced. The number of necrotic or apoptotic fibres is not different in normal and diabetic mice, as well as the number of infiltrating cells. However the number of $CD31^+$ cells is reduced in diabetic mice. HMGB1 restores reperfusion in diabetic mice and the number of $CD31^+$ cells is normalized as well (106).

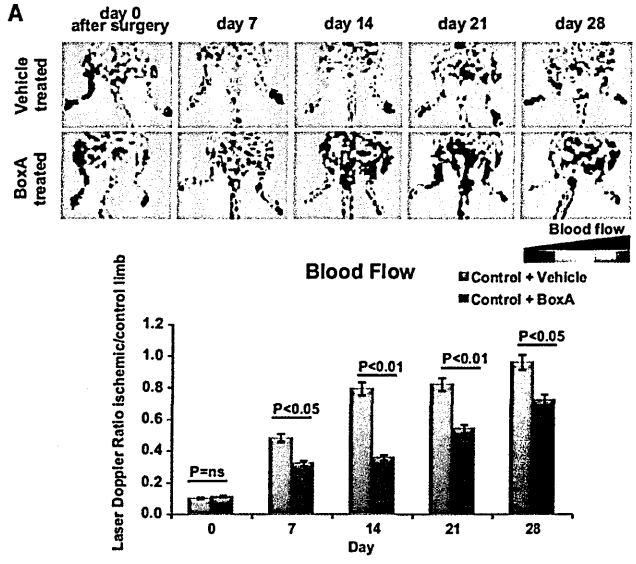

Figure 25 - Representative evaluation of the ischemic (right) and non-ischemic (left) hind limbs immediately after and on days 7, 14, 21, and 28 after surgery. Blood flow recovery is impaired in BoxA-treated mice compared with vehicle-treated mice (106).

Angiogenesis-activated endothelial cells have to migrate, proliferate and sprout into the stroma, leading to the formation of vascular loops and finally capillary tubes. HMGB1 *in vitro* enhances endothelial cell proliferation, migration and tube formation in a RAGE-dependent manner.

HMGB1 increases the repair of a disrupted endothelial cell monolayer through augmenting the sprouting activity in a RAGE dependent fashion (107). HMGB1 pro-angiogenic effect is at least partially heparin dependent (108). Also the pro-angiogenic effect of HMGB1 involves TLR4 signalling. In a model of coroidal neovascularization, local treatment with HMGB1 increases the number of vessels in normal mice while fails to induce vessel formation in $TLR4^{-/-}$ mice. Moreover peritoneal macrophages from

control mice produce VEGF, bFGF and TGFβ upon stimulation with HMGB1, while peritoneal macrophages from $TLR4^{-/-}$ mice fail (109).

Angiogenesis and lymphangiogenesis share many features. HMGB1 has been found also to increase proliferation, migration and tube formation of lymphatic cell lines in a time and dose dependent manner (110).

The so-called angiogenetic switch, the initiation of angiogenesis, is a key step in tumour progression and dissemination. It ensures the correct oxygen and nutrient supply to the growing tumour. It is promoted by the hypoxic microenvironment that is established upon initial tumour enlargement. Hypoxia triggers necrotic cell death of tumour cells and necrotic areas show increase expression of VEGF and their pro-angiogenic molecules (111).

5. Putting the puzzle together: what is the contribution of distinct sources of Hmgb1 to tissue repair? The need for a new animal model

5.1 HMGB1 and muscle repair

HMGB1 and muscle repair are intimately linked to inflammation, and the features of the inflammatory response modulates HMGB1 activity. Appropriate inflammatory responses are needed for successful tissue healing. There are relative few studies pointing to a possible role for HMGB1 in muscle repair. HMGB1 has proved to be important in the repair of ischemia/reperfusion injury through control of vascularization and in cardiac repair through control of cardiac stem cell differentiation (102, 106). Moreover we and other have identified HMGB1 as a chemotactic molecule for unconventional myogenic cells such as mesoangioblasts (76, 77). HMGB1 has also an effect on myoblast proliferation, differentiation and migration (78).

RAGE engagement leads to the expression of TGFβ and PDGF (112). RAGE is expressed in skeletal muscle and it is developmentally regulated. It has a myogenic role when engaged by HMGB1 through MAPK signalling pathway. In contrast when engaged by S100B protein it has an apparently opposite action, at least *in vitro* (49). In a very recent paper it has been demonstrated that HMGB1/RAGE interaction controls satellite cell homeostasis. In $Rage^{-/-}$ mice the number of $Pax7^{+}$ (i.e. quiescent) satellite cells is increased and it increases further following muscle damage. Regeneration is delayed of nearly one week in these mice, probably due to an excessive satellite cell proliferation, that inhibits differentiation. Pax7 overexpression indeed blocks myogenin expression, while RAGE engagement leads to its expression. Thus it appears that RAGE signalling physiologically represses Pax7 transcription in satellite cells by driving myogenin expression (113).

5.2 Limitations in HMGB1 study

Most of the studies cited have important limitations. The studies on ischemia/reperfusion model in normal mice have been carried out by injecting HMGB1 pharmacological inhibitors into damaged muscle. In this case the outcome observed is the result of the total block of extracellular HMGB1, without dissecting the relative role of leukocyte-associated HMGB1 and HMGB1 passively released by dying fibres. In the case of diabetic mice and ischemia/reperfusion study, exogenous HMGB1 has been administered to mice. Thus the results obtained do not reflect directly the role of the endogenous protein (106). The same approach was used in the studies about skin and cardiac wound healing that thus present the same limitations (3, 104). The study on rat myoblast proliferation and differentiation is only *in vitro* (78), as well as the study about the role of macrophage-released HMGB1 in mesoangioblast migration (76). The paper on HMGB1 role in mesoangioblast migration *in vivo* has been carried out by injecting HMGB1-coated heparin beads into muscles, again not addressing the role of the

endogenous protein (77). The role of RAGE has been addressed *in vivo* but without distinguishing the two sources of HMGB1, the passively released by necrotic fibres and the actively secreted by inflammatory cells (49, 113). Finally the role of HMGB1 in driving MHC class I antigen overexpression in muscle fibres has been addressed on isolated fibres and with recombinant protein administered, thus avoiding the study of the endogenous protein (114).

5.3 An original mouse model to address HMGB1 dynamics in vivo

To better define HMGB1 role in tissue repair it would be necessary to establish:

- an appropriate sterile damage model to study the molecule *in vivo*. As described muscle damage is an ideal model. A better description of HMGB1 expression in acutely damage muscle is reported is section 1 of the RESULTS
- a mouse model in which HMGB1 is lacking selectively in the haematopoietic system, to dissect the relative role of leukocyte HMGB1. This model was not available at the beginning of my PhD project.

Theoretically a mouse with all the tissue wt and only the haematopoietic compartment *Hmgb1*$^{-/-}$ is needed. The easiest way to obtain such a model is to transplant a bone marrow from *Hmgb1*$^{-/-}$ donor into wt recipient. Unfortunately *Hmgb1*$^{-/-}$ mice are not viable and die short after birth because of severe hypoglycaemia. Even when injected with glucose they die few days after. Long-living pups die at three weeks of age and are smaller than their wt counterparts. Moreover they are deaf, blind, display marked kyphosis, bone and muscle atrophy (115). Thus they are not available nor for *in vivo* study nor to be used as bone marrow source for transplantation. We have decided to move to another source of haematopoietic precursors, the foetal liver. Foetal liver is the haematopoietic organ in late intrauterine life. We decided to use foetal liver at gestational day E14.5, reported as the peak of the liver haematopoiesis (116). In section

2.3 of the RESULTS I will present the set up work to define the best condition to transplant foetal liver into adult, lethally irradiated recipient. The set-up work has been carried out on wt CD45.2^{+} foetal liver that have been transplanted into adult CD45.1^{+} recipient. In section 2.4 I will report the results I have obtained about muscle repair in mice transplanted with Hmgb1 deficient and proficient foetal livers. Hmgb1$^{-/-}$ foetal liver have been obtained by crossing male *Hmgb1*$^{+/-}$ X female *Hmgb1*$^{+/-}$. Thanks to this original model the relative role of leukocyte HMGB1 can be addressed *in vivo* in a sterile tissue repair model.

In the next section I am going to present several acute damage models described in literature, with some advantages and drawbacks, to explane why we have chosen the cardiotoxin-induced muscle damage model.

5.4 The choice of an appropriate acute damage model

Four main methods to induce acute muscle injury on mice are reported in literature:

i) Exercise/contraction injury

ii) Glycerol intramuscular injection

iii) Ischemia-reperfusion injury

iv) Toxin(s) intramuscular injection

Each method has got its own peculiar characteristics. Herein I am going to briefly review and compare these methods to show why in the present study I have chosen the injection of cardiotoxin in the skeletal muscles of mice.

i) Exercise training consists of high-repetition, aerobic-type activity: swimming, treadmill running, and voluntary-wheel running. Exercise intensity ranges from submaximal exercise to maximal exhaustive exercise. The exercise protocols ranges from 1 wk to several months and the duration and type of the exercise-training protocols is from 2 to 60 min of swimming each day or 15 min to several hours of treadmill

running per day. Many of the studies allow the animals to exercise ad libitum on an exercise wheel (117). A large number of studies have shown that eccentric exercise causes injury in normal humans and animals (118, 119). Several studies have been performed to help elucidate the mechanisms and subsequent adaptation of skeletal muscle to contraction-induced injury. This information, theoretically, would help assess what types of training would be either beneficial or deleterious to muscle. Some authors proposed that microinjuries to the sarcolemma and their subsequent repair may be an important mechanism that regulates muscle atrophy, homeostasis, and hypertrophy. In a model of rat contraction injury even when no disruption of the sarcolemma was detectable by ordinary light microscopy, the presence of albumin within the muscle was an indication of microinjury to the sarcolemma. The microinjury to the sarcolemmal is an early form of exercise-induced injury. This injury could be repaired or, if severe, progress to fibre necrosis (120). In the case of my project this is not the ideal model for several reason:

a. Lots of protocols are available. Each of them is very well characterised at histological but not at immunological levels. Few reports are available on the role of specific immune cell population. Since I have to dissect the role of tissue and leukocyte Hmgb1, this is a big limitation
b. All protocols described in literature are stressful for the animal, that before being submitted to exercise would have already undergone foetal liver transplantation after lethal irradiation
c. Repair kinetics are very variable among protocols described

ii) Glycerol injection is not as stressful as the exercise injury. The damage is obtained by direct administration of glycerol with a simple intramuscular injection. The damage is sterile and the repair is quick, since a structure similar to untreated muscle is restored in 28 days. However inflammatory cells are virtually absent in this model, as shown in Figure 26.

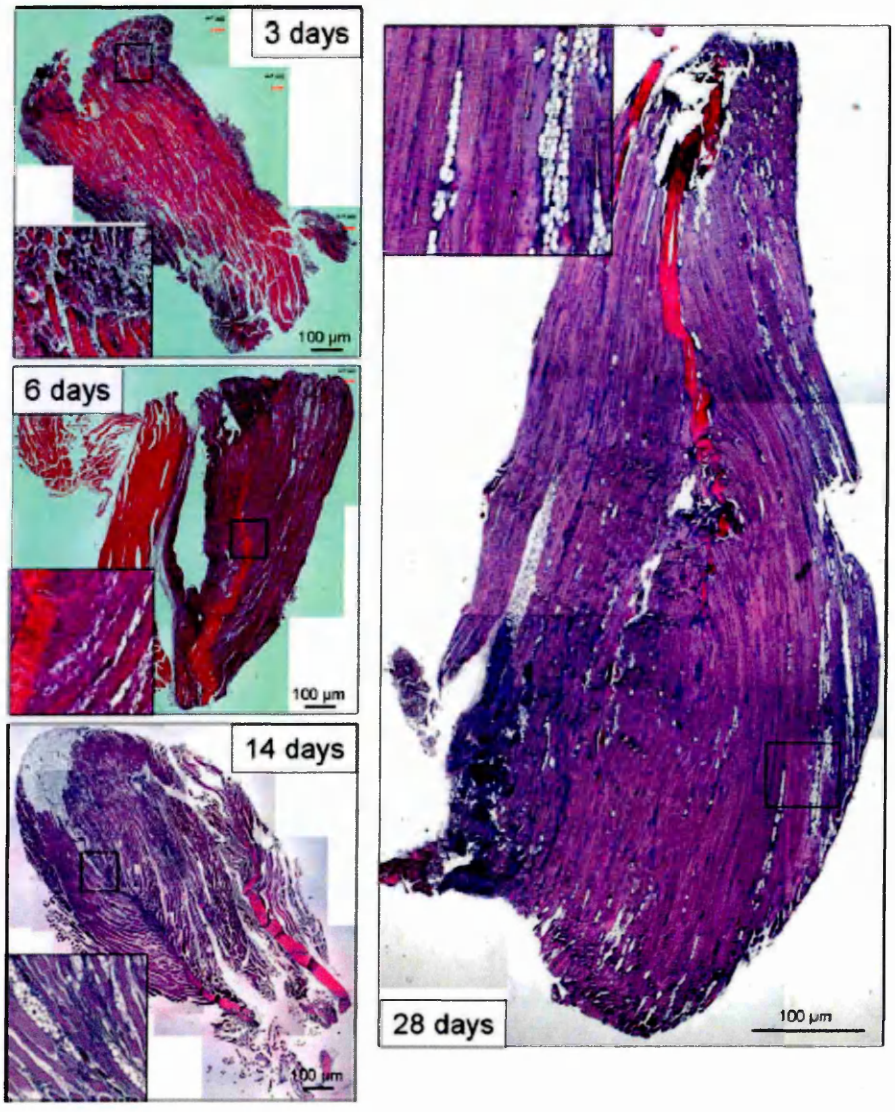

Figure 26 - Kinetic analysis of glycerol induced muscle regeneration. Histological modifications in skeletal muscle were analyzed by hematoxylin-eosin-safranin staining after intra-muscular injection of 25 µL of glycerol 50% (HBSS, v/v) in the TA of 3 month-old B6D2 female. Muscles were sampled at indicated times and paraffin-embedded before analysis. Scale bar = 100 µm (121).

This model is used to study the pathophysiology of fat deposition in muscle. The quantity of fat deposition varies depending on the age, sex and strain of the mouse (121). Since we need to dissect the relative contribution of muscle and leukocyte Hmgb1 this model cannot be used. The absence of inflammation is a non-physiological event since normally skeletal muscle damage is accompanied by leukocyte infiltration (122). In the ideal model to solve my biological issue there should be the *restitutio ad*

integrum of the skeletal muscle. The presence of extensive fat deposition mirrors an aberrant repair process.

iii) Muscle damage due to ischemia-reperfusion is characterized by oedema, infiltration of inflammatory cells, and disruption of normal muscle cell architecture (123). Theoretically it would be the ideal model to address my issue. However skeletal muscle fibers are known to survive up to 4 hr of ischemia (124), so cellular injury is likely to be initiated only after a prolonged period of ischemia. This is the major limitation of this model: to induce ischemia a long surgical procedure in general anesthesia is required. Furthermore, in studies in rodents a patchy pattern is observed with normal and necrotic muscle fibers (123).

iv) Toxins used to induce skeletal muscle damage, such as cardiotoxin or notexin, are small peptides of low molecular weight. Upon i.m. injection into mice, the toxin induces early morphological alterations in the periphery of muscle fibers, indicating that the plasma membrane is the first cellular structure to be affected. Afterwards, necrotic cells have a clumped appearance, which then changes to a more hyaline histological pattern. Removal of necrotic material by phagocytes around day 3 after injection is followed by skeletal muscle regeneration, with the presence of myoblasts, myotubes and fully regenerated myofibers. The *resitutio ad integrum* of the tissue is achieved by day30 from toxin injection. The toxin induces a rapid and drastic drop in muscle creatine and creatine kinase contents, as well as an increase in serum levels of the enzymes lactic dehydrogenase and creatine kinase. Moreover, total muscle calcium increased significantly after toxin administration. The injection of toxins is non invasive, it is followed by a detectable and well characterized inflammatory reaction and the muscle is able to restore the original architecture in one month from the injection (2, 42, 125, 126). The major drawback of this model is that the hit is non physiological, as it would be in the case of exercise injury. Despite this I have induced acute damage by injection of a toxin, since it ensures me a quick, well characterized

repair of an inflammatory, sterile damage. I have injected a mix of long and short cardiotoxins from Sigma-Aldrich derived from the venom of the snake *Naja mossambica mossambica.* A brief description of the histological and immunological characteristics of the model is reported in the first section of RESULTS as well as a description of Hmgb1 expression in this model.

MATERIALS AND METHODS

1. Muscle damage induction and repair evaluation

All procedures involving animals are performed accordingly to the Institutional Animal Care and Use Committee (IACUC). Wild-type C57BL/6 female mice 8 weeks old (from Charles River Laboratories, Calco, Italy) were injected intramuscularly (i.m.) with cardiotoxin (CTX, 100 μl, 10 μM within the quadriceps and 50 μL, 10 μM within the tibialis anterior [TA]) (*Naja mossambica mossambica*; Sigma-Aldrich, Germany). Mice were sacrificed at 1, 3, 7, 10, and 15 days after injury. Injured muscles were collected and frozen. Immunohistochemical and Immunofluorescence analysis have been performed as described later. Muscle damage, remodelling, and repair were evaluated by hematoxylin and eosin (H&E) on 6-μm-thick muscle sections.

2. BoxA treatment

At day0 CTX (50 μL, 10 μM, Sigma-Aldrich, Germany) and BoxA (diluted in CTX solution, 10 μg/TA, HMGBiotech, Milan, Italy) are co-injected into TA muscle. The treatment with BoxA is repeated i.m. every other day for the first week after damage. Then mice are treated i.m. at day9, 12, 14 and 24. Control mice (sham group) received the vehicle alone (saline solution) according to schedule. Mice are followed by MRI before treatment and at day 1, 3, 5, 6, 10, 14, 30. MRI procedure is described in the following paragraph. 6 or 7 mice are sacrificed at day7, 15, and 30. Three mice/group are sacrificed at day 1 and 3 for muscle weight analysis. Muscle are retrieved and weighted immediately after isolation.

3. Magnetic Resonance Imaging (MRI)

3.1 MRI acquisition

MRI acquisition were performed using a 7T horizontal 30 cm bore, 300.3 MHz unit (Bruker, BioSpec 70/30 USR, Paravision 5.0, Germany), with a maximun 675 mT/m

gradient, a maximum rise time of 140 μs and with a linear MRI transmitter coil (inner diameter of 72 mm) and 1H rat heart receive-only coil array with four internal preamplifiers. The laser cross-hair positioning of mice was reproducible and operator independent. A Multi-Slice Multi Echo (MSME) T_2 map with fat suppression was used (TR=1938 ms; TE=10,73/171,68; FOV=20x20; matrix=256x256 mm; spatial resolution=0,078x0,078 mm/pixel; NSA=4). The acquisition of the Diffusion Tensor Image (DTI) in 30 directions was performed using the following parameters: TR= 3750 ms; TE= 33 ms; FOV=30x30; matrix=128x128; NSA= 1; diffusion gradient duration=4ms; diffusion gradient separation=20ms and *b* value of 0 sec/mm^2 or 700 sec/mm^2. The EPI-Diffusion Map was acquired with TR=3000 ms, TE=30 ms, 6 *b* value directions, diffusion gradient duration=7 ms, diffusion gradient separation=14 ms, NSA=2. The DTI and EPI-Diffusion Map sequences shared the same matrix size (128x128 mm) and the same spatial resolution (0,234 x 0,234 mm/pixel). All sequences were acquired with a slice thickness of 1mm and a gap of 1mm.

3.2 Data processing

For each mouse at each time point five subsequent slices have been considered. For each slice two regions of interest (ROI), one on the TA (damaged muscle) and one on the G (control muscle) were evaluated by two independent operators. For each mouse four serial sections of seven μm thickness with 30 μm interslice distance were collected and stained as described above. A semiquantitative (0 to 5) score for infiltrate evaluation was established and an expert pathologist evaluated blinded all sections. 0 is considered as not infiltrated muscle. 5 is the most infiltrate muscle. Muscle with intermediate infiltration levels are evaluated accordingly. The score was subsequently correlated with T_2-rt. In the same sections a second blinded independent observer have counted the central-nucleated fibres. The average for each mouse was then correlated to fractional anisotropy (F.A.) from DTI sequence.

4. Foetal liver transplantation and chimerism assessment

Hmgb1 heterozygous mice colony is propagated in the SPF Facility of San Raffaele Institute. An Hmgb1 heterozygous female and male are crossed. Foetuses at day E14.5 post coitum and livers are retrieved and smashed mechanically. After filtration on a 40 μm cell strainer (BD Falcon, USA), single cell suspension from one foetal liver is resuspended in 200 μL of sterile saline solution and 100 μL/mouse are injected. Recipient mice are lethally irradiated (900nrad) the day before with an X-ray source (Gilardoni, Italy). Mice are kept in SPF condition all throughout the experiment. After 6 weeks chimerism on peripheral blood (PB) is verified on PB from the tail vein. 100 μL PB/mouse are collected in 20 μL Heparin (Hospira, Illinois, USA; 5000 UI/mL). 30 μL/FACS tube are dispensed. After addition of 50 μL blocking buffer (PBS+10% FBS, Lonza, Italy) and incubation at RT for 15 minutes, primary antibody is added: anti-mouse CD45.1 PE (BD Bioscience, clone A20), anti-mouse CD45.2 FITC (BD Bioscience, clone 104), anti-mouse CD11b APC (BioLegend, San Diego, CA, USA, clone M1/70). Anti-CD45.1, CD45.2 and anti-CD11b have been added at a final concentration of 2 μg/mL and 5 μg/mL respectively. After washing red blood cells are lysed using lysis buffer (BD Bioscience). Cells are fixed in PFA 4% (Sigma-Aldrich) and stored at 4 °C until acquisition. BM cells have been flushed and cells are processed and labeled as above. Spleen and inguinal lymph nodes were incubated twice (30' each at 37 °C) with collagenase A, B, D mix (Roche). The retrieved suspension is filtered. Single cells have been labeled and processed as above. Flow cytometry has been carried out with FACS-Canto flow cytometer and the Flow Jo Software v. 8.6.1 (Tree Star Inc., Ashland, OR, USA).

5. Flow cytometry on total muscle

Muscles are dissociated by enzymatic digestion with collagenase type V (Sigma-Aldrich) (0.5 mg/ml) and dispase (Invitrogen, Life Technologies Europe, Paisley, UK) (3.5 mg/ml) at 37 °C for 40 min. Retrieved cells are labelled as above. Primary antibody is added and incubation is left 20' at +4 °C. The following antibodies are used: anti-mouse CD45.1 PE (BD Bioscience, clone A20), anti-mouse CD45.2 FITC (BD Bioscience, clone 104), anti-mouse, CD45 V450 (BD Bioscience, clone 30-F11), anti-mouse Ly6G FITC (BioLegend, clone 1A8), anti-mouse CD11b APC (BioLegend, clone M1/70), anti-mouse F4/80 PE (BioLegend, clone BM8), anti-mouse CD3 APC (BD Bioscience, clone 145-2c11), anti-mouse NK1.1 PerCP (BD Bioscience, clone PK136), anti-mouse CD19 PE (BD Bioscience, clone 1D3), anti-mouse CD86 PE (BD Bioscience, clone GL1). Final concentration for anti-CD45.1, CD45.2, CD45 and Ly6G is 2 μg/mL. Final concentration for all other antibodies is 5 μg/mL. To reveal purified anti-mouse CD163 (Santa-Cruz Biotechnology, Santa Cruz, CA, USA, rabbit polyclonal) we have used anti-rabbit FITC secondary antibody BD Bioscience, goat polyclonal). After labelling cells are fixed in PFA 1%, washed and analyzed by flow cytometry using FACS-Canto flow cytometer and the Flow Jo Software v. 8.6.1 (Tree Star Inc.).

6. mRNA analysis

Muscle total cellular RNA is extracted using TRIZOL (Invitrogen), following the manufacturer's recommendations. RNA (1 μg) is used for quantitative polymerase chain reaction (PCR) analysis for first-strand synthesis of complementary DNA with the high capacity complementary DNA Reverse Transcription kit (Applied Biosystems) according to the manufacturer's instructions.

Quantitative PCR is performed using SYBRgreen PCR Master Mix (Applied Biosystems, Life Technologies Europe). Results are quantified using ABI7900 machine (Applied Biosystems). The level of RNA is normalized to the corresponding level of GAPDH messenger RNA (mRNA) for muscle lysates or total cells lysates. Sequences

of primers (Primm, Milan, Italy) used in quantitative real-time PCR are as follows (5' to 3' sequence): hif1α (Fw: TCA AGT CAG CAA CGT GGA AG; Rv: TAT CGA GGC TGT GTC GAC); vegfβ (Fw: CCT GGA AGA ACA CAG CCA AT; Rv: GGA GTG GGA TGG ATG ATG TC); ang2 (Fw: CAC AGC GAG CAG CTA CAG TC; Rv: ATA GCA ACC GAG CTC TTG GA); glut1 (Fw: GCT GTG CTT ATG GGC TTC TC; Rv: AGA GGC CAC AAG TCT GCA TT); CAIX (Fw: GGA GTC CCT TGG GTT AGA GG; Rv: GAT GTC TAC CGG GGA CTG AA); myoD (Fw: ACG GCT CTC TCT GCT CCT TT; Rv: GTA GGG AAG TGT GCG TGC T); pax7 (Fw: GAC TCG GCT TCC TCC ATC TC; Rv: AGT AGG CTT GTC CCG TTT CC); myogenin (Fw: GAC ATC CCC CTA TTT CTA CCA; Rv: GTC CCC AGT CCC TTT TCT TC); igf1 (Fw: GTG TGG ACC GAG GGG CTT TTA CTT C; Rv: GCT TCA GTG GGG CAC AGT ACA TCT C); tnfα (Fw: TCC CAG GTT CTC TTC AAG GGA; Rv: GGT GAG GAG CAC GTA GTC GG); il6 (Fw: CTC TGC AAG AGA CTT CCA TCC AGT; Rv: CGT GGT TGT CAC CAG CAT CA); il10 (Fw: ATT TGA ATT CCC TGG GTG AGA AG; Rv: CAC AGG GGA GAA ATC GAT GAC A); gapdh (Fw: TCC ACT CAT GGC AAATTC AA; Rv: TTT GAT GTT AGT GGG GTC TCG).

7. Western blot analysis on $CD45^+$ cells and total muscle lysates

Cells are retrieved from damaged muscles at days 1, 3, 5, 7, 10 and 15 after injection of CTX. Muscles are dissociated by enzymatic digestion as above. Cells expressing the CD45 marker are purified using magnetic beads (Milteny Biotec, GmbH). The purity is verified by flow cytometry after incubation with FITC-labelled anti-CD45.2 mAb (final concentration 5 μg/ml; BD Pharmingen, clone 104). $CD45^+$ infiltrating cells and whole muscle are lysed in Tris 10mM pH 8.0, NaCl 150mM, Nonidet P40 1%, sodium dodecyl sulphate 0.1%, EDTA 1mM, in the presence of protease inhibitors cocktail [containing 4-(2-aminoethyl) benzenesulfonyl fluoride (AEBSF), pepstatinA, E-64, bestatin, leupeptin, and aprotinin; Sigma-Aldrich]. Lysates are centrifuged at 16,000g for 5 min at 4 °C. For Western blot analysis, equal amounts

of protein (20 μg) are resolved by sodium dodecyl sulphate polyacrylamide gel electrophoresis and transferred onto Immobilon-P (Millipore). After Ponceau S (Sigma-Aldrich) staining to verify correct transfer, membranes are saturated in Tris-HCl 20mM, pH7.6, NaCl 150mM (Tris-buffered saline [TBST]), containing non-fat milk 5% and Tween 20 0.1%. Mouse Hmgb1 is revealed using mouse monoclonal anti-Hmgb1 (final concentration 0.1 μg/ml, kindly provided by Dia.Pro. Diagnostic Bioprobes, Milan, Italy). To normalize results membranes are blotted using mouse monoclonal anti-βactin (final concentration 0.1 μg/ml; Sigma-Aldrich, clone AC15), or mouse monoclonal anti-GAPDH (final concentration 0.1 μg/ml; Sigma-Aldrich, clone GAPDH-71.1) antibodies. All antibodies were diluted in TBST 5% non-fat milk. Incubation was performed overnight at 4 °C for primary antibodies and 1h at room temperature for the second-step reagents. Primary antibodies are revealed with HRP-conjugated secondary antibodies (final concentration 0.2 g/ml; GE Healthcare Europe GmbH) and a chemiluminescence kit (ECL, Western blotting detection reagents; GE Healthcare Europe GmbH).

8. ELISAs

For determination of the concentration of IL10, TNFα and IGF1 we have used DuoSet kit (R&D Systems) following manufacturer's instruction. For determination of Hmgb1 concentration we have used Shino Test Corporation (Tokyo, Japan) ELISA kit following manufacturer's instruction. Data acquisition is performed on a Microplate Reader (Bio-Rad, Hercules CA, USA) and data analysis is performed using Microplate Manager Software (v. 5.2.1, BioRad). Data are expressed in pg/mL.

9. Immunohistochemistry

Frozen sections (7 μm thick) are fixed in paraformaldehyde (PFA) 4% (Sigma-Aldrich) for 10' and washed twice in PBS. Endogenous peroxidase has been quenched using 0.1% H_2O_2 in methanol for 10' at RT. After washing Avidin/Biotin blocking kit (Vector Laboratories) is used following manufacturer's instruction. Sections are washed twice with PBS and blocked for 1h at RT in PBS + 5% BSA + 5% goat serum. Primary antibodies are incubated overnight at 4 °C. To assess CD68 expression we used rat anti-mouse CD68 (AbD Serotec) diluted 1:100 in blocking buffer. For CD31 we used rat anti-mouse CD31 (BD Bioscience, clone MEC13.3) diluted 1:100 in blocking buffer. To reveal CD68 and CD31 we used a goat anti-rat biotin-conjugated secondary antibody (eBioscience) diluted 1:300 in blocking buffer. Secondary antibody is incubated 1h at RT and then revealed using streptavidin HRP and chromogen. Streptavidin HRP (1:200 in PBS, Invitrogen) is incubated 20' at RT. Chromogen (NovaRed,Vector Laboratories) is prepared following manufacturer's instruction and developed under an optical microscope (Nikon).

10. Immunofluorescence

10.1 Pax7 and MyoD staining

Frozen sections (10 μm thick), are fixed in PFA 4%, washed and subjected to antigen retrieval by incubation in boiling citric acid pH6 for 10'. Sections are then cooled on ice for 30', left 1h at RT in PBS + 5% BSA (Sigma-Aldrich) + 1% normal goat serum + 5% FBS + 0.1% Triton X100 (Sigma-Aldrich). Primary antibodies are incubated overnight at 4 °C. To detect Pax7 we have used the supernatant of a mouse anti-Pax7 hybridoma (Developmental Studies Hybridoma Bank, University of Iowa, Iowa City, USA) diluted 1:5 in blocking buffer; to detect MyoD we have used a rabbit anti-mouse MyoD polyclonal antibody (Santa Cruz Biotechnology) diluted 1:25 in blocking buffer. For Pax7 an AlexaFluor anti-mouse 488 antibody (Invitrogen) is used diluted 1:500. For MyoD an AlexaFluor anti-rabbit 594 antibody (Invitrogen) is used

diluted 1:500. Nuclei are counterstained using Hoechst 33348 (Invitrogen) diluted in PBS and incubated for 10' at RT. Mounting is performed using H_20 and glycerol. Photographs are taken at 40x magnification on Nikon Eclipse 55i microscope (Nikon, Tokyo, Japan). Pictures were captured with digital sight DS-5M digital camera (Nikon) using LuciaG Software (Laboratory Imaging, Prague, CZ).

10.2 Hmgb1 staining

Frozen section (10 μm thick) are fixed in PFA 4% (Sigma-Aldrich) for 10' and washed twice in PBS. Sections are then left 2h at RT in blocking buffer: PBS + 5% BSA + 5% FBS + 0.1% Triton X100 (Sigma-Aldrich). Expression of Hmgb1 is revealed using a polyclonal rabbit anti-mouse Hmgb1 antibody (Abcam, USA) diluted 1:500 and an AlexaFluor anti-rabbit 594 antibody (Invitrogen) diluted 1:500. Nuclei are counterstained using Hoechst 33348 (Invitrogen). Mounting is performed as above. Photographs are taken at 40x magnification on a Photographs are taken at 40x magnification on Nikon Eclipse 55i microscope (Nikon, Tokyo, Japan). Pictures were captured with digital sight DS-5M digital camera (Nikon) using LuciaG Software (Laboratory Imaging, Prague, CZ).

10.3 Myosin Heavy Chain (MyHC) and CD11b staining on cell culture

After 48 hours of differentiation (see 12.2) differentiated satellite cells are identified assessing the expression of MyHC. Cells are fixed for 15' in PFA 4%, washed in PBS and blocked 1h at RT in blocking buffer: PBS + 5% BSA + 5% FBS + 0,1% Triton X100. We have stained satellite cells with MF20 hybridoma supernatant diluted 1:5 in blocking buffer and macrophages with rat anti-mouse CD11b antibody (clone M1/70, BioLegend) diluted 1:500. Both antibodies are incubated overnight at 4 °C. MyHC is revealed using AlexaFluor anti-mouse 488 antibody, CD11b is revealed using AlexaFluor anti-rat 594 antibody, both diluted 1:500. Nuclei are counterstained

using Hoechst 33348. After washing, pictures are taken at 20x magnification. The InCell Analyzer 1000 (GE Healthcare) instrument has been used for high throughput acquisition (see 12.3).

11. Murine macrophage differentiation and polarization

11.1 Murine macrophage differentiation

BM is flushed from C57BL/6 female mice (6-8 weeks old, Charles River). BM progenitors are extracted as described (127). The cells are challenged with complete medium: α-MEM (GIBCO, Invitrogen) + 10% FBS + 100 ng/mL recombinant murine (rm) M-CSF (Miltenyi Biotec) and differentiated for 5 days in Petri dish for bacteria (BD Falcon), diameter 10 cm, splitted and cultured two more days in the same medium. The resulting macrophage population is referred to as "M0".

11.2 Murine macrophage polarization

M0 macrophages are detached on ice using cold PBS and then resuspended in α-MEM (GIBCO, Invitrogen) + 10% FBS (Lonza). M0 cells are then counted. To obtain pro-inflammatory, M1-like cells, M0 cells are resuspended at a concentration of 500 000 cells/mL in α-MEM (GIBCO, Invitrogen) + 10% FBS + 50 ng/mL rmIFNγ (PeproTech) and cultured for 48h. To generate anti-inflammatory, M2-like cells, M0 are resuspended in α-MEM (GIBCO, Invitrogen) + 10% FBS + 10 ng/mL rmIL10 (R&D Systems) + 10 ng/mL rm M-CSF (Miltenyi Biotec, GmbH) and cultured 96h, with half of the complete medium refreshed after 48h.

12. Satellite cell isolation, expansion and co-colture with murine macrophages

12.1 Satellite cells isolation and expansion

6 weeks old C57BL/6 female mice (Charles River) are sacrificed and TA, quadriceps, gastrocnemius and triceps are retrieved. Muscles are dissociated by enzymatic digestion with collagenase type V (Sigma-Aldrich) (0.5 mg/ml) and dispase

(Invitrogen) (3.5 mg/ml) at 37 °C for 40 min. Digested cells are resuspended in IMDM (Gibco, Invitrogen) + 10% FBS. Cells from each mouse are plated into two separate tissue culture dish (10 cm diameter, BD Falcon) and maintained in incubator at 37 °C, 5% CO_2 for 2h. During pre-plating new tissue culture dishes are coated with collagen (Sigma-Aldrich) for 30' at room temperature. Collagen is then retrieved from dishes. During the pre-plating phase contaminant cell populations (endothelial cells, fibroblasts, etc) adhere. Floating cells are retrieved and plated in Ham F10 medium (Sigma-Aldrich) containing 20% Hyclone (Gibco, Invitrogen). Cells from each mouse are plated into three collagen-coated dishes. Satellite cells are propagated at 37 °C, 5% CO_2 until they reach confluence. Every 3 days half of the complete medium is refreshed.

12.2 Satellite cells differentiation

Proliferating satellite cells are detached using trypsin/EDTA cocktail (Lonza). Cells are then centrifuged (1500 rpm, 5', RT), counted and plated into Matrigel (Sigma-Aldrich) coated multiwell plates. Typically, 100 000 cells/well are plated in 12 wells plate in 1 mL complete medium. Differentiation medium is DMEM (Lonza) + 2% horse serum (HS, Vector Laboratories). Complete differentiation occurs in 48h, at 37 °C, 5% CO_2. Satellite cells differentiation assay is performed also using 500µL of differentiation medium and 500µL of conditioned supernatants from polarized macrophages, either obtained from Hmgb1 wt and Hmgb1 KO FLT mice. As a control satellite cells are differentiated in 500µL differentiation medium + 500µL of α-MEM containing 10%FBS and the recombinant cytokines used for macrophage polarization (see 11.2).

12.3 Satellite cells – Macrophages co-colture

Satellite cells are retrieved from collagen-coated dish using Trypsin/EDTA cocktail. Macrophages are detached using PBS + 5mM EDTA on ice. Cells are

resuspended in α-MEM + 10%FBS. Macrophages and satellite cells are mixed at 1:1 ratio into Matrigel coated 12 wells plate and cultured for 48h at 37 °C, 5% CO_2.

12.4 Differentiation assessment and quantification

Differentiated satellite cells are identified by MyHC expression as described above (see 10.3). For each well 20 to 30 photograph are taken using InCell Analyzer 1000 at 20x magnification. Each condition is tested in double or in triplicate, as indicated in figure legend. Each photograph is manually counted clustering positive cells with one nucleus, positive fibres with 2 to 4 nuclei and positive fibres with more than 5 nuclei. Results are graphed as average ± standard deviation (SD) for each condition and each cluster of fibre size.

13. Statistical analysis

13.1 General

Data are expressed as means ± SD. Statistical analysis was performed using Student's t-test for unpaired data or one-way ANOVA followed by a Dunnett's or Newman-Keuls *post hoc* test when appropriate. Values of $p<0.05$ were considered statistically significant (Graph Pad Prism, v. 4.0 Software, La Jolla, CA, USA).

13.2 MRI statistics

Data are expressed as means ± s.e.m.. Statistical analysis was performed using Student's t-test for unpaired data or one-way ANOVA when appropriate; correlation was evaluated using Pearson test (Prism 4.0, GraphPad Software, Inc.). Values of $P<0.05$ were considered statistically significant

RESULTS - 1

As mentioned in the INTRDUCTION the aim of my PhD project is to dissect the relative role of tissue and leukocyte Hmgb1 in the context of sterile damage and repair. Acute skeletal muscle damage is often associated with excessive exercise or commonly when a person tears a muscle. Acute muscle damage is a sterile condition normally accompanied by inflammation (2, 122). Therefore it is an ideal model to address our scientific question. I have induced acute muscle damage by the injection of cardiotoxin (CTX). In the next section I will briefly describe the histological and immunological characteristics of this model. Moreover I will show the expression of Hmgb1 during muscle repair to verify that the protein is expressed both by muscle myofibres and infiltrating leukocytes.

1. Characteristics of CTX-induced acute damage model

1.1 Kinetic of repair of CTX injected muscle

I have injected cardiotoxin (CTX) directly in *tibialis anterior* (TA) and quadriceps (Q) muscles bilaterally as depicted in figure 1.1 (panel A). I have then stained using hematoxylin and eosin (H&E) sections from TA muscles at distinct time points, as shown in figure 1.1 (panel B). At day1 after CTX injection a massive death of muscle fibers and few infiltrating cells are evidenced. At day3 mononuclear cell infiltration is substantially increased. At day5 infiltrating cells persist and some regenerating, centrally nucleated fibres appear. At day7 and day10 infiltrating cells progressively disappear. The described regeneration is not substantially different depending on mice genetic background and recapitulates in a relative short time the homeostatic response of a tissue to a sterile injury. Thus this represents an ideal model to study the role of Hmgb1 in tissue repair.

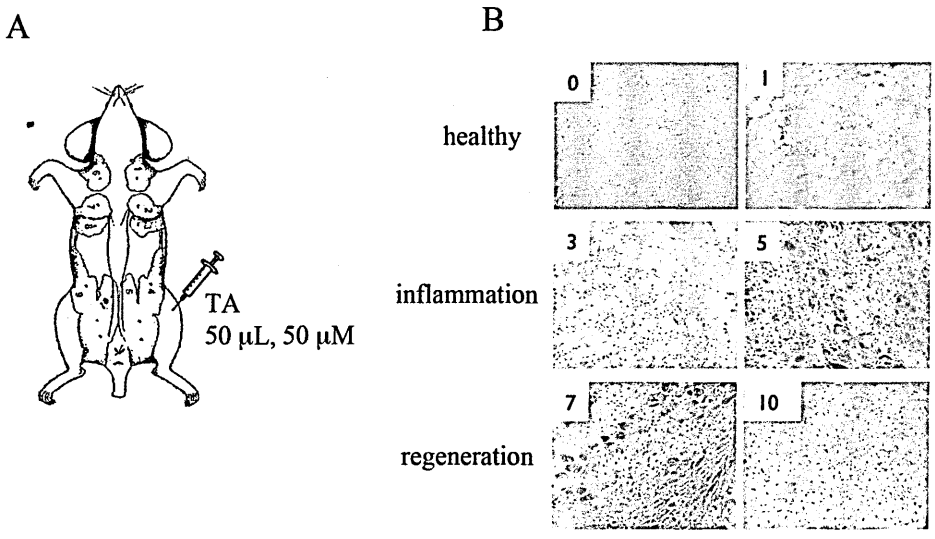

Figure 1.1 – Kinetic of the response of skeletal muscle to a sterile injury **A.** Cardiotoxin (CTX) is injected into *tibialis anterior* (TA) muscle as shown in the cartoon. **B.** Injured TA are retrieved and stained with H&E staining at various times (20x magnification). After CTX injection there is tissue necrosis in appearance (day1); at later time points inflammatory leukocytes infiltrate the muscle. From day5 centrally nucleated, regenerating fibres appear. The full regenerative phase starts at day7; by day10 the inflammatory infiltrate is virtually disappeared. By day30 (not shown) the muscle is completely healed.

1.2 Immunological characterization of CTX injected muscle

To demonstrate that CTX injection does not affect the composition of peripheral blood of injected animals I have analyzed the peripheral blood by cytofluorimetric analysis (Figure 1.2). On the gate of $CD45^+$ cells I have analyzed the expression of CD11b for myeloid cells, F4/80 for monocyte/macrophage lineage, CD3 for T lymphocyte and CD19 for B lymphocyte. The expression of CD11b and F4/80 is virtually unchanged in CTX injected *vs.* healthy mice. There is a slight decrease in the percentage of $CD3^+$ cells from day1 after CTX injection that however is not statistically significant. The percentage of $CD19^+$ cells seems to be increased. However the basal percentage of $CD19^+$ cells is already slightly higher in the CTX injected group. Also in

this case the differences are not statistically significant. Also on a biological point of view a difference of 1-5% in the presence of specific peripheral blood population is encompass in the normal variability that can be found from mouse to mouse.

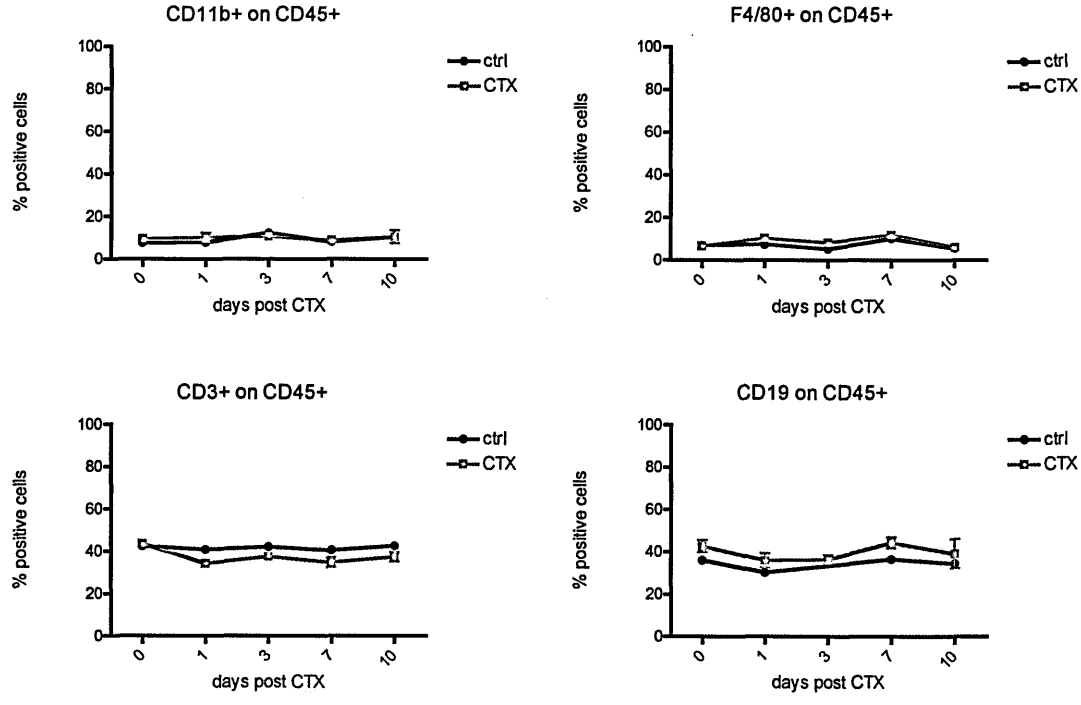

Figure 1.2 – The injection of CTX does not perturb the general composition of peripheral blood. 3 mice/group are injected either with CTX or vehicle. Tail vein bleeding is performed at the indicated time points and peripheral blood is analyzed by cytofluorimetric analysis. The graphs show the average of the percentage of the indicated marker on the total $CD45^+$ population ± SD. t-test for unpaired data is applied at each time point.

Michela Vezzoli in the lab has shown that CD45+ cells, so *bona fide* leukocytes, peak at day3 after CTX injection. The same kinetic has been described for macrophages, that thus are the predominant infiltrating population at early time points after CTX injection (75). Macrophages in CTX injected muscle display the typical scavenger phenotype of tissue-repairing macrophages. They express CD163 since day3 after damage but its expression is lost at later time points (day7 and 10). The expression of CD206 is instead stable and it persists all throughout the damage and repair process

(42). Finally Lidia Bosurgi in the lab has confirmed the crucial role of macrophages in muscle repair after CTX injection (128), as already reported in a model of notexin injection (2).

The next step has been to verify whether and how Hmgb1 is expressed.

1.3 Hmgb1 expression during damage and repair after CTX injection

Immunofluorescence (IF) reveals Hmgb1 expression (red) in TA sections before injury and at later times (day3 and day7). Nuclei are counterstained with Hoechst (blue). Hmgb1 is normally expressed in some but not all nuclei (Figure 1.2, panel A, left picture). As expected Hmgb1 expression in quiescent myofibres is mostly restricted in the subsarcoplasmatic muscle domain, where nuclei are located. A western blot analysis confirms that Hmgb1 is present in healthy muscle, albeit at low levels (Figure 1.2, panel B, lane "0"). Hmgb1 is released upon active tissue injury: at day1 after CTX injection there is a ten-fold increase in the serum concentration of Hmgb1, as reported in Figure 1.2 (panel D). Hmgb1 levels abate at later times, when dead fibres disappear and regeneration takes over (day3 and day5). IF for HMGB1 at day3 and day7 indicates that mononuclear infiltrating cells also express Hmgb1 (Fig. 1, panel A). The result is confirmed by western blot for Hmgb1 on CD45+ leukocytes retrieved from damaged/regenerating muscles at distinct time points. Infiltrating leukocytes consistently express the protein at any time point analyzed.

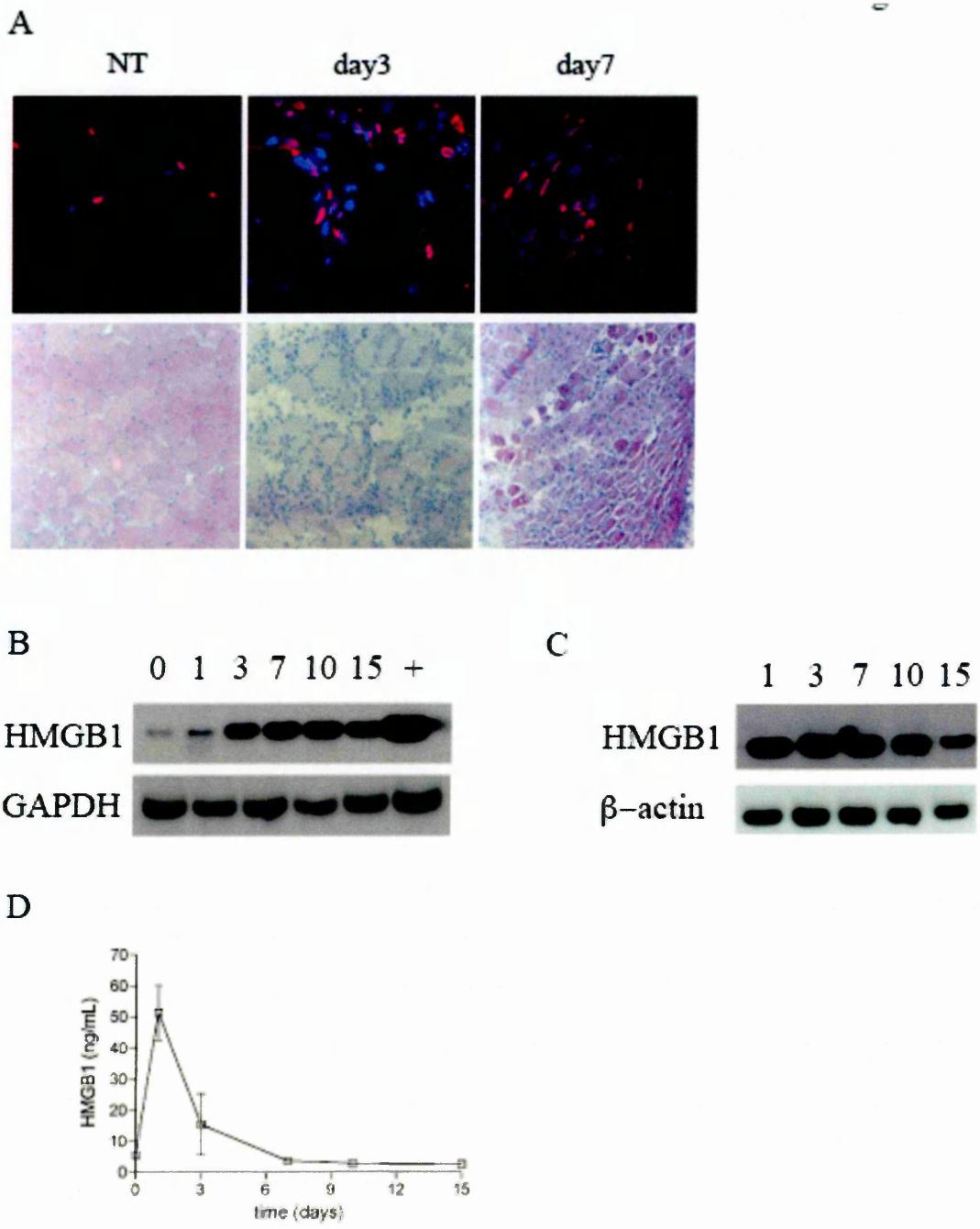

Figure 1.3 – Local and systemic Hmgb1 expression in injured and regenerating muscles. **A.** Immunofluorescence for Hmgb1 before damage and at day3 and day7 after tissue damage (top panels, red colour). Nuclei are counterstained with Hoechst 33348. Pictures shown are at 40x magnification. H&E staining of tissue at the same time points are shown in the bottom panels. Hmgb1 expression is restricted to subsarcoplasmatic domain in healthy muscle (NT). It is also expressed by infiltrate (day3) and by central nuclei of regenerating fibres (day7) **B.** Western blot for mouse Hmgb1 on total muscle lysates. Hmgb1 is present in healthy muscle. Hmgb1 increases after acute damage and remains high till day15. GAPDH is used as housekeeping protein. **C.** Western blot for mouse Hmgb1 on $CD45^{+}$ leukocytes retrieved at distinct time points from damaged muscle by magnetic beads sorting. Infiltrating cells express Hmgb1 at any time point analyzed. Identical quantity of total protein is loaded on each lane **D.** Hmgb1 is

measured by ELISA on sera collected from damaged mice at distinct time point after CTX injection. At day1 there is the peak of circulating Hmgb1, together with the peak of muscle fibres death.

2. MRI as a tool to study acute muscle damage

An obvious limitation of the experiments described so far is the impossibility to non-invasively follow muscle response to injury in single mouse. To overcome this problem, I have focused on the establishment of a magnetic resonance imaging (MRI) approach to longitudinally obtain information on the muscle characteristics without the need of sacrificing animals at each time point.

2.1 Introduction to MRI

A non-invasive tool for quantitative and dynamic assessment of the skeletal muscle modifications during acute damage and regeneration would find several important preclinical and clinical applications.

Magnetic Resonance Diffusion Tensor Imaging (DTI) enables to describe the skeletal muscle architecture investigating the differential diffusion of water in different directions of space (129). Due to fibrillar structure of normal skeletal muscles, the diffusion of water is greater along fibres orientation than in other directions of space. The diffusion of water on a specific direction is a physical property called anisotropy. The anisotropic diffusion, characterizing the intact skeletal muscles, is easily quantified by DTI, measuring the fractional anisotropy (FA) (130). In case of injuries affecting the myofibres integrity, the anisotropic property of skeletal muscles is perturbed because of loosing of a preferential direction of diffusion. Heemskerk et al demonstrated the decrease of FA after an ischemic injury. They studied C57BL/6 mice before femoral artery ligation and at distinct time points after surgery. They performed a comparison between the modification of MR parameters and the qualitative visual assessment of histological changes. The FA dropped after the ischemic injury and progressively increased during the muscle regeneration (131), suggesting that FA could be an

interesting parameter to monitor muscle damage and regeneration. The main limitation of this study is that the authors compared histology and magnetic resonance results only in a qualitative and not in a quantitative way. Moreover the FA values are mathematically derived from MRI sequence and not directly investigated, as I will show later in our study.

A commonly accepted MRI sign of muscle damage is an increased signal in T2-weighted images linked to T2 relaxation time (T2rt) lengthening. The increase in the T2rt values mirrors several phenomena, such as muscle oedema, inflammation and necrosis (132-134). T2rt could help to obtain valuable information in the follow-up of cardiotoxin-induced muscle injury mouse model. However only a very preliminary study without any direct histological comparison is currently available in literature. On ischemic muscular injury, the modification of T2rt occurring during muscle after damage have been assessed. T2rt was increases at day 3 after femoral artery ligation and is followed by a progressive normalization; however, any direct correlation is performed between the T2rt changes and the histological modifications.

Multiparametric MRI could therefore represent a very promising tool for quantitative monitoring the structural changes occurring after a muscle injury, however further data about the comparison between the MRI parameters and the histological changes in preclinical model of muscle damage were required when I started my PhD project. The following experiments are aimed at prospectively evaluating a multiparametric MRI protocol as a non-invasive and quantitative tool to assess muscle injury and to monitor muscle healing process, obtaining dynamic information about inflammatory infiltrate and fibres regeneration.

2.2 Analysis of TA muscle by MRI

In figure 2.1, panel A a sagittal (sag), coronal (cor) and axial sections of mouse hind limb is shown. All images are T1 weighted. All analysis are performed on ten slices with 1mm interslice distance (open red rectangles). The reference section

analyzed is axial (dotted red line). By such an approach we simultaneously sample the whole muscle length, from the knee to the footpad. For each sequence, graphs show the average ± standard deviation of 5 slices. Values are calculated on specific regions of interest (ROI). One ROI is placed on the TA muscle that will undergo damage. The control ROI is placed on the gastrocnemius (G), at the opposite side of the leg.

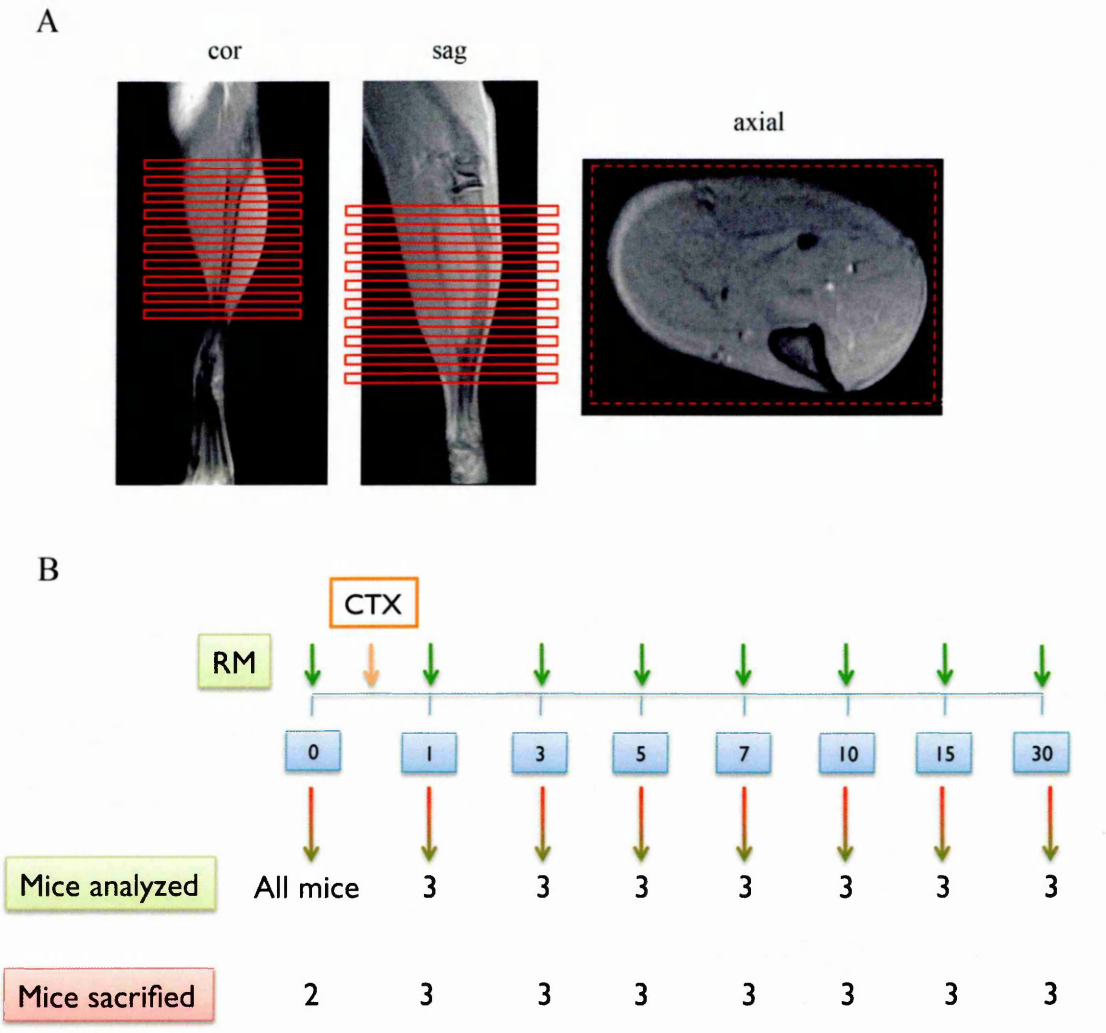

Figure 2.1 – Establishment of an MRI imaging approach to the study of muscle damage and repair *in vivo*. **A.** A coronal (cor), sagittal (sag) and axial section of a healthy muscle leg. Red boxes highlight the area analyzed. Images shown here are from an anatomical T1 sequence to study the best positioning for the mouse into the instrument. **B.** Experimental design to validate MRI as a valuable tool to follow muscle healing *in vivo*. Green arrows indicate the time points at which MRI is performed. Orange arrow indicates the time of CTX injection. Coloured arrows indicate the time points at which mice are analyzed and sacrificed.

To validate quantitatively and qualitatively MRI as a tool to describe muscle injury and healing we have designed an *ad hoc* experiment in collaboration with the Radiology department (Figure 2.1, panel B). Sequences used are T2 map, diffusion tensor imaging (DTI) and diffusion map. In following subchapter each sequence is described and analyzed. The whole cohort of mice has been investigated before any injury (0) and 2 mice are sacrificed immediately to compare histology with MRI images. Mice are then injected with CTX and followed by 7T MRI at day1, 3, 5, 7, 10, 15 and 30 after muscle damage. At each time point 3 animals are sacrificed, TA isolated and frozen for subsequent histological analysis.

2.3 MRI as a tool to assess muscle oedema and inflammation

Oedema is visualized on T2 weighted MRI images as hyper intense (white) areas. T2 relaxation time (T2rt) value is related to the extent of the oedema: the higher the T2rt, the more extended the oedema. Oedema is expected to appear after tissue damage in the TA muscle (red line on graphs), but not in control muscle (G, green line on graphs) and is related to the inflammatory status of the tissue. The simultaneous assessment of TA muscle histology (Figure 1.4, panel A, top line) and T2 weighted images (Figure 2.2, panel A, middle line) reveals a good association between high T2rt values and qualitative or semiquantitative results in H&E stained tissues (Figure 2.2 and nor shown). In the bottom line the T2rt profiles of one representative mouse per time point are shown. In figure 2.2 panel B I report the dynamic changes of T2rt at distinct time points after tissue damage. As expected the T2rt peaks between day3 and 5, at the top of the inflammatory response. Control muscle (G) is virtually unaffected by oedema in TA muscle.

In collaboration with Antonella Monno in the lab I have set up a score to evaluate the entity of infiltration in H&E sections. 0 corresponds to the absence of infiltration, while 5 correspond to the most infiltrated section. For each mouse 4 serial

sections are evaluated and each dot in the graph represents the average of 3 mice per time point. The histological score and the number of CD45+ cells (*bona fide* leukocytes) extracted from damaged muscles at each time point (Figure 1.4, panel C and D) have been significantly correlated with the T2rt, suggesting that this parameters reflects the overall extent of oedema and inflammation in the injured and regenerating tissue.

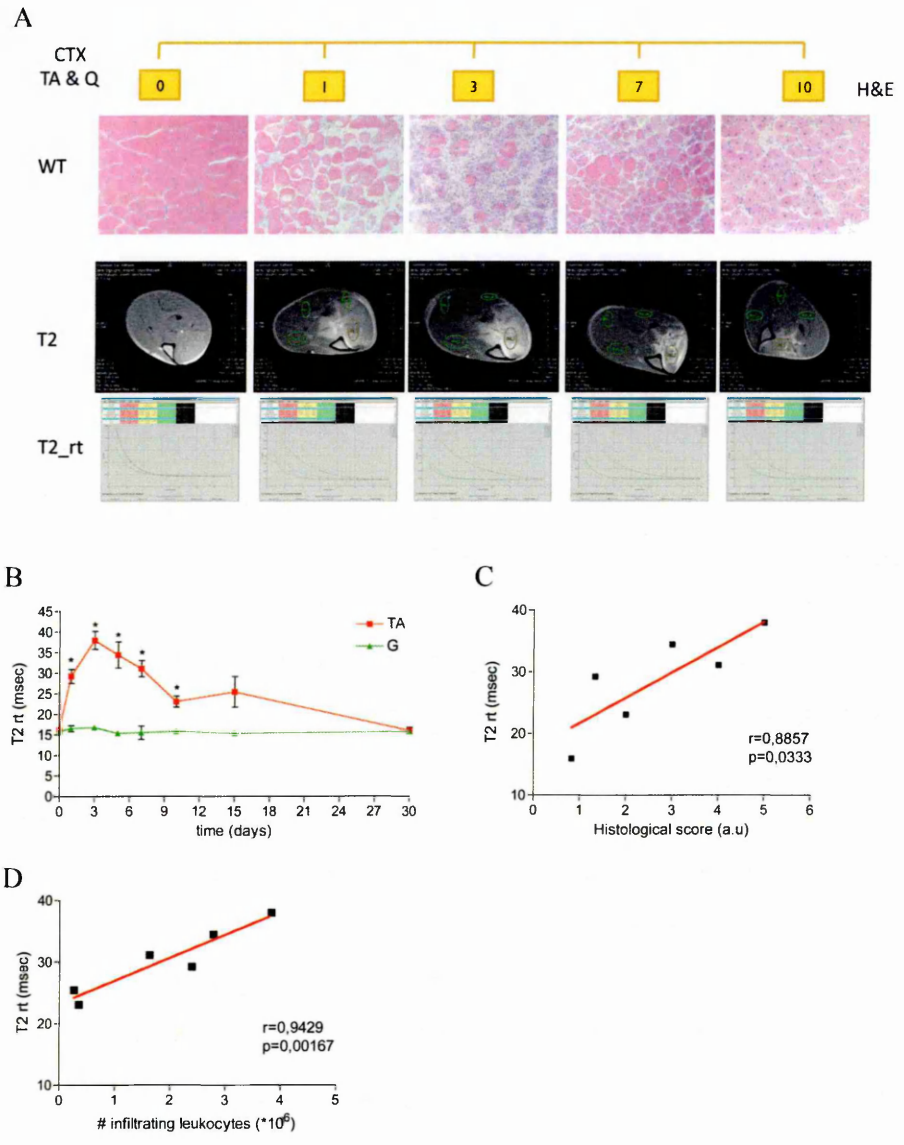

Figure 2.2 - T2 map sequence can be used to follow muscle oedema. **A.** Qualitative comparison between MRI images (intermediate line) and histological sections (H&E, 20x magnification, top line) at distinct time points. In bottom line relaxation time plots are reported **B.** T2rt analysis is performed on TA (damaged, red line) and gastrocnemius (G, control, green line). T2rt values are reported. 3 animals are analyzed for each time point. Average ± SD is reported. Each time point is compared with basal values for statistical analysis. One-way ANOVA is applied. * $p<0.05$ **C.** T2rt mean values at each time point are

correlated with histological score, expressed as arbitrary units (a.u.). **D.** T2rt was correlated with the number of muscle infiltrating leukocytes, retrieved by immunomagnetic sorting. For both **C** and **D** correlation was evaluated using Person test. $p<0.05$ was considered as statistically significant.

2.4 MRI is a valuable tool to study tissue architecture during muscle damage

Muscle in physiological conditions is a bundle of fibres oriented in the same direction. Water inside fibres is oriented in the same direction. Mechanical constrains thus restrict the kinetics of water molecules: accordingly, in an axial section of a mouse leg, the preferential direction of water is orthogonal. This pattern of movement is visualized by the blue colour in the images (Figure 2.3, panel A, time 0). When fibres are disrupted water randomly diffuses into the muscle. The black colour reflects the lack of preferential direction in the movement of water molecules (Figure 2.3, panel A, 1 and 3 days after CTX injection). The reconstitution of the fibres corresponds to a predominant blue pattern in the DTI analysis. Variations in the Fractional Anisotropy (F.A., y axis, Figure 1.6, panel B and C) reflect these events. TA has in normal condition a F.A. = 0,3. After injury the F.A. value drops (day1, F.A.=0,09). Values rise when regeneration starts (day5) and return to normal levels by day30. The control muscle (G) is in contrast virtually unaffected. We have counted the number of fibres in a given section and the number of regenerating fibres, identified based on the nuclear position (i.e. central in regenerating fibres, peripheral in resting fibres). F.A. values at day 3 (2 mice), day 5 (3 mice), day7 (3 mice) have been correlated with the number of centrally nucleated fibres/FOV as a surrogate marker of the extent of muscle regeneration (Figure 2.3, panel C).

Diffusion constant parameter represents a further qualitative parameter to assess tissue regeneration. It estimates the speed of water and is expressed in mm^2/sec. The lower the diffusion constant, the higher is the cellular density of a tissue. Figure 2.3 panel D illustrates the dynamic changes of diffusion constant during muscle damage and healing process. The speed of water increases after injury reflecting the loss of

cellular density. The diffusion constant drops and returns to basal levels by day30, reflecting effective tissue healing.

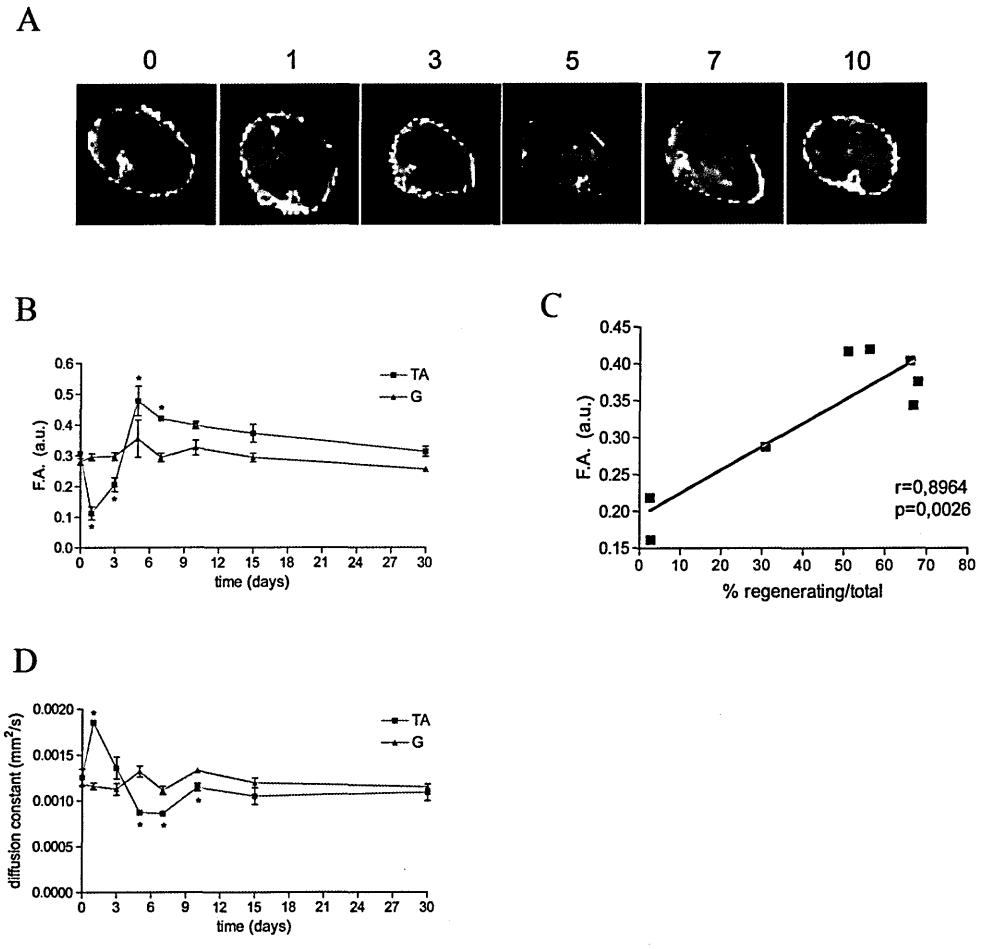

Figure 2.3 – Fractional anisotropy and diffusion constant can be used to quantitatively assess and prospectically follow variations of the muscle architecture. **A.** Qualitative analysis of axial section with diffusion tensor imaging. Blue colour represents an orthogonal direction of water molecules. **B.** Quantitative analysis for water direction in damaged and repairing TA. On the x axis time is reported. On the y axis the fractional anisotropy (F.A.) values are indicated. For each time point we report the average ± SD of three mice for F.A. For each mouse 5 slices are analyzed both on TA (red line) and G (green line) muscle. Each time point is compared with basal values for statistical analysis. One-way ANOVA is applied. * $p<0.05$ **C.** For each mouse the percentage of regenerating fibres is calculated and then correlated with the F.A. values at distinct time points (day3, day5, day7). Each dot represents a mouse. Correlation was evaluated using Person test. $P<0.05$ was considered as statistically significant **D.** On x axis there is time while on y axis is the value of diffusion constant. For each time point we report the average ± SD of three mice for diffusion constant. For each mouse 5 slices are analyzed both on TA (red line) and G (green line) muscle. Each time point is compared with basal values for statistical analysis. One-way ANOVA is applied. * $p<0.05$

DISCUSSION – 1

The injection of CTX to induce muscle damage is an ideal model to study the immunological events underlying muscle repair. The kinetic of skeletal muscle repair is quick and in 7-10 days almost all fibres display a centrally-nucleated appearance typical of regenerating fibres. The decrease in the number and in the size of regenerating fibres is a quantitative parameter that can be assessed as a sign of aberrant repair. Since the aim of the study is to dissect the relative role of leukocyte Hmgb1 respect to tissue Hmgb1 the CTX injection should not perturb peripheral blood leukocyte composition. The analysis of monocyte, T and B lymphocyte on peripheral blood after CTX injection demonstrate that this is the case. The slight decrease, albeit not significant, of $CD3^+$ T lymphocytes is consistent with a report in literature (135) that cardiotoxin-III is an inducer of activation-induced apoptosis of human $CD8^+$ T lymphocytes. Small amounts of cardiotoxin-III are present in our mixture of cardiotoxin and, moreover, only a fraction of circulating $CD3^+$ T cells is constituted by $CD8^+$ activated lymphocytes. Finally the fraction of CTX mixture that from the muscle reaches the systemic distribution is probably too low to induce a greater effect on T lymphocyte viability. B cell increase observed at day7 after CTX injection can be justified by the fact that a tissue damage with massive cell death is often accompanied by the rising of a self-limiting autoimmune reaction with the production of low-titer autoantibodies (136).

To define the CTX injection model as an ideal system to address my scientific question Hmgb1 should be present both in muscle and in infiltrating leukocytes. Hmgb1 is present in total muscle lysates from undamaged muscle. The immunofluorescence analysis showed that Hmgb1 in healthy muscle is located preferentially in nuclei of myofibres and, possibly, of satellite cells. The systemic release of Hmgb1 in correspondence of muscle necrosis at day1 is a further evidence that Hmgb1 is passively released by dying muscle fibres, according to its role as an alarmin (1, 51, 54). CD45+ cells isolated from damaged muscles at distinct time points after CTX injection express

Hmgb1 at any time point analyzed, thus confirmed that the protein in our model is expressed also by inflammatory cells. Immunofluorescence analysis at day3 and 7 showed some nuclei of mononucleated infiltrating cells that are negative for Hmgb1 staining. Those cells could have already secreted Hmgb1 upon activation by cytokines present in the microenvironment (60, 93).

After the choice of the appropriate acute damage model I needed to set up a non-invasive tool to follow muscle damage *in vivo*, since no tools were available at the beginning of the project. In collaboration with the Centre for Experimental Imaging and with the Radiology department of the institute I have performed a longitudinal study to compare histological and MRI findings in a qualitative and quantitative manner. The aim of the present study was to validate a multiparametric MRI protocol for the dynamic and quantitative monitoring of skeletal muscle damage and healing. As presented in the introduction, the dynamic of regeneration are known from histological studies. However, histology has several limitations both in patients and in preclinical models as tool to investigate muscle damage: (i) the excision of muscle samples is a further trauma that could lead to confounding results; (ii) biopsies allow to obtain only segmental information without a panoramic assessment; (iii) the mice has to be killed to collect muscles and investigate their architecture. A non-invasive tool for longitudinal monitoring of muscle regeneration would be fundamental help in basic research, as well as in the investigation of immunological aspects of several myopathies, including muscular dystrophies and autoimmune polymyositis. For our study we used the acute muscle damage model based on intra muscle CTX injection as it is useful to study both tissue and inflammatory dynamics. We monitored the changes of T2rt, speed of water diffusion and FA at distinct time points after CTX injection and we performed correlations with data from quantitative analysis of histological samples.

In normal muscle the T2-rt is shorter than in other parenchymal tissues because of the strong contribution of the intracellular muscle compartment in which water T2 is

very short. From a physical point of view, the T2rt modification observed are likely to be linked to muscle oedema. T2 rt is a parameter to follow muscle oedema after tissue damage. We investigated the possibility that, besides oedema, it could be a more general parameter to follow inflammation, both on its humoral and cellular component. T2rt proved to positively correlate with the number of infiltrating cells and the histological score based on the infiltration level and the morphological appearance of the muscle. Consistently with the results reported in literature the diffusion constant (speed of water inside the tissue) increases at day 1 after injury and suddenly was back at basal level at day 3 (134). As already suggested these modifications could reflect the changes in fibre size, especially because the diffusion of water measured in skeletal muscles largely reflects the diffusion in the intracellular space (134). Therefore, the myocytes swelling observed immediately after injury is likely to determine the diffusion constant increase at day 1. The mismatch between diffusion constant and T2rt results at day 1 and 3 after injury indicates that the two parameters reflect distinct processes, being the former related to muscle structure and the latter to muscle inflammation. The diffusivity at later time points (day 5 and 7) becomes lower than in untreated muscle. The phenomenon can be explained by the fact that fibre size of regenerating cells is inconstant and lower than healthy fibres (137). Even more interesting are the changes of FA. Albeit specular to the modification of diffusion constant, the FA changes are larger. The intact skeletal muscle is characterized by an anisotropic diffusion of water (FA $\approx$ 0.3), similarly to healthy white matter of the brain (138, 139). At day 1 the tissue integrity is disrupted and, as expected, we observe the loss of the skeletal muscle anisotropic feature. Between day 5 and 7 the FA shows a fast increase above basal levels. The increase can be explained by the appearance of regenerating fibres. In fact at day 5 and 7 the centrally nucleated fibres, albeit present, are still immature and with a reduced diameter. At the same time points histology unveils that muscles are full of mononuclear infiltrating cells. Given that water diffusion is mainly intracellular and that

intercellular spaces are filled by inflammatory cells, it is easy to figure out an increase in FA. By day 30 histological sections show a progressive normalization of fiber diameter and a decrease in infiltration. Thus, as expected, water diffusion normalized as well. Based on these considerations, the FA changes seem to express the centrally nucleated fibers appearance and maturation. In conclusion, our study contributes to demonstrate that a multiparametric MRI protocol, including T2-mapping and DTI, could be considered an effective non invasive tool to obtain a panoramic monitoring of muscle damage and repairing process with a quantitative readout.

RESULTS – 2

1. Hmgb1 action in injured/regenerating muscle

In a first set of experiments I have used a pharmacological approach to study the contribution of extracellular Hmgb1 to muscle damage.

1.1 Schedule for pharmacological blockade of extracellular HMGB1

In a first set of experiment I have injected the competitive antagonist for Hmgb1, BoxA, at the site of injury. BoxA is injected together with CTX into TA muscle and the treatment is repeated (Figure 1.1, panel A). Control muscles have received the vehicle with the same schedule (saline/BoxA green arrow, CTX-saline orange arrow). MRI is carried out as indicated by blue arrow. 6-7 mice are sacrificed at day7, 15, 30 (red arrow) and various aspects of muscle assessed. 3 animals are sacrificed at day1 and 3 only for muscle weight analysis. Each mouse receives saline on one leg and BoxA in the controlateral leg.

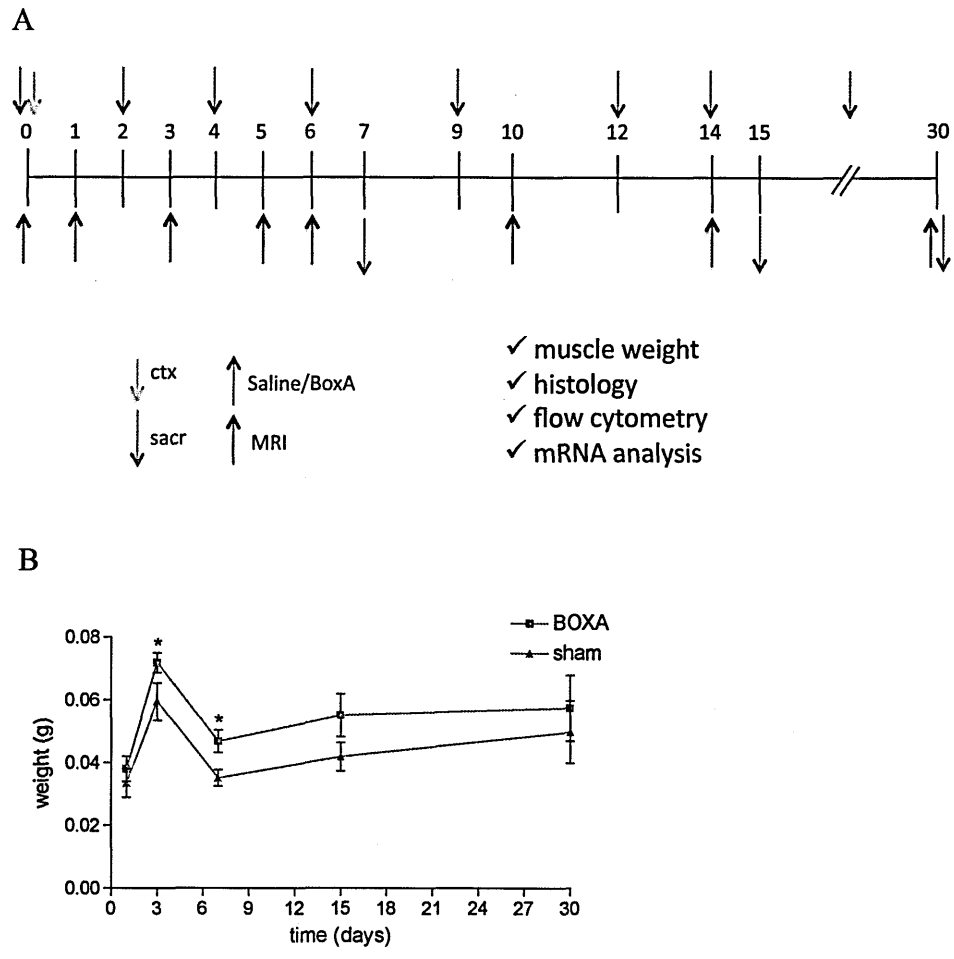

Figure 1.1 – Effects of Hmgb1 in injured and regenerating muscle. **A.** Schedule of BoxA treatment. BoxA is injected in TA together with CTX. Blue arrow indicates MRI analysis, red arrow indicates sacrifice of mice. 7 animals are sacrificed at day7 and 14, 6 animals at day30 and 3 at day1 and 3 for muscle weight analysis only. **B.** Muscle weight *vs.* time is graphed. Data from BoxA and sham treated mice are compared at each time point using a t-test for paired data. $p<0.05$ is considered as statistically significant (*). Red line represents BoxA treated muscles, green line represents sham treated muscles.

The weight of treated TA muscles is significantly higher than sham treated counterparts at day 3 and 7. The difference is lost at day15 and 30 and is not present at day1 (Figure 1.1, panel B and Figure 1.2).

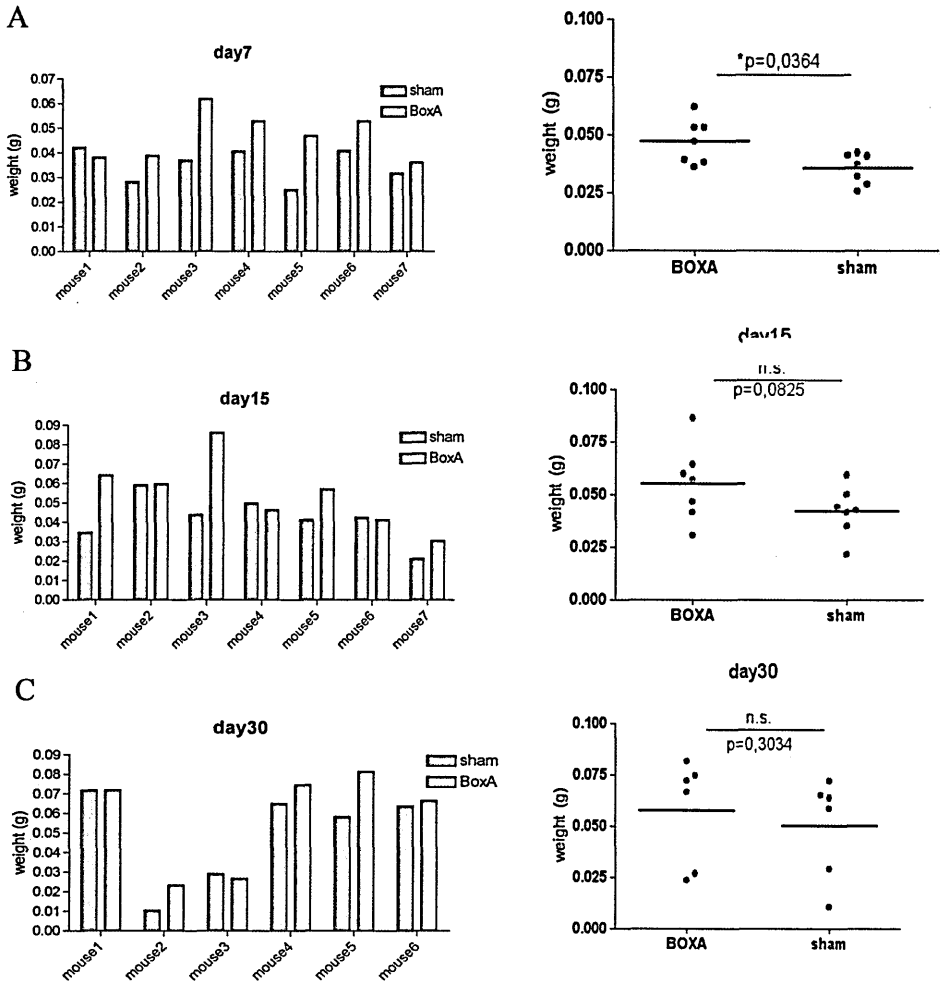

Figure 1.2 – Hmgb1 has an effect on muscle weight. **A. B. C.** Left histograms reports the comparison of each BoxA treated TA *vs.* sham treated controlateral TA. Right graph represents the comparison between the two groups of mice at day7. Non parametric analysis is applied. Associated p is indicated in the graph.

The aim of the project is to verify whether the leukocyte Hmgb1 is involved in the control of muscle repair. Since extracellular Hmgb1 is both of muscle and leukocyte origin, the first step is to verify whether the general blockade of extracellular Hmgb1 brings to a defect in the inflammatory response following muscle injury or in the process of healing. After administration of BoxA we have qualitatively and quantitatively investigated the inflammatory response in injured and repairing muscle.

1.2 Hmgb1 controls inflammation in muscle damage

Weight assessment represents a rather crude approach, which possibly reflects tissue oedema and infiltration and possibly other events. In collaboration with the radiology department and Centre for Experimental Imaging of our institute I have thus used MRI to investigate and quantitatively detail the events occurring during the homeostatic response to muscle injury. I have analyzed oedema with T2 map sequence (Figure 1.3, panel A). T2rt are compared in sham and BoxA treated muscles. Oedema is slightly higher in BoxA treated mice at day1 and lower at day7, possibly reflecting a perturbation of the development of oedema in BoxA treated muscles. To assess the extent of inflammatory infiltrate I have analyzed by cytofluorimetric analysis the percentage of $CD45^+$ cells after enzymatic digestion of muscles (Figure 3.3, panel B, left column). The same analysis is performed at day15 (Figure 3.3, panel B, right column). At both time points I have failed to detect significant difference between sham and BoxA treated muscles. Also the number of $CD45^+$ cells is unchanged. This indicated that the difference in T2rt, albeit statistically significant, might be of limited biological relevance, since the extent of inflammation is comparable.

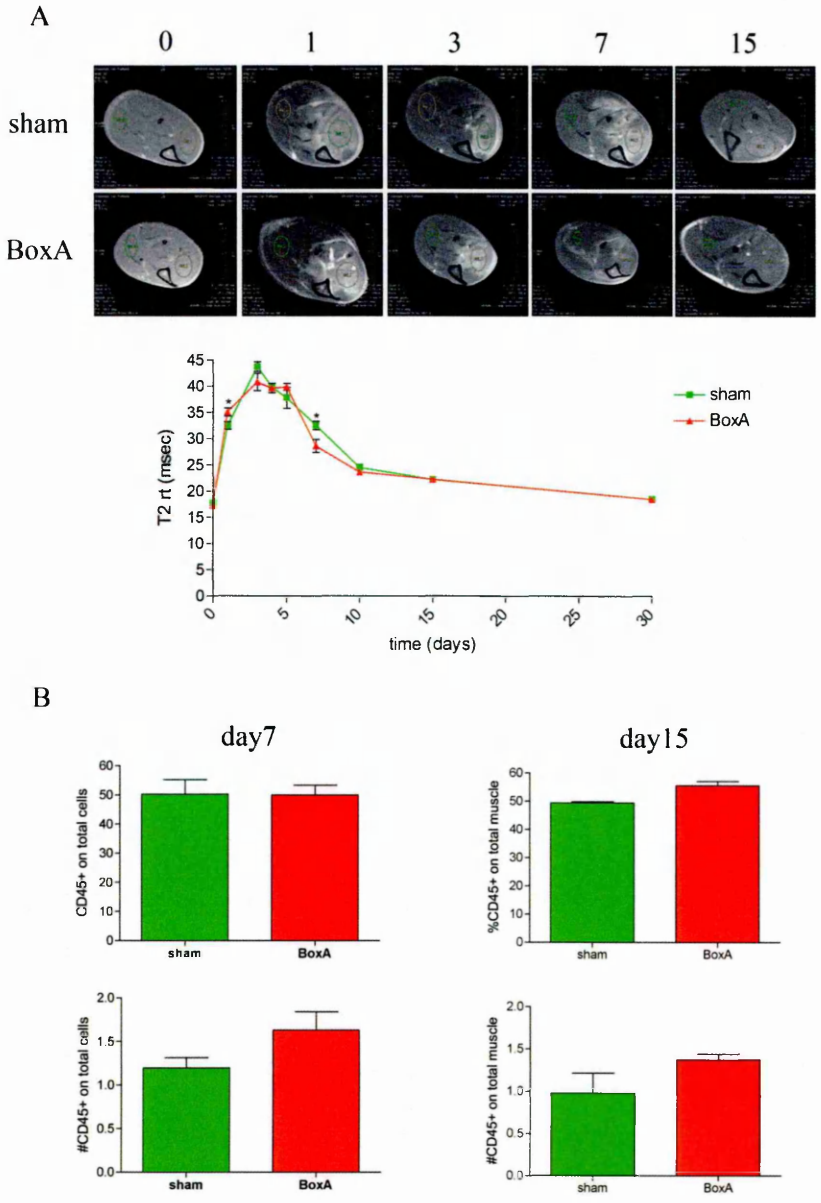

Figure 1.3 – Hmgb1 partially controls the size of oedema but not the number of infiltrating cells. **A.** On top panels qualitative analysis of T2 Map images is reported. We graphed T2rt values on y axis and time on x axis. For each time point we report the average ± SD of six mice. At each time point T2rt is compared between BoxA (red line) and sham (green line) treated TA. One-way ANOVA is applied. *$p<0.05$ **B.** The percentage of $CD45^+$ cells (top graphs) and the number of $CD45^+$ cells (bottom graphs) on total muscle cells is analyzed by flow cytometry at day7 and day15 in sham (green bars) and BoxA (red bars) treated TA. t-test for unpaired data is applied. $p<0.05$ is considered as statistically significant. No differences are detected in flow cytometry analysis.

I have also assessed by flow cytometry whether the pharmacological blockade of Hmgb1 influences the distribution of the various inflammatory populations, by

selectively enhancing or dampening the recruitment of different cells. To this aim I have analyzed the expression of lineage markers, such as Ly6G (granulocytes), CD11b (myeloid cells), CD3 (T lymphocytes), CD19 (B lymphocytes) and NK1.1 (NK cells). Hmgb1 blockade by BoxA reduces macrophage infiltration at day7 (Figure 1.4, panel A), while they are over represented at day15 (Figure 1.5, panel A), possibly reflecting a delayed kinetics of macrophage attraction. T lymphocytes are reduced at day15 (Figure 1.5, panel B). The effect on macrophages and T lymphocytes is apparently specific since other leukocyte population are unaffected, such as B lymphocytes, NK and NK-T ($NK1.1^{+}$-$CD3^{+}$) (Figure 1.4 panel B, Figure 1.5 panel B).

Of interest, not only the kinetics of macrophage infiltration changes, but their functional polarization is also influenced, as verified at day15 by the relative expression of receptors that tag pro-inflammatory ($CD45^{+}CD11b^{+}F4/80^{+}CD86^{+}$) *vs.* regenerative macrophages ($CD45^{+}CD11b^{+}F4/80^{+}CD163^{+}$) (Figure 1.5, panel A).

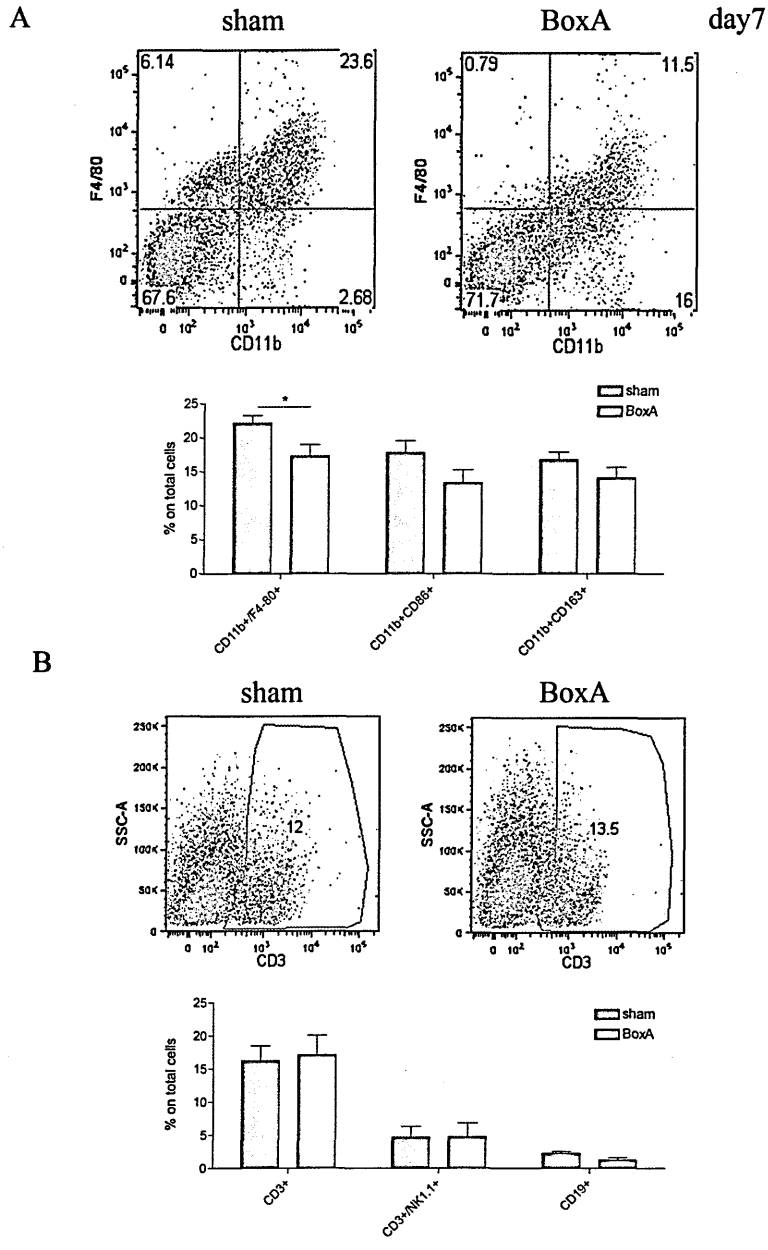

Figure 1.4 – Hmgb1 influences the recruitment of macrophages at day7 after acute damage. **A.** The percentage of $CD45^+CD11b^+F4/80^+$, $CD45^+CD11b^+F4/80^+CD86^+$ and $CD45^+CD11b^+F4/80^+CD163^+$ cells on total muscle cells is compared in sham *vs.* BoxA treated muscles. **B.** Cytofluorimetric dot plot represent the percentage of $CD45^+CD3^+$ cells on total muscle cells. The percentages of $CD45^+CD3^+$, $CD45^+CD3^+NK1.1^+$ and $CD45^+CD19^+$ are compared at day7 in sham *vs.* BoxA treated muscles. Both in **A** and in **B** green bars represent sham treated muscles, red bars represent BoxA treated mice and three mice per group are analyzed. Bars are average ± SD. *$p<0,05$.

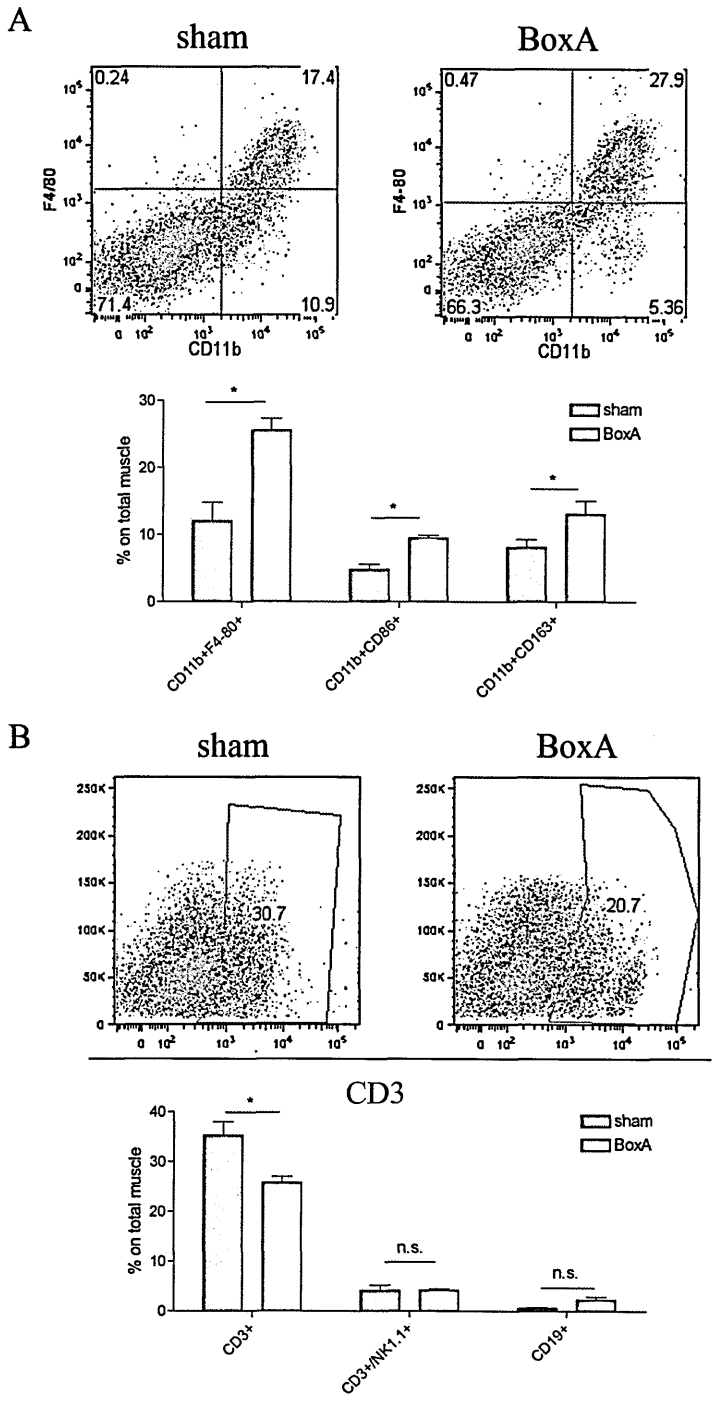

Figure 1.5 – Hmgb1 influences macrophage and lymphocyte recruitment in damaged muscle at day15. **A.** The percentage of $CD45^+CD11b^+F4/80^+$, $CD45^+CD11b^+F4/80^+CD86^+$ and $CD45^+CD11b^+F4/80^+CD163^+$ cells on total muscle cells is compared in sham *vs.* BoxA treated muscles. **B.** Cytofluorimetric dot plot represent the percentage of $CD45^+CD3^+$ cells on total muscle cells. The percentages of $CD45^+CD3^+$, $CD45^+CD3^+NK1.1^+$ and $CD45^+CD19^+$ are compared at day7 in sham *vs.* BoxA treated muscles. Both in **A** and in **B** green bars represent sham treated muscles, red bars represent BoxA treated mice and three mice per group are analyzed. Bars are average ± SD. *$p<0,05$.

3.3 HMGB1 partially influences muscle healing

To investigate muscle architecture during damage and repair we use both histology and MRI. H&E staining is performed on TA treated or not with BoxA at day7,15 and 30 after muscle damage. Results are reported in Figure 3.6, panel A. there is a transient delay in tissue repair at day15, when some necrotic areas (blue spots) are still present in the tissue. However by day30 sham and BoxA treated TA have both repaired correctly. MRI analysis reveals that fractional anisotropy (F.A.) is higher in BoxA treated *vs.* sham treated TA.I Since macrophages influence muscle repair (2, 43, 128) and results suggest that macrophage recruitment and polarization are at least partially dependent on extracellular Hmgb1, the following step has been to investigate whether the restoration of muscle architecture is impaired after BoxA treatment.IFA On the other hand F.A. is lower at day7 in BoxA *vs.* sham treated TA, while it is higher at day3, possibly reflecting a lower percentage of centrally nucleated fibres (Figure 1.6, panel B).

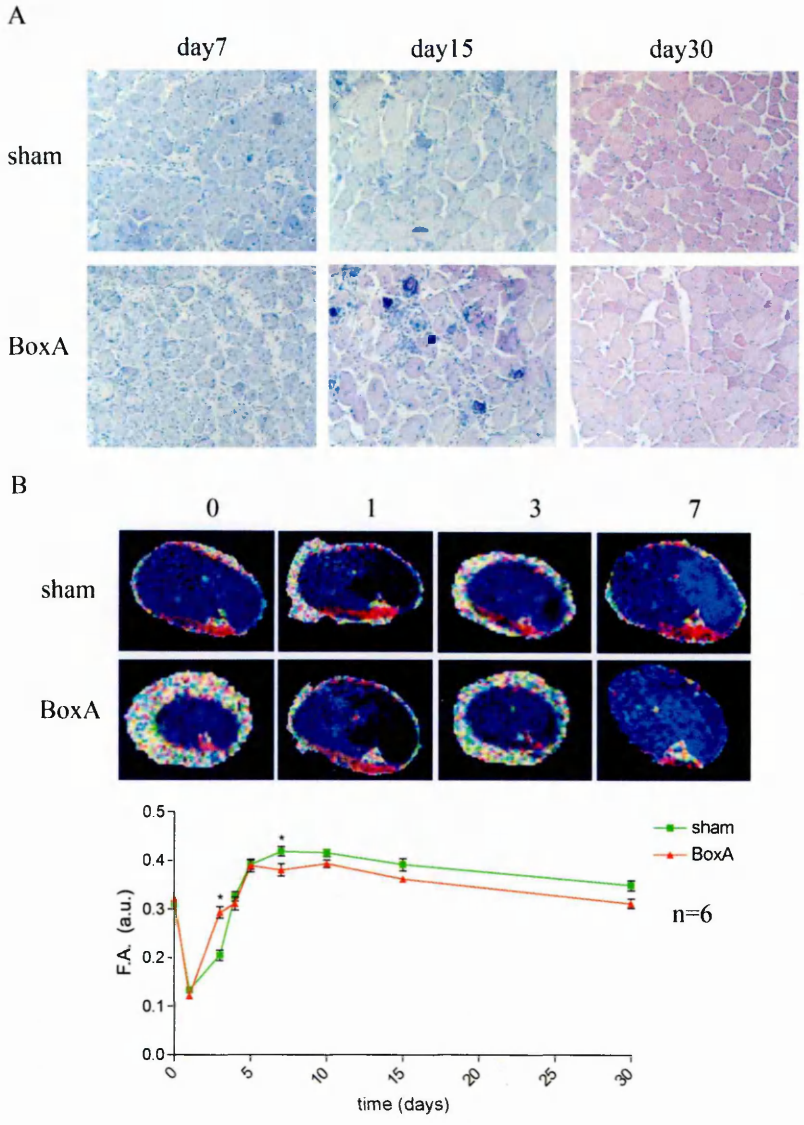

Figure 1.6 – Hmgb1 partially affects muscle repair. **A.** H&E staining is performed on sections from frozen samples. 3-6 mice per group per time point are investigated. Representative pictures for each group and for each time point are reported (20x magnification). **B.** Diffusion tensor imaging is performed on six mice/group. On the x axis time is reported. On the y axis the fractional anisotropy (F.A.) values are indicated. For each time point we report the average ± SD of three mice for F.A. For each mouse 5 slices are analyzed both on BoxA (red line) and sham (green line) muscle. At each time point BoxA treated and sham treated muscles are compared for statistical analysis. Non parametric test is applied. * $p<0.05$

	Muscle repair	Oedema	#CD45+ infiltrating cells	Macrophage infiltration	CD45+CD11b+ F4/80+CD163+	CD45+CD11b+ F4/80+CD86+	Lymphocyte infiltration	Other cell infiltration
day7	/	+	/	-	/	/	/	/
day15	-	/	/	+	+	+	-	/

Table 1 – Sum up of results obtained with pharmacological blockade of Hmgb1. It has been highlighted that extracellular Hmgb1 partially controls muscle healing at day15. Hmgb1 controls oedema formation at day7 but not the number of infiltrating cells. It controls macrophage infiltration and partially macrophage phenotype. Hmgb1 regulates T-lymphocyte attraction at day15 while it does not impact on the infiltration of other cell population.

BoxA is a quick and dirty approach to study Hmgb1. It blocks both the Hmgb1 that is passively released by dying fibres and the Hmgb1 that is actively secreted by immune cells. The main goal of the present study is to elucidate why both the alarmin and the cytokine function of Hmgb1 are needed for tissue repair. I have set up an ad hoc animal model to address this issue: a mouse that is Hmgb1 proficient in all tissues and that lacks Hmgb1 only in the haematopoietic tissue. To obtain such a mouse the most intuitive approach is to perform a bone marrow transplantation from $Hmgb1^{-/-}$ mice into WT recipient. However $Hmgb1^{-/-}$ pups die at p1 because of severe hypoglycaemia and they are not suitable as sources for bone marrow transplantation. Foetal liver is the site of haematopoiesis in the intrauterine life. The peak of foetal haematopoiesis is at day E14.5. I set up a model of foetal liver transfer to transplant $Hmgb1^{-/-}$ precursors into lethally irradiated adult recipient.

In the next section I will present data about the set up of the foetal liver transplantation protocol. In this first part I have transferred WT foetal livers into WT recipients, to give the proof of principle that transplantation is working. In the last chapter of result I will show you the characterization of mice transplanted with $Hmgb1^{-/-}$ *vs.* $Hmgb1^{+/+}$ foetal livers.T, post-translational modification

2. <u>Foetal liver transplanted mice have good chimerism in peripheral blood and in primary and secondary lymphoid organs</u>

To dissect the role of leukocyte and muscle Hmgb1 we need a mouse model lacking one of the two sources of Hmgb1. We decided to generate a mouse model without Hmgb1 in the haematopoietic system. The easiest way would be to transfer bone

marrow from an *Hmgb1*$^{-/-}$ donor into an *Hmgb1*$^{+/+}$ recipient. However, as mentioned in the introduction, *Hmgb1*$^{-/-}$ mice are not viable (115). Thus we have focused our strategy on generating a chimera starting from foetal liver, the anatomic site deputed to haemopoiesis in the foetus.

2.1 Chimerism assessment

I have first transferred WT foetal liver cells into WT recipients. To distinguish donor and recipient cells I have taken advantage of the CD45.1 and CD45.2 mismatch. Donor cells express the CD45.2, while recipient mice express the CD45.1 allelic variant. By cytofluorimetric analysis it is relatively easy to assess the percentage of donor and recipient cells in a given tissue.

I have analyzed the PB of 17 mice transplanted with 1:1 or 1:2 ratio donor:recipient ratio (Figure 2.1, panel A). Six weeks after transplantation the majority of circulating leukocytes is of donor origin. A negligible amount of cells is of recipient origin (<10%). In the BM of 12 mice 10 weeks after transplantation (Figure 2.1, panel B) the majority of leukocyte is of donor origin. A negligible amount of cells is of recipient origin (<1%). BM also contains a percentage of cells that are not of haematopoietic origin, possibly vessels or stromal cells. Virtually all CD11b^{+} cells are CD45.2^{+}, i.e. of donor origin (Figure 2.1, panel B, bottom right dot plot).

I have evaluated chimerism in secondary lymphoid organs, such as spleen (Figure 2.2, panel A), inguinal lymph nodes (LN, Figure 3.8, panel C) and in peritoneal liquid (Figure 2.2, panel B) 10 weeks after transplantation. The chimerism is consistently highly satisfactory with a negligible residual percentage of recipient cells (<5-10%). As expected the highest percentage of recipient cells is found in peritoneal liquid, probably because of the difficulty to erase the resident population with irradiation.

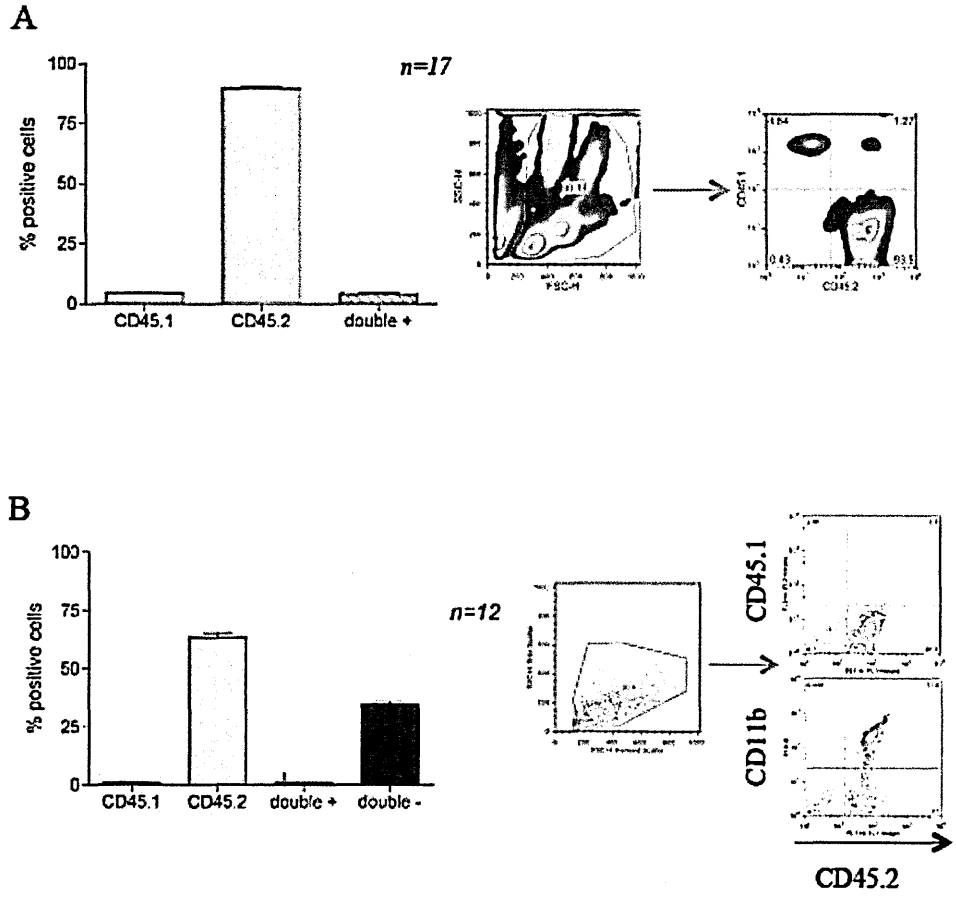

Figure 2.1 – A good chimerism is reached in peripheral blood and bone marrow of transplanted mice. **A.** Cytofluorimetric analysis of PB performed on 17 mice for the expression of CD45.1 and CD45.2. Alive cells are gated and doublets are excluded. On the alive, single cell population the analysis for CD45.1 and CD45.2 expression is performed. Qualitative appearance of dot plots is reported on the right. On the left there is the quantitative representation of results. In the histograms average ± SD is reported (n=17). **B.** Cytofluorimetric analysis of BM performed on 12 mice for the expression of CD45.1 and CD45.2. Alive cells are gated and doublets are excluded. On the alive, single cell population the analysis for CD45.1, CD45.2 and CD11b expression is performed. Qualitative appearance of dot plots is reported on the right. On the left there is the quantitative representation of results for CD45.1 and CD45.2 expression. In the histograms average ± SD is reported (n=12). For CD11b expression one representative dot plot is reported on the right.

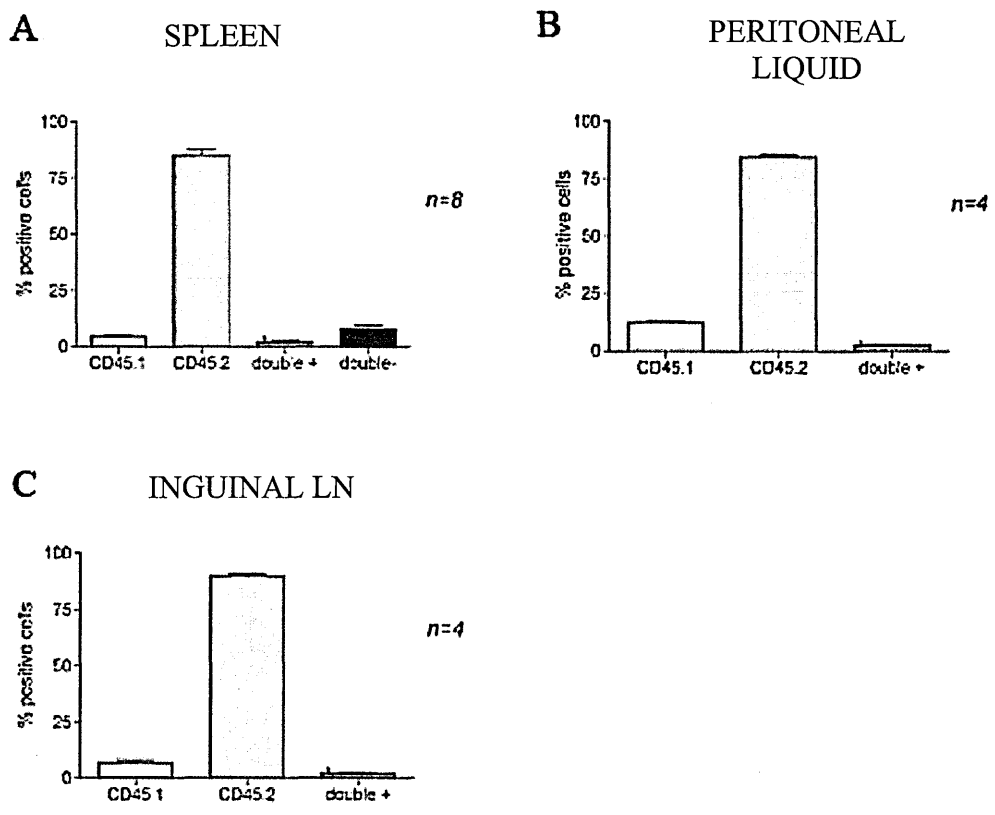

Figure 2.2 – Efficacy of foetal liver as a source of haematopoietic precursors. The fraction of cells of donor (CD45.1+) and of recipient (CD45.2+) origin has been evaluated in the spleen (**A.** n=8), peritoneal liquid (**B.** n=4) and inguinal lymph nodes (**C.** n=4).

2.2 Muscle regeneration after transplantation with foetal liver precursor cells

Healthy TA has similar features in the two groups of mice, indicating that irradiation *per se* does not detectably perturb the tissue architecture (Figure 2.3, panel A). At day3 after injury the extent of necrosis and infiltration are similar. At day7 regeneration simultaneously occurs in the two groups of mice. Transplanted mice have an apparently more sustained leukocyte infiltration even if the difference is not significant. At day10 the two groups of mice are comparable.

The greatest part of circulating cells is of donor origin. To be sure that donor and not recipient cells are preferentially recruited at the site of muscle damage I have stained for CD45.2 (marker of donor cells) muscle sections at day3 and day7 after injury (Figure 2.3, panel B).

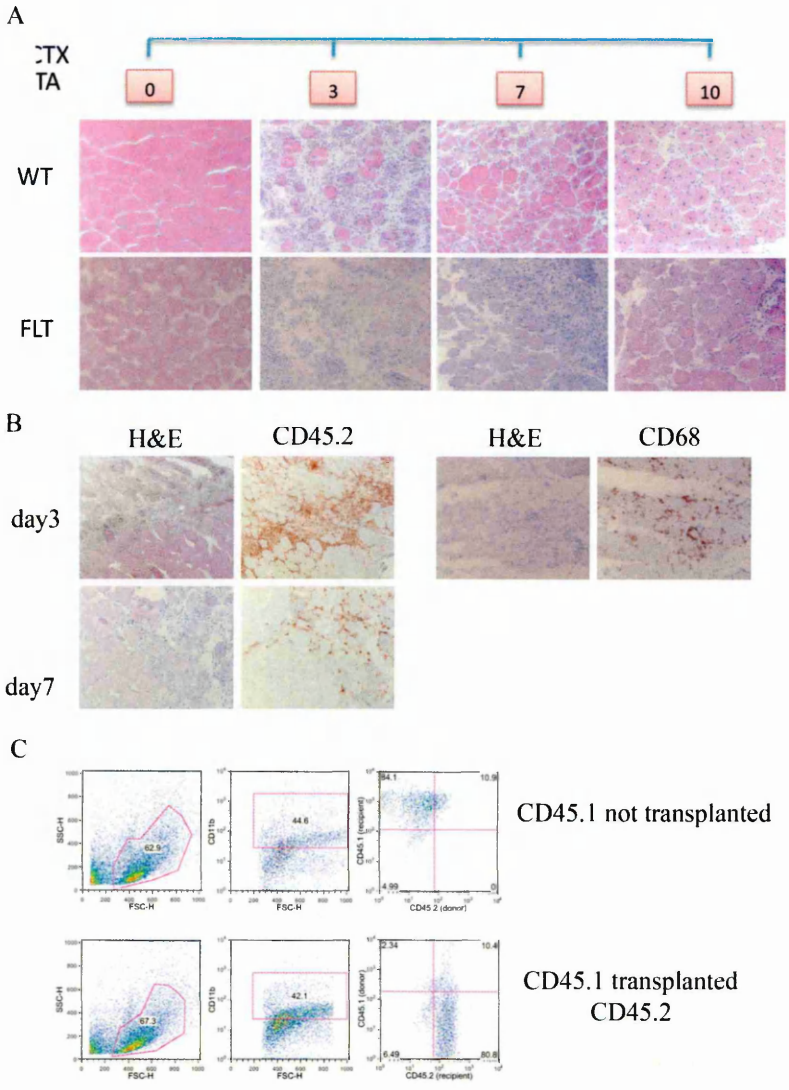

Figure 2.3 – Cells of donor origin are effectively recruited at sites of muscle injury. **A.** Injury is induced in 12 untreated (WT) or 12 transplanted animals (FLT). Representative pictures (20x magnification) are reported **B.** Muscle sections are stained for CD45.2 and CD68. Representative pictures of one out of three animals analyzed are shown (20x magnification) **C.** The percentage of $CD45.1^+$ cells is analyzed on $CD11b^+$ cells from damaged muscles. The analysis is performed on a transplanted animal (bottom dot plots) but also on a CD45.1 not transplanted mouse, as a positive control for CD45.1 labelling.

The vast majority of infiltrating leukocytes are $CD45.2^+$. Moreover most of them express the CD68 marker. Results obtained with immunohistochemistry are confirmed physically retrieving leukocytes from the tissue and studying them by flow cytometry (Figure 2.3, panel C). The analysis reveals that in the gate of $CD11b^+$ cells (bona fide macrophages) the greatest part of the cells (around 90%) is $CD45.2^+$, so of donor origin,

thus confirming that the procedure of foetal liver transplant ensures good chimerism both in lymphoid organs and in inflamed muscles.

To better define the oedema in transplanted mice I have analyzed them using the MRI sequences introduce before. TA muscles of injured mice transplanted or not with FL precursors have been analyzed using MRI before and at day3, 7 and 15 after damage. T2rt and F.A. are reported in Table 2. Transplantation does not influence T2rt trend in damaged TA. T2rt peaks at day3 after injury. At day7 the T2rt is still high; later on it declines as expected (see Table 2).

T2rt (msec)	day0	day3	day7	day15
Untransplanted TA	16,165±0,477	37,977±0,606	31,103±1,972	25,401±3,721
Untransplanted G	15,793±0,606	16,730±0,536	15,494±1,616	15,334±0,607
Transplanted TA	16,594±0,724	39,506±2,513	34,568±2,103	21,383±1,496
Transplanted G	16,493±0,598	16,814±0,310	15,861±0,696	17,751±0,652

Table 2 – Transplantation does not influence T2rt trend during muscle damage and repair. TA = tibialis anterior, G = gastrocnemius. n=3 at each time point. t-test for unpaired data is applied. No significant differences are detected between transplanted and untransplanted mice.

Foetal liver transplant does not impinge the kinetics of skeletal muscle response to sterile injury, as assessed by FA. During damage phase FA drops as expected (day3) and then promptly recovers (see Table 3) as it happens for untransplanted mice.

F.A. (a.u.)	day0	day3	day7	day15
Untransplanted TA	0,306±0,008	0,206±0,023	0,421±0,02	0,373±0,003
Untransplanted G	0,280±0,011	0,297±0,013	0,294±0,014	0,255±0,007
Transplanted TA	0,309±0,009	0,157±0,023	0,350±0,022	0,391±0,003
Transplanted G	0,275±0,013	0,287±0,013	0,295±0,016	0,282±0,003

Table 3 – Transplantation does not influence F.A. trend during muscle damage and repair. TA = tibialis anterior, G = gastrocnemius. n=3 at each time point. T-test for unpaired data is applied. No significant differences are detected between transplanted and untransplanted mice.

3. Leukocyte Hmgb1 controls muscle repair through regulation of angiogenesis

3.1 Effective chimerism in lethally irradiated WT mice transplanted with Hmgb1$^{-/-}$ foetal liver cells (FLT)

Before analyzing muscle repair in transplanted mice it is necessary to verify whether transplantation procedure of *Hmgb1*$^{-/-}$ foetal livers ensures good chimerism at peripheral level. Figure 4.1 panel A demonstrates that transplanted Hmgb1$^{-/-}$ precursors effectively engraft, as assessed by the relative expression of CD45.1 and CD45.2 markers. I have then verified the Hmgb1 expression in circulating leukocytes by western blot analysis (Figure 3.1, panel B). A negligible amount of Hmgb1 is indeed express, possibly reflecting residual recipient circulating leukocytes. Since no one before produced a model in which circulating white blood cells do not express Hmgb1 we have further characterized our model by haemochrome analysis (Figure 3.1, panel C). *Hmgb1*$^{-/-}$ FLT mice have fewer platelets and circulating leukocytes than their controls. The number of red blood cells is unchanged in the two groups of mice.

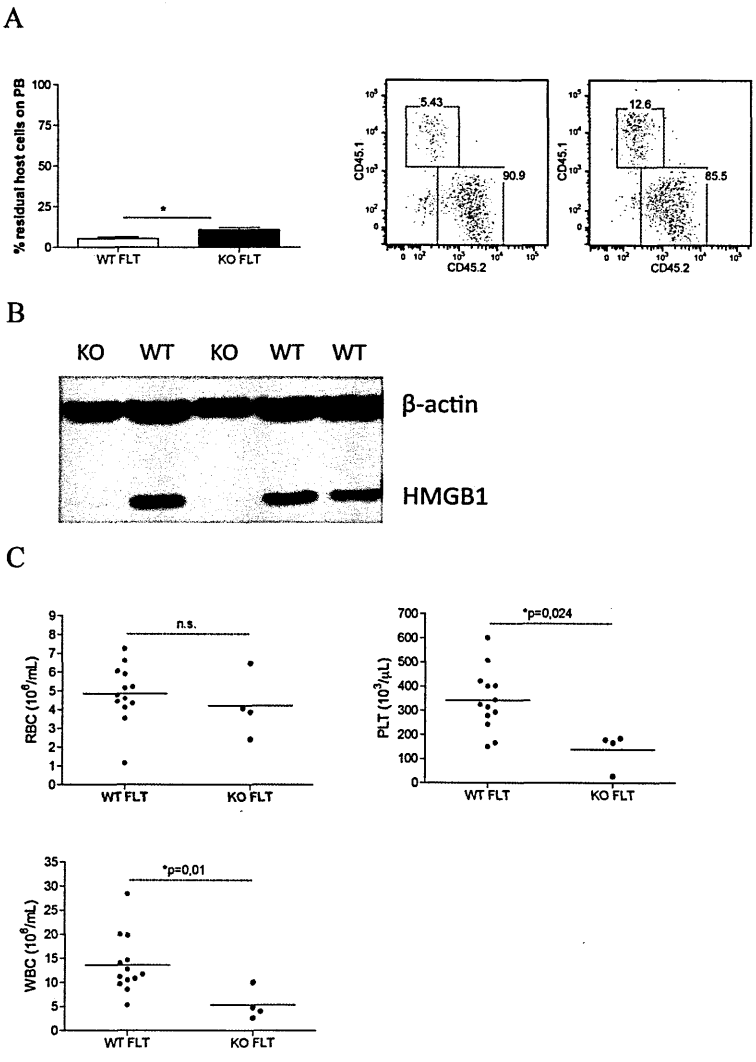

Figure 3.1 – Hmgb1$^{-/-}$ FLT mice express negligible amount of Hmgb1 in circulating leukocytes but have altered haemochromes. **A.** Chimerism analysis on WT FLT *vs* KO FLT mice. Cytofluorimetric analysis on peripheral blood (PB) of 7 mice/group (left panels). Residual host cells on PB have been identified as CD45.1^{+}. **B.** Western blot analysis on WT FLT and KO FLT circulating white blood cells for HMGB1. β-actin has been used as loading control. **C.** Haemochrome analysis on PB of WT FLT (n=14) vs KO FLT (n=4) mice. The number of red blood cells (RBC, upper left panel), platelet (PLT, upper right panel) and white blood cells (WBC, bottom panel) have been evaluated. Data are analyzed by t-test for unpaired data. p<0,05 was considered as statistically significant (* = p<0.05, n.s. = not significant).

3.2 Hmgb1$^{-/-}$ FLT mice have normal PB and BM populations of white blood cells

As mentioned in the introduction Hmgb1 has several roles in controlling immune responses (1, 51, 54, 81, 83). For this reason it is important to verify if, together with a reduction in the number of circulating white blood cells, there is also an impairment in the composition of leukocyte populations. I have analyzed by flow

cytometry the composition of the $CD45^+$ population of both PB and BM 6 and 12 weeks after transplantation respectively (Figure 3.2). In panel A the comparison between a representative WT and KO FLT mouse is reported. WT and KO FLT mice do not differ in any of the population analyzed. The result is confirmed by the quantification performed on 4 independent mice (Figure 3.2, panel B). The same analysis is performed on BM. In the gate of CD45+ population several lineage markers are analyzed. No differences are seen between WT and KO FLT mice (Figure 3.2, panel C and D). These results highlight that, despite a lower number of circulating white blood cells, the composition of leukocytes is comparable between *Hmgb1*$^{+/+}$ and *Hmgb1*$^{-/-}$ FLT mice.

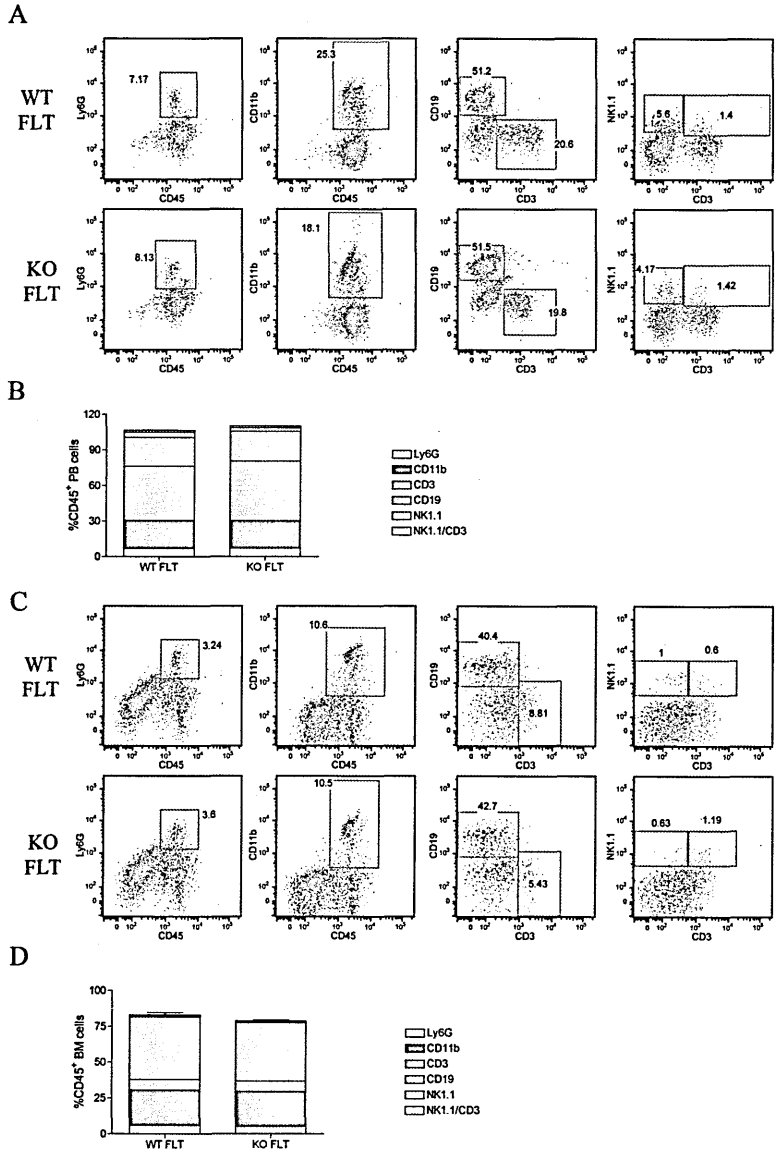

Figure 3.2 – Hmgb1$^{-/-}$ FLT mice have normal leukocyte lineage distribution in PB and BM. **A.** PB cells from WT FLT and KO FLT mice are analyzed by flow cytometry (n=4). Representative dot plots from one Hmgb1 KO FLT and one Hmgb1 WT FLT mouse are reported. **B.** The percentage of lineage markers (Ly6G, CD11b, CD3, CD19, NK1.1) is calculated on CD45^{+} cells and reported in the colored histogram. **C.** Bone marrow cells from WT FLT and KO FLT mice are analyzed by flow cytometry (n=3). Representative dot plots from one Hmgb1 KO FLT and one Hmgb1 WT FLT mouse are shown. **D.** The percentage of lineage markers (Ly6G, CD11b, CD3, CD19, NK1.1) was calculated on CD45^{+} cells and reported in the colored histogram.

3.3 Leukocyte Hmgb1 controls muscle repair

After the characterization of peripheral blood and bone marrow the next step has been to verify whether *Hmgb1*$^{-/-}$ FLT mice display alterations in muscle repair after acute damage. Thus it is possible to dissect the relative role of tissue and leukocyte derived Hmgb1 in the context of sterile damage repair. *Hmgb1*$^{-/-}$ FLT mice and their controls are then damaged by CTX and repair is evaluated. At first we analyzed TA muscles by MRI. F.A. is analyzed at distinct time points (Figure 3.3). No differences between TA from WT and KO FLT mice are present, indicating a similar level of tissue necrosis at early time points and of myofibre regeneration at later time points. However this analysis does not give information about muscle morphology.

I analyzed by histology TA muscles from WT and KO FLT mice both at day7 and day15 after CTX injection (Figure 3.4 and Figure 3.5 respectively). H&E staining is performed. I have counted the number of centrally nucleated fibres at day7 and I have measured the diameters of regenerating fibres at day15. The number of centrally nucleated fibres is lower at day7 in TA from Hmgb1 KO FLT mice. Moreover at day7 there is a greater fat presence in TA from KO FLT mice, as unveiled by RedOil staining.

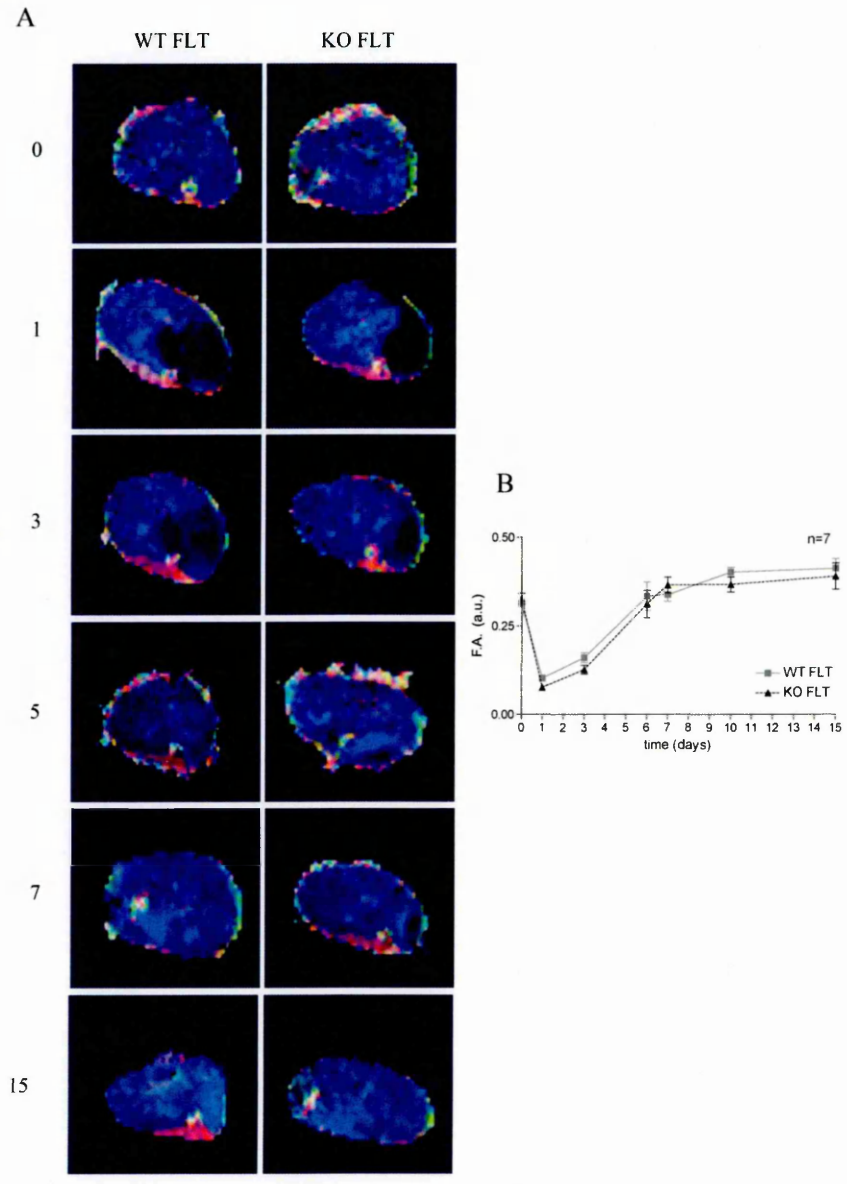

Figure 3.3 – F.A. is not different in TA from WT and KO FLT mice. **A.** CTX damaged tibialis anterior (TA) muscles from WT FLT and KO FLT mice are analyzed using MRI. Qualitative comparison between Hmgb1 WT FLT and Hmgb1 KO FLT mice at distinct time points is reported. **B.** Quantitative analysis of DTI sequence in the two groups of mice (n=7 in each group). F.A. is evaluated at distinct time points in five slices/mouse. One-way ANOVA is applied at each time point to compare TA from Hmgb1 WT FLT and Hmgb1 KO FLT mice. $p<0.05$ is considered statistically significant. No significant differences are detected.

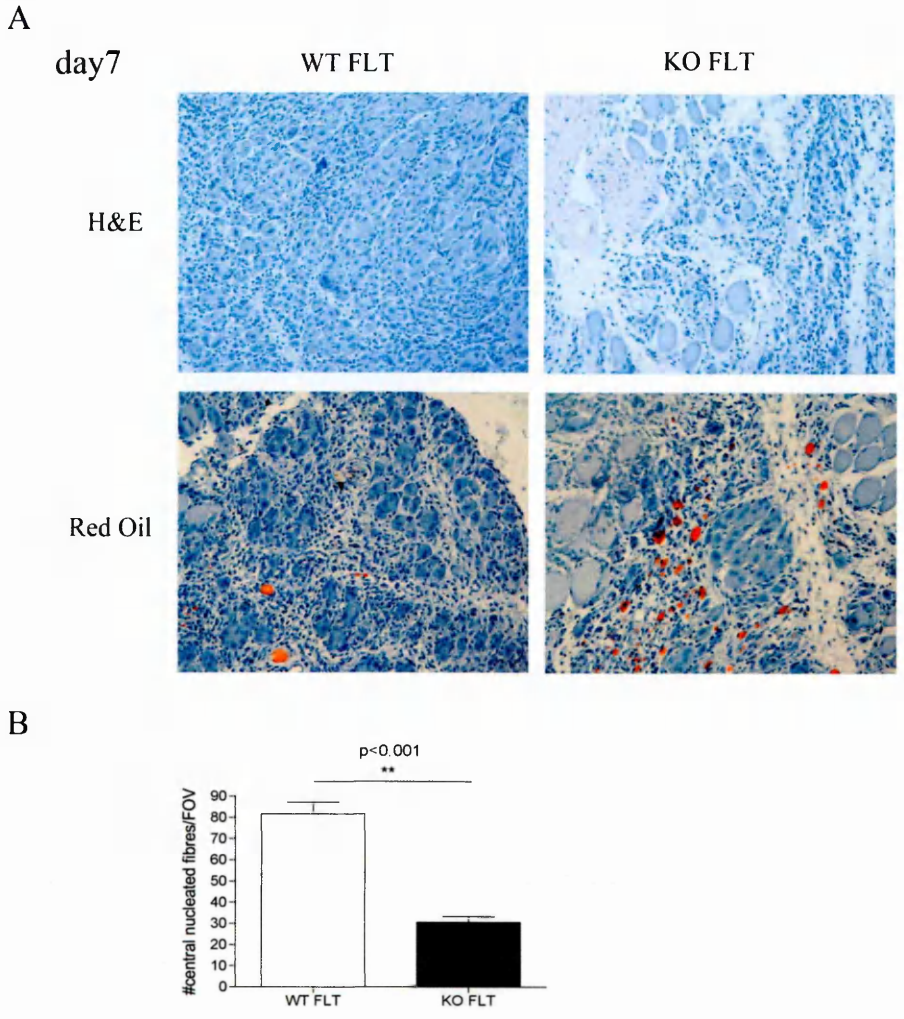

Figure 3.4 – Hmgb1 is important for correct repair at day7. **A.** day7 CTX injected TA muscles are displayed with hematoxylin and eosin staining (H&E, **A**-upper panels) and the number of centrally nucleated fibers was counted (n=3, 10 successive slices for each mouse, **B**). On the same muscle a Red Oil staining was performed (**A** - lower panels).

The measurement of fibre diameter (cross sectional area, c.s.a.) at day15 reveals that regenerating fibres in TA from KO FLT mice are dramatically smaller (Figure 3.5). This further support a role for leukocyte Hmgb1 in guiding muscle repair.

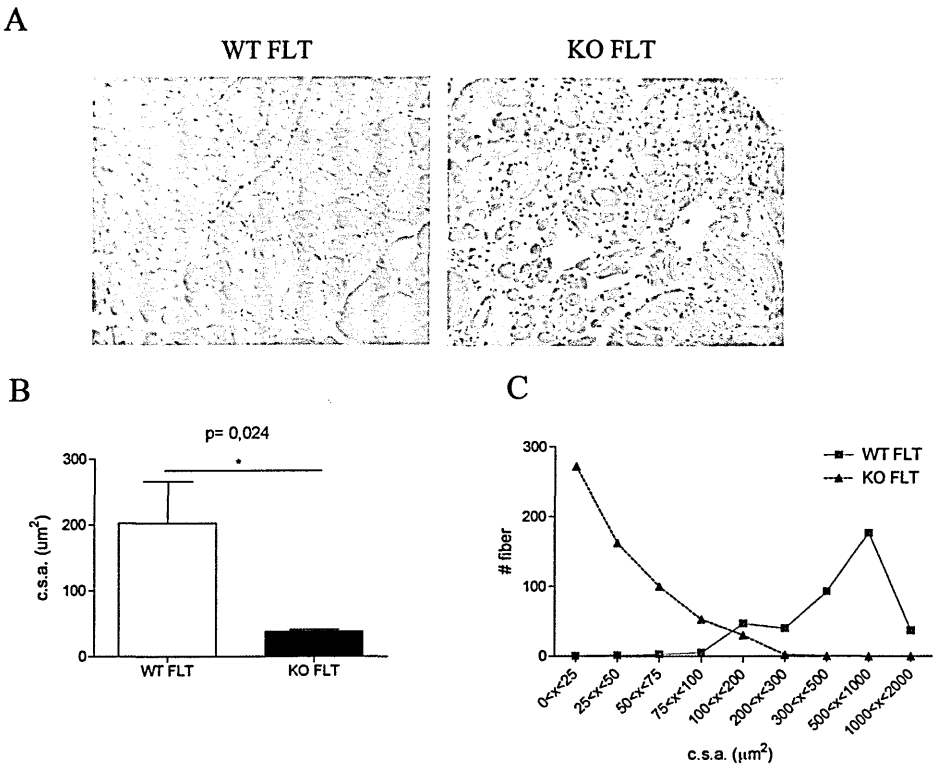

Figure 3.5 – Leukocyte Hmgb1 controls muscle repair at day15. **A.** day15 CTX treated muscles are analyzed by H&E (n=3 per group). Representative pictures from TA muscles at day15 after CTX injection stained with H&E are reported **B.** Fiber diameter (cross sectional area, c.s.a.) is measured (left panel) in 10 serial section/mouse. 3 mice per group are analyzed. All data are compared using t-test for unpaired data. $p< 0.05$ was considered as statistically significant. *$p<0.05$ **C.** The result is visualized also by the comparison (right panel) between one representative mouse per group. C.s.a range are defined (x axis) and the number of fiber within a given range is reported (y axis).

Our data suggest that leukocyte Hmgb1 controls muscle repair. The reason why leukocyte Hmgb1 should control muscle repair remain elusive. Three main hypotheses can explain the phenotype observed:

1. Leukocyte Hmgb1 controls inflammation, macrophage recruitment and/or macrophage polarization, known to be instrumental in repairing muscle (122)
2. Leukocyte Hmgb1 controls satellite cell biology
3. Leukocyte Hmgb1 controls angiogenesis in repairing muscle

3.4 Leukocyte Hmgb1 controls neither inflammation nor macrophage polarization

First I have defined whether Hmgb1 is involved in the control of oedema during damage and repair process. Hmgb1 WT and KO FLT mice are analyzed by MRI to investigate oedema in damaged TA muscle (Figure 3.6). Qualitative comparison between the two groups of mice reveals no apparent differences. Quantitative analysis of T2rt confirms that no difference in the extent of oedema is present. A slight, albeit not significant, increase in T2rt is detected at day5 and day7 in Hmgb1 KO FLT mice, possibly unveiling a tendency to an increase in recruiting leukocytes at the site of damage.

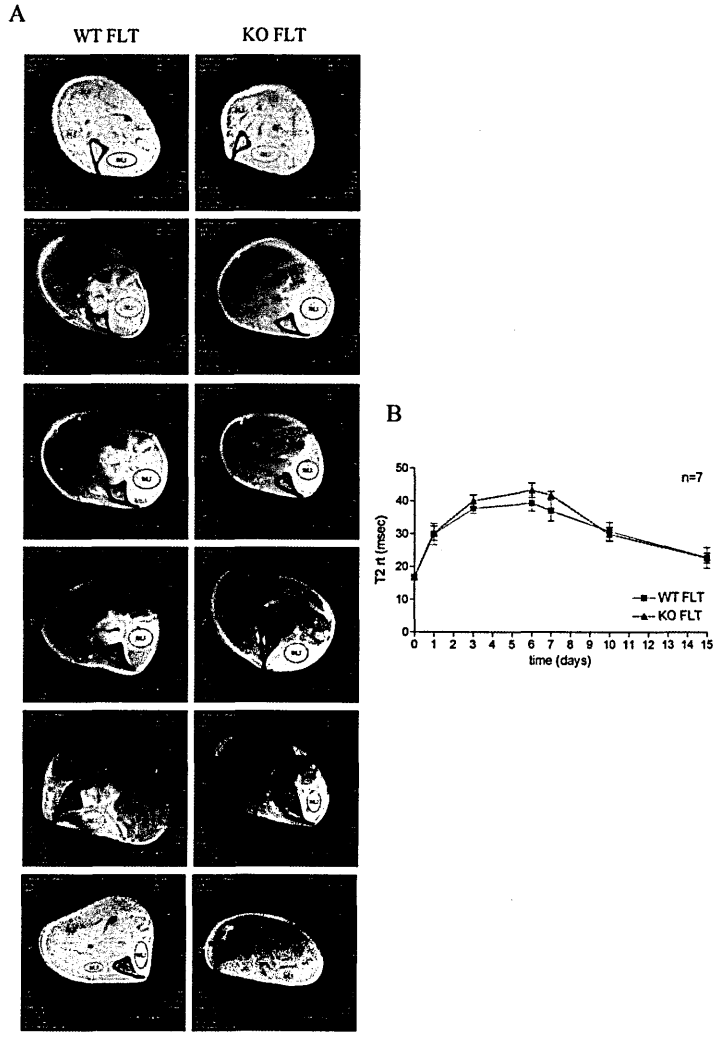

Figure 3.6 – Leukocyte Hmgb1 does not affect the extent of the oedema in damaged muscle. **A.** CTX damaged TA muscles from WT FLT and KO FLT mice are analyzed using MRI (n=7 in each

group). Qualitative comparison between Hmgb1 WT FLT and Hmgb1 KO FLT mice at distinct time points is reported **B.** From T_2 Map sequence T_2-rt is calculated in the two groups of mice at distinct time points. One-way ANOVA is applied at each time point to compare TA from Hmgb1 WT FLT and Hmgb1 KO FLT mice. $p<0.05$ is considered statistically significant. No significant differences are detected.

To better define how the infiltration is composed inside damaged and repairing muscles I have performed cytofluorimetric analysis. First I have verified chimerism at the site of damage. TA muscles from both WT and KO FLT mice at day7 after CTX injection are processed by enzymatic digestion. To verify chimerism in the tissue I have labelled digested muscles for both CD45.1 and CD45.2 (Figure 3.7, panel A). A minimal percentage of residual recipient cells is detected (<10% in both groups of animals), thus ensuring that the difference in the number of circulating white blood cells is not accompanied to an aberrant recruitment of leukocytes at the site of damage.

Since leukocytes such as macrophages are crucial for muscle repair (128), it is necessary to investigate if the leukocyte populations that are present at the site of injury depend or not on their own Hmgb1 for the recruitment. I have labelled cells from muscle digestion for CD45 together with several lineage markers such ad CD11b, CD3, CD19 and NK1.1 (Figure 3.7, panel B and C). Ly6G is not used for the present analysis since granulocytes infiltrate muscle only till day1 after CTX injection. In particular in the gate of $CD45^+$ cells I have analyzed the percentage of $CD11b^+$ cells (*bona fide* macrophages, Figure 3.7 panel B). No differences are revealed, as confirmed also by the quantitative analysis performed on 3 mice/group. No differences are also present between all the other lineages analyzed comparing WT and KO FLT mice (Figure 3.7, panel C). Finally I have analyzed the expression of macrophage polarization markers on $CD45^+CD11b^+$ cells (Figure 3.7, panel D). I have used CD86 as marker for pro-inflammatory macrophages and CD163 for anti-inflammatory macrophages. The cytofluorimetric analysis reveals no differences between the two groups of mice for

what concerns leukocyte infiltration. It seems that the percentage of $CD11b^{+}$ cells is reduced. The slight reduction in CD11b+ cells is accompanied by a modest increase in the percentage of CD3+ and NK1.1+ cells. None of these differences are statistically significant and also the biological impact of such small variations is likely to be irrelevant. The big defects in muscle repair are seen when at least 50% of the total infiltrating macrophages is eliminated by the use of clodronate-lyposome approach (128).

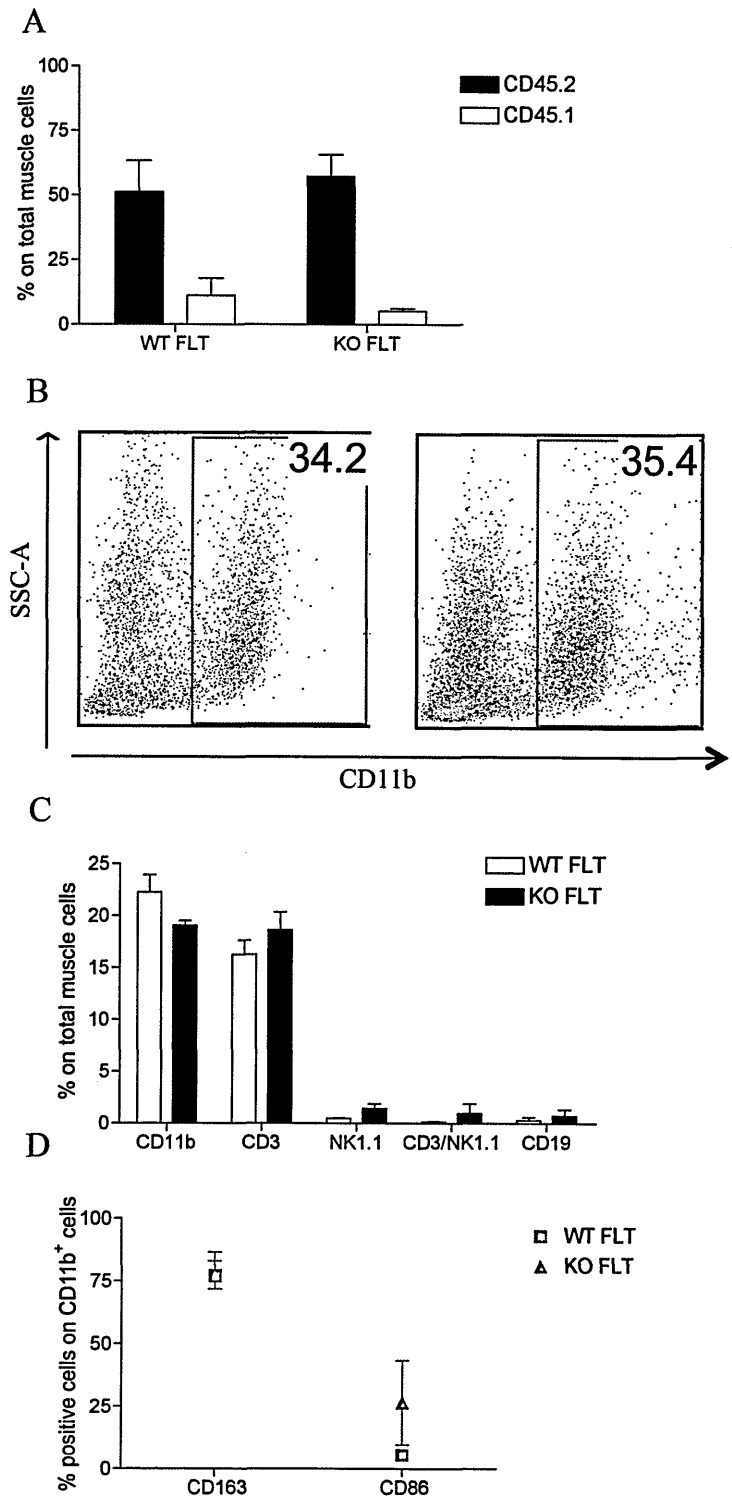

Figure 3.7 – Leukocyte Hmgb1 barely controls inflammatory cell recruitment at the site of damage at day7 after CTX injection. **A.** Total muscle cells after enzymatic digestion are analyzed by flow cytometry at day7 after CTX injection. $CD45.1^+$ and $CD45.2^+$ cell percentage is compared between the two groups of mice. **B.** $CD11b^+$ cells percentage on total muscle cells is analyzed. Representative dot plots are shown. **C.** Infiltrate composition is analyzed in 3 mice/group. White bars represent Hmgb1 WT FLT mice, black bars represent Hmgb1 KO FLT mice. Data are compared using t-test for unpaired data.

$p<0.05$ is considered statistically significant. No differences are detected. **D.** The percentage of $CD11b^+CD163^+$ and the percentage of $CD11b^+CD86^+$ are analyzed on total muscle cells from muscle digestion in the two groups of mice at day7 after CTX damage.

For what concerns macrophage polarization the analysis unveils a difference in the percentage of $CD45^+CD11b^+CD86^+$ cells. The difference is at the limit of statistical significance ($p=0.06$). However it could reflect a role for leukocyte Hmgb1 in controlling, at least partially, macrophage polarization. It is interesting that the percentage of $CD45^+CD11b^+CD163^+$ cells is unchanged. Some of the $CD11b^+$ cells in Hmgb1 WT FLT mice do not express nor CD163 nor CD86. They could express other pro- or anti-inflammatory markers, such as CD80 or CD206 respectively. In the group of Hmgb1 KO FLT mice the sum of $CD45^+CD11b^+CD86^+$ and of $CD45^+CD11b^+CD163^+$ cells is 100%. However it is not excluded that they could express other markers too. Collectively the results suggest that there could be a relevant increase in the proportion of macrophages with antigen presenting ability, a feature normally associated with pro-inflammatory macrophages. However the percentage of macrophages with scavenger (i.e. pro-healing) ability seems to be unchanged. To confirm a possible role of leukocyte Hmgb1 in controlling macrophage polarization or at least antigen presenting molecule expression I have moved to an *in vitro* system. The difference highlighted *in vivo* is affected by the variability among animals. Moreover an analysis on cytokine expression will be performed on total muscle to verify whether the phenotypical change observed has functional consequences.

I have derived macrophages from bone marrow of transplanted animals. I have polarized *in vitro* both Hmgb1 WT and KO macrophages. I have then analyzed their phenotypes by cytofluorimetric analysis and their cytokine secretions by ELISA. I have derived resting macrophages from BM of WT and KO FLT mice. Resting macrophages are then polarized using either IFNγ to obtain pro-inflammatory (M1-like) macrophages

or IL10 to obtain anti-inflammatory (M2-like) macrophages (Figure 3.8, panel A and B respectively). WT and KO macrophages do not differ in their expression of several cell surface marker, such as lineage markers (CD11b, F4/80), antigen presenting and co-stimulatory molecules (H2-k^b, CD40, CD86) or scavenger molecules (CD163, CD206). A decrease in MHC class II antigen (I-Ab) is unveiled. The difference is not statistically significant and points exactly in the opposite direction respect to the increase of CD86 observed *in vivo*. The analysis of Hmgb1 receptors RAGE and TLR4 is hampered by the lack of good antibodies for cytofluorimetric analysis. Taken together these results suggest that Hmgb1 does not really shape macrophage polarization. It is more likely that it partially affects the antigen presentation ability of macrophages. This would be consistent with what is published in literature about the role of Hmgb1 from dendritic cells in shaping activation and Th1 polarization in CD4+ naïve T lymphocytes (94, 95). In any case this is unlikely to deeply affect muscle repair. The scavenger/regenerative ability of macrophage is likely to be the key feature of macrophages to mediate muscle repair (43, 122). However the scavenger receptor expression is unchanged both *in vivo* and *in vitro*.

To definitively rule out the possibility for Hmgb1 to control macrophages polarization I have tested cytokine secretion *in vitro* by pro-inflammatory and tissue repairing macrophages. I have analyzed TNFα, typical of pro-inflammatory macrophages and IL10, typical of tissue repairing macrophages (8). Finally I have tested IGF-1, a molecule able to foster satellite cell proliferation and differentiation in regenerating muscle (140-142).

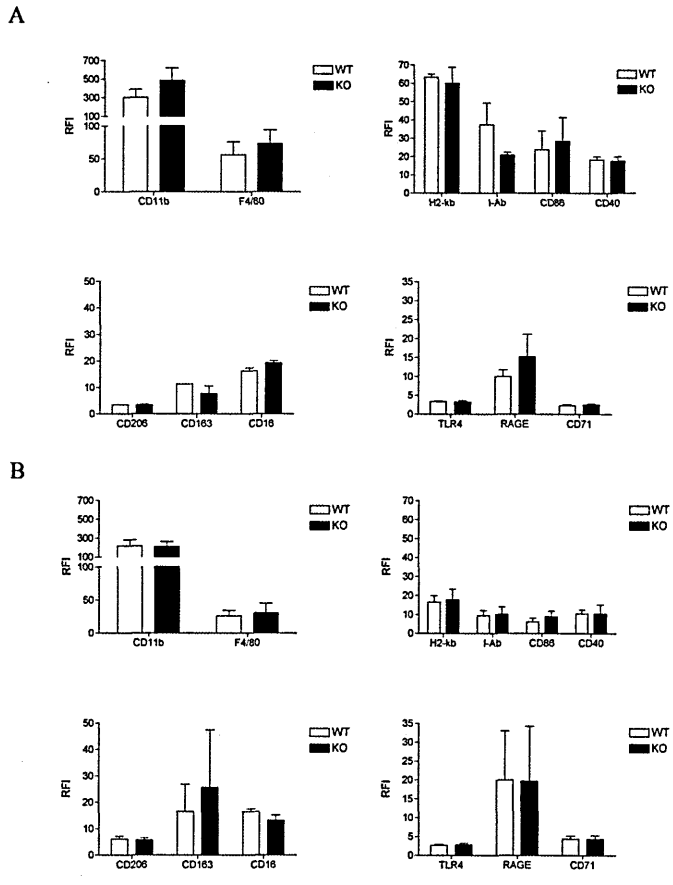

Figure 3.8 – Leukocyte Hmgb1 does not control the expression of specific polarization cell surface marker of macrophages. **A.** Flow cytometry analysis of cell surface markers of WT vs KO pro-inflammatory macrophages (M1, n=3). **B.** Flow cytometry analysis of cell surface markers of WT vs KO anti-inflammatory macrophages (M2, n=3). **A, B.** Fluorescence is quantified using Relative Fluorescence Intensity (RFI, y axis). Results are analyzed by t-test for unpaired data and values $p<0.05$ are considered as statistically significant. No significant differences are detected.

Also ELISAs for TNFα, IL10 and IGF1 do not reveal differences between WT and KO derived macrophages, regardless of their polarization (Figure 3.9). This finding suggests that leukocyte Hmgb1 is not involved in shaping macrophage polarization since at functional level there is not any difference in the secretion of cytokine.

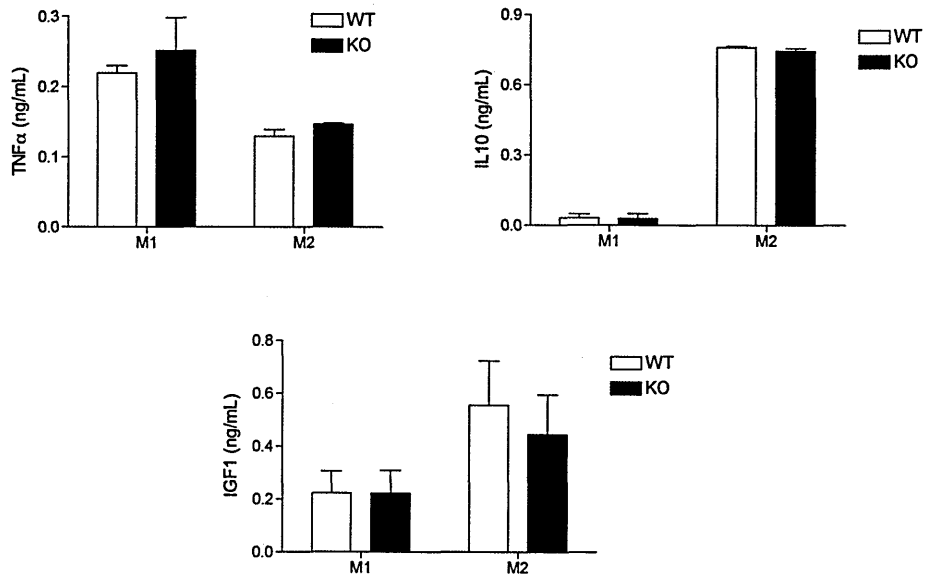

Figure 3.9 – Leukocyte Hmgb1 does not control the expression of cytokines specific for pro (M1) or anti-inflammatory (M2) macrophage phenotypes. ELISAs are performed on conditioned supernatants from M1 and M2 macrophages, either WT or KO (n=3). Results are analyzed by t-test for unpaired data and values $p<0.05$ are considered as statistically significant. No significant differences are detected.

To further characterize inflammatory status of muscle I have sacrificed 3 mice/group before CTX injection and at day 5, 10 and 15 after damage; I have then isolated mRNA from total muscle (TA) and performed real time RT-PCR. I have analyzed il6, tnfα and il10 (Figure 3.10). In Hmgb1 KO transplanted mice mRNA of il6, tnfα and il10 fail to peak at early time points after tissue damage (day5). This could hyporeactivity of leukocytes in damaged muscle could be part of a bigger defect in the control of immune responses mediated by soluble factors. This issue would be better addressed in the paragraph 3.6.

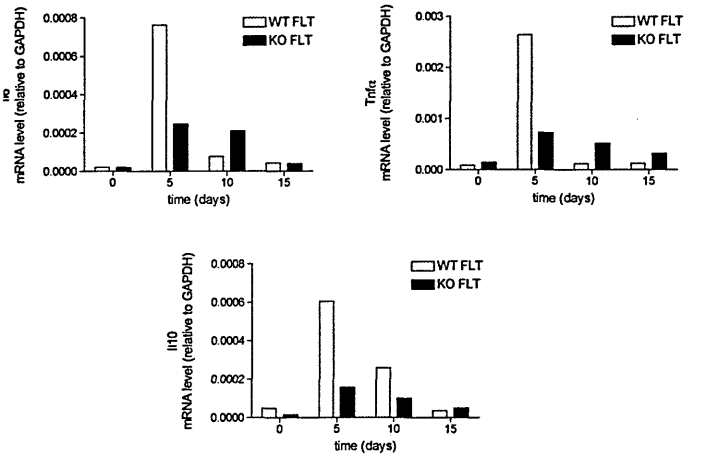

Figure 3.10 – Leukocyte Hmgb1 partially controls cytokine mRNA expression on total muscle. RT real time PCR on total muscle tissue for cytokines at distinct time points after muscle damage is performed. Il6 (left panel), Tnfα (centre) and Il10 (right panel) were analyzed. Results are representative of one out of two series of animals.

Our data suggest that leukocyte Hmgb1 does not control macrophage polarization in repairing muscle. Our data do not rule out the possibility that leukocyte Hmgb1 is involved in modulating antigen presentation ability of macrophages. However leukocyte Hmgb1 does not control the expression of scavenger receptors *in vivo* and *in vitro*, nor the secretion of cytokines by polarized macrophages *in vitro*. *In vivo* cytokines mRNA is modulated by leukocyte Hmgb1 at early time points after tissue damage. At the beginning of the repair phase (day7) the gross composition of the infiltration is not depending on leukocyte Hmgb1. The analysis performed so far do not allow for a definitive conclusion about the functional activity of all infiltrating leukocytes. However the few differences revealed cannot account for the big healing defect observed in Hmgb1 KO FLT mice. Thus I have further characterized the homeostatic response of WT and KO FLT mice to injury by analyzing muscle and satellite cell behaviour.

3.5 Leukocyte Hmgb1 barely influences satellite cell biology

I have analyzed the mRNA expression of some transcription factors related to myogenesis such as Pax7, MyoD, Myogenin and I have also analyzed the pro-myogenic factor Igf-1. The analysis is performed at distinct time points on total muscle mRNA. The expression of Pax7 and Igf1 is lower at day5 and 15 in Hmgb1 KO *vs.* WT transplanted mice. However at day7 we know from histology that the number of regenerating fibres is lower. Some of the factors analyzed, such as Igf1, are expressed both by inflammatory cells and muscle fibres. Thus it is not sufficient the qPCR analysis to establish whether the difference is a cause or an effect of the delayed repair.

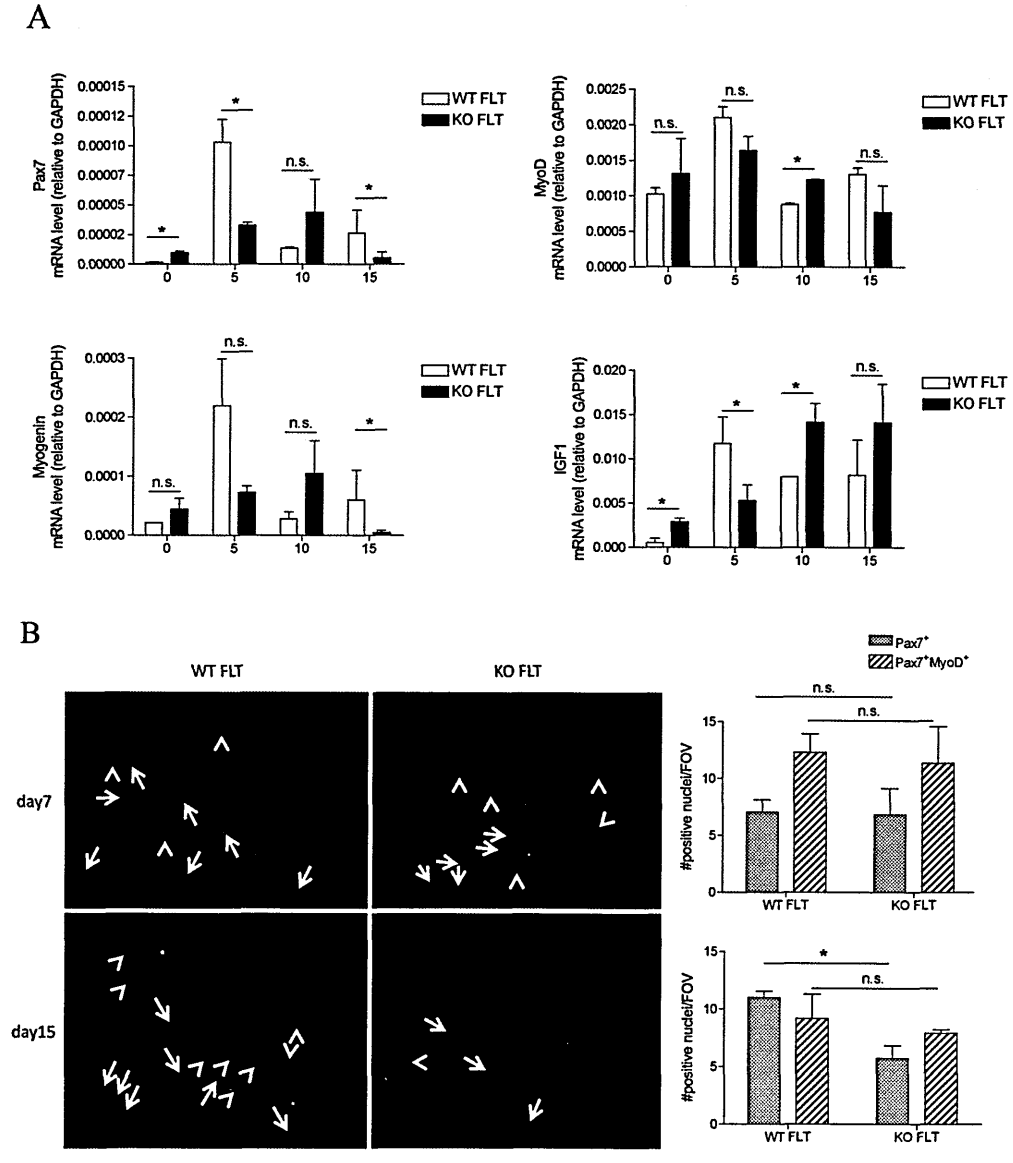

Figure 3.11 – Leukocyte Hmgb1 possibly controls the coming back to a quiescent state of satellite cells. **A.** RT real time PCR on total muscle tissue for transcription factors related to satellite cell function and

myogenesis is performed. *Pax7* expression level is shown in the upper left panel. *MyoD* is shown in the upper right panel. *Myogenin* is shown in lower left panel. *Igf1* expression level is reported in the lower right panel. n=3 per group per time point. **B.** Immunofluorescence for Pax7 (green) and MyoD (red) is performed on frozen section from both WT FLT and KO FLT mice to verify satellite cell activation. At day7 and day15 the number of $Pax7^+$ (arrowheads) and $Pax7^+MyoD^+$ (arrows) satellite cells is counted. Sections from 3 mice/group per each time point are used for cell count (40x magnification). All results are analyzed by t-test for unpaired data and values $p<0.05$ are considered as statistically significant (* = $p<0.05$, n.s. = not significant).

To clarify this point I have stained frozen sections from WT FLT and KO FLT mice at day7 and 15 after CTX injection. The sections are stained for Pax7 and MyoD. I then count the number of $Pax7^+$ or $Pax7^+MyoD^+$ cells. The number of quiescent or early activated, $Pax7^+$ cells is not different in the two groups of mice at day7. At day15 the number of quiescent cells is lower in Hmgb1 KO transplanted mice. The number of activated, double positive cells is not different either at day7 and day15. Our data collectively suggest that leukocyte Hmgb1 is not involved in satellite cell activation at early time points. We cannot exclude that it controls the coming back to a quiescent state of activated satellite cells.

Differentiation is a key step in satellite cell biology. Macrophages have been demonstrated to deeply interact with satellite cells in this phase (44, 47, 143). To verify the role of leukocyte Hmgb1 I have co-cultured pro- (M1 like) or anti-inflammatory (M2 like) macrophages with satellite cells in the presence or in the absence of BoxA. Moreover I have repeated the same co-culture with both WT and KO derived macrophages. Finally I have differentiated satellite cells in the presence of conditioned supernatants from both WT and KO polarized macrophages. Positive controls are satellite cells in differentiation medium (DMEM+5% Horse Serum). Negative controls are satellite cells in growth medium (Ham F10+20% Hyclone). Differentiation is quantified by counting the number of Myosin Heavy Chain (MyHC) positive myotubes with one nucleus, from 2 to 4 nuclei and with more than 5 nuclei.

First I report that BoxA *per se* does not influence satellite cell differentiation (Figure 3.12, panel A). Also satellite cells express Hmgb1 during proliferation and then down regulate it upon differentiation (Figure 3.12, panel B).

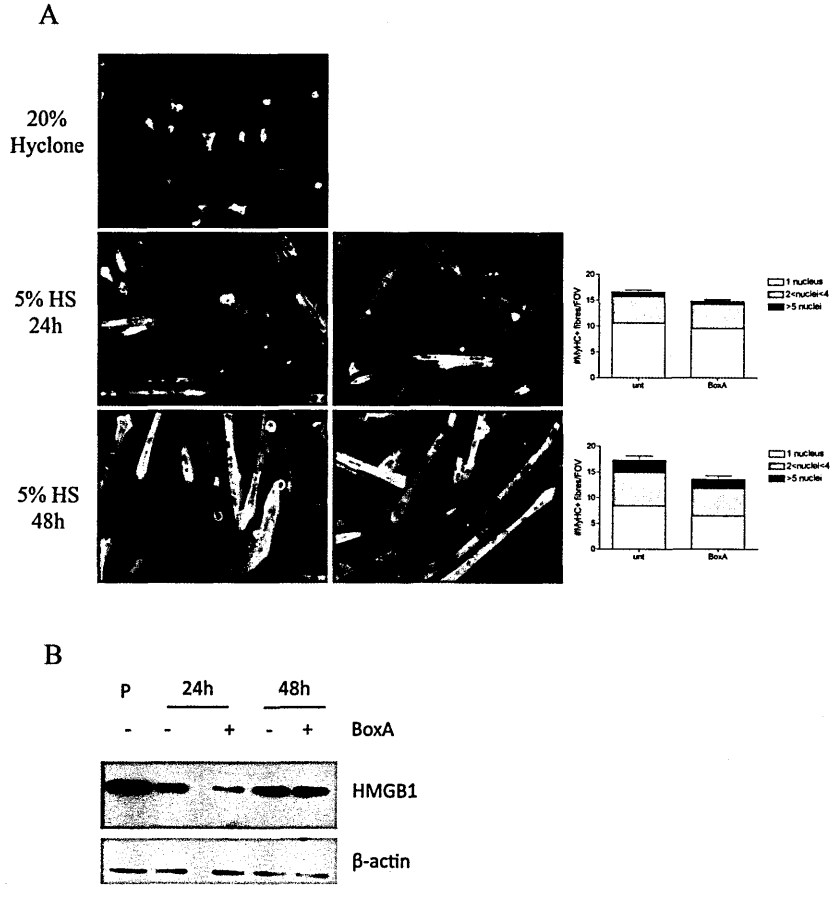

Figure 3.12 – BoxA does not impair satellite cells differentiation. **A.** Satellite cells are left in growth medium (20% Hyclone) as negative control. Satellite cells are differentiated in 5% Horse Serum (HS) for either 24h or 48h in the presence (right pictures) or in the absence (left pictures) of BoxA. In the Immunofluorescence blue is Hoechst 33342 (i.e. nuclei), green is MyHC (i.e. differentiated satellite cells). Quantitative results are reported in the histograms. White is the number of $MyHC^+$ myotubes/field of view (FOV) with one nucleus. Grey is the number of $MyHC^+$ myotubes/FOV with 2 to 4 nuclei. Black is the number of $MyHC^+$ myotubes/FOV with 5 nuclei. Average ± SD of three independent experiments performed in double is reported. Results are compared using ANOVA. $p<0.05$ is considered statistically significant. No significant differences are detected **B.** Hmgb1 expression in proliferating satellite cells (P), differentiating satellite cells (24h) and in differentiated satellite cells (48. Differentiating and differentiated satellite cells are analyzed in the presence or in the absence of BoxA. β-actin is used as housekeeping protein.

Blocking Hmgb1 with BoxA does not influence satellite cell differentiation, both if co-cultured with pro- and anti-inflammatory macrophages (Figure 3.13).

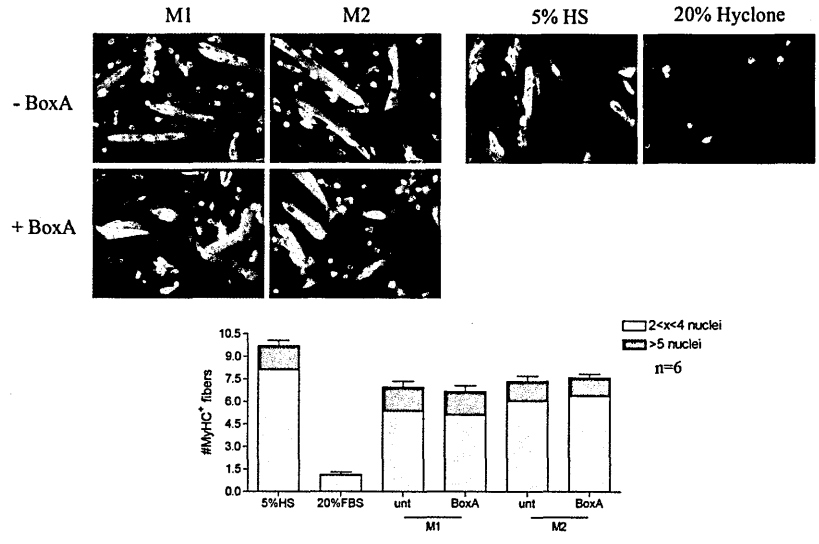

Figure 3.13 – Extracellular Hmgb1 does not control satellite cell differentiation. Co-culture is performed in permissive condition for satellite cell differentiation. Green = MyHC, red = CD11b (macrophages), blue = nuclei (20x magnification). Co-culture is performed in the presence or in the absence of BoxA using both M1 and M2 macrophages. Quantitative results are reported in the histograms. Grey is the number of $MyHC^+$ myotubes/FOV with 2 to 4 nuclei. Dark grey is the number of $MyHC^+$ myotubes/FOV with >5 nuclei. Average ± SD of six independent experiments performed in triplicate is reported. Results are compared using ANOVA. $p<0.05$ is considered statistically significant. No significant differences are detected.

The co-culture is repeated using pro- and anti-inflammatory macrophages both WT and KO derived. No differences are detected in any of the condition analyzed (Figure 3.14).

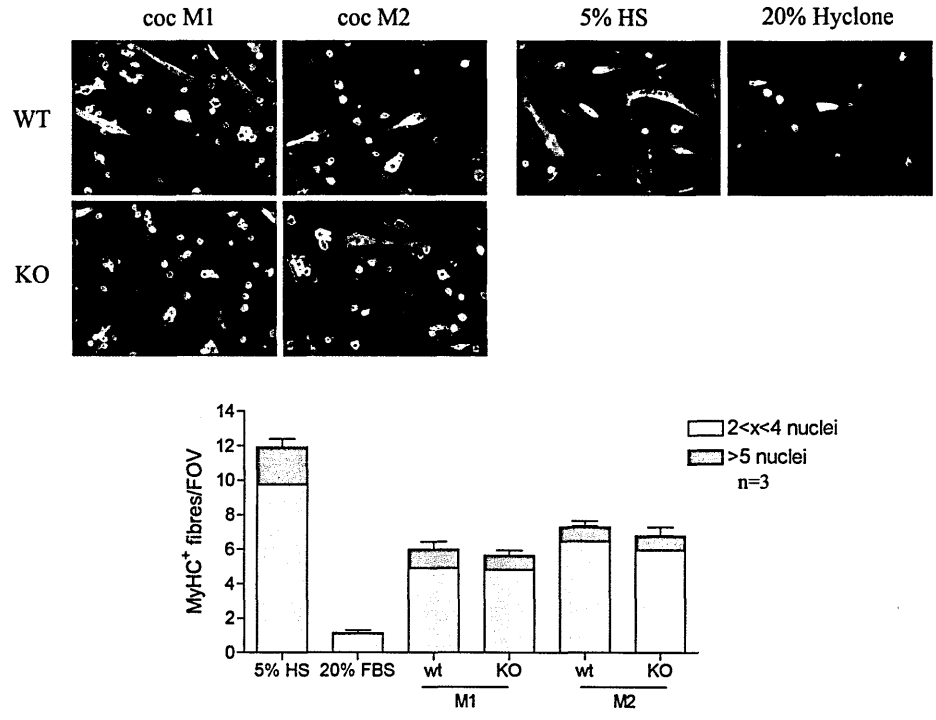

Figure 3.14 – Macrophage Hmgb1 does not influence satellite cell differentiation. Co-culture is performed in permissive condition for satellite cell differentiation. Green = MyHC, red = CD11b (macrophages), blue = nuclei (20x magnification). Quantitative results are reported in the histograms. Grey is the number of $MyHC^+$ myotubes/FOV with 2 to 4 nuclei. Dark grey is the number of $MyHC^+$ myotubes/FOV with >5 nuclei. Average ± SD of three independent experiments performed in triplicate is reported. Results are compared using ANOVA. $p<0.05$ is considered statistically significant. No significant differences are detected.

To definitively rule out the role of macrophage Hmgb1 in the differentiation process of satellite cells I have grown the satellite cells in permissive condition for differentiation in the presence of conditioned supernatants from both WT and KO pro- and anti-inflammatory macrophages. Data confirm that macrophage Hmgb1 does not influence satellite cells differentiation (Figure 3.15). As a control satellite cells are differentiated in the presence of the cytokine used to polarize macrophages (i.e. IFN-γ and IL10).

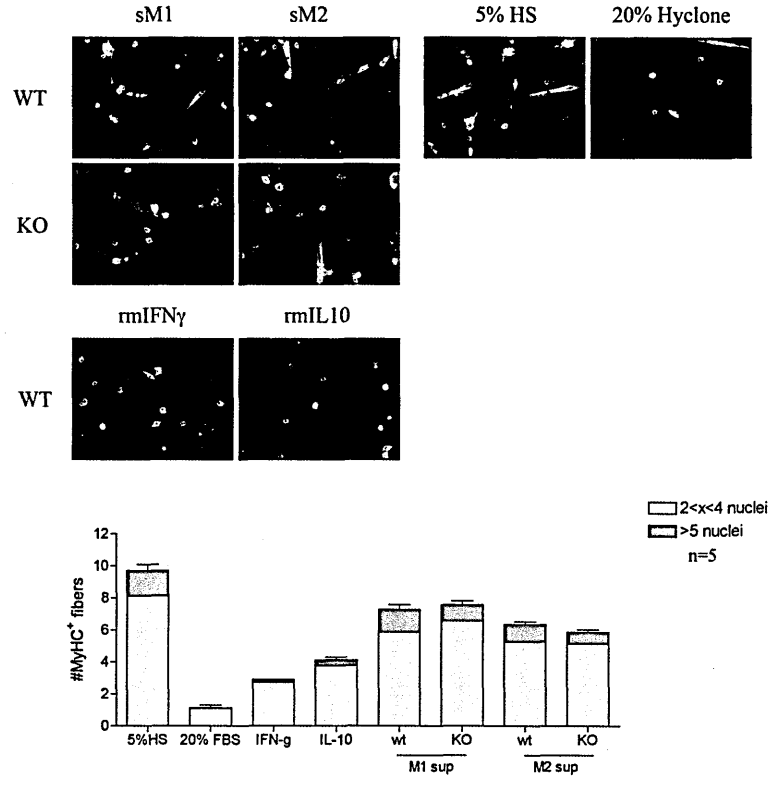

Figure 3.15 – Macrophage Hmgb1 does not influence satellite cell differentiation. Macrophage Hmgb1 does not impair satellite cell differentiation. Satellite cells are plated in permissive condition for differentiation. Green = MyHC, blue = nuclei (20x magnification). Quantitative results are reported in the histograms. Grey is the number of $MyHC^+$ myotubes/FOV with 2 to 4 nuclei. Dark grey is the number of $MyHC^+$ myotubes/FOV with >5 nuclei. Average ± SD of five independent experiments performed in double is reported. Results are compared using ANOVA. $p<0.05$ is considered statistically significant. No significant differences are detected.

Collectively our data suggest that leukocyte Hmgb1 does not control nor influence satellite cell activation and differentiation. We cannot exclude that Hmgb1 play a role in controlling the step back to quiescence of activated satellite cells. However this is not sufficient to explain the dramatic phenotype we observe in muscle already at day7 after damage.

3.6 Leukocyte Hmgb1 controls angiogenesis in repairing muscle

Up to now our results suggest that a modest influence of leukocyte Hmgb1 on inflammatory response is detectable. Leukocyte Hmgb1 does not influence satellite

cells activation during early phase of regeneration (day7). It could be of importance for the control of the coming back to quiescence of satellite cells. However these findings do not explain the dramatic phenotype observed. As mentioned in the introduction correct vascularization is instrumental to healing (6, 11, 16, 144). Hmgb1 has been recently described as an angiogenic molecule (106-108). Thus I have analyzed the role of leukocyte Hmgb1 in the control of vascularization after sterile damage.

To verify whether Hmgb1 controls angiogenesis in repairing muscle I have stained day7 TA for CD31 (Figure 3.16, panel A). The number of vessels has been counted. The analysis reveals that Hmgb1 KO FLT mice display a lower number of vessels respect to Hmgb1 WT FLT mice, indicating a role for leukocyte Hmgb1 in controlling vessel remodelling.

The question is how Hmgb1 controls angiogenesis. I have verified whether leukocyte Hmgb1 controls in a paracrine manner the expression of angiogenic factors in damaged muscle. I have analyzed mRNA expression on total muscle of Vegfβ and Angiopoietin II (AngII) (Figure 3.16, panel B). Vegfβ levels are similar in the two groups of mice. On the contrary AngII levels are dramatically reduced in Hmgb1 KO FLT mice at day5. Our data suggest that leukocyte Hmgb1 controls the transient up-regulation of AngII in early regenerative phase, necessary to allow new vessel sprouting (24). As a consequence at day10 there are higher levels of AngII in KO FLT *vs.* WT FLT muscles. However the peak of AngII expression never reaches the expression levels observed in WT FLT muscles at day5.

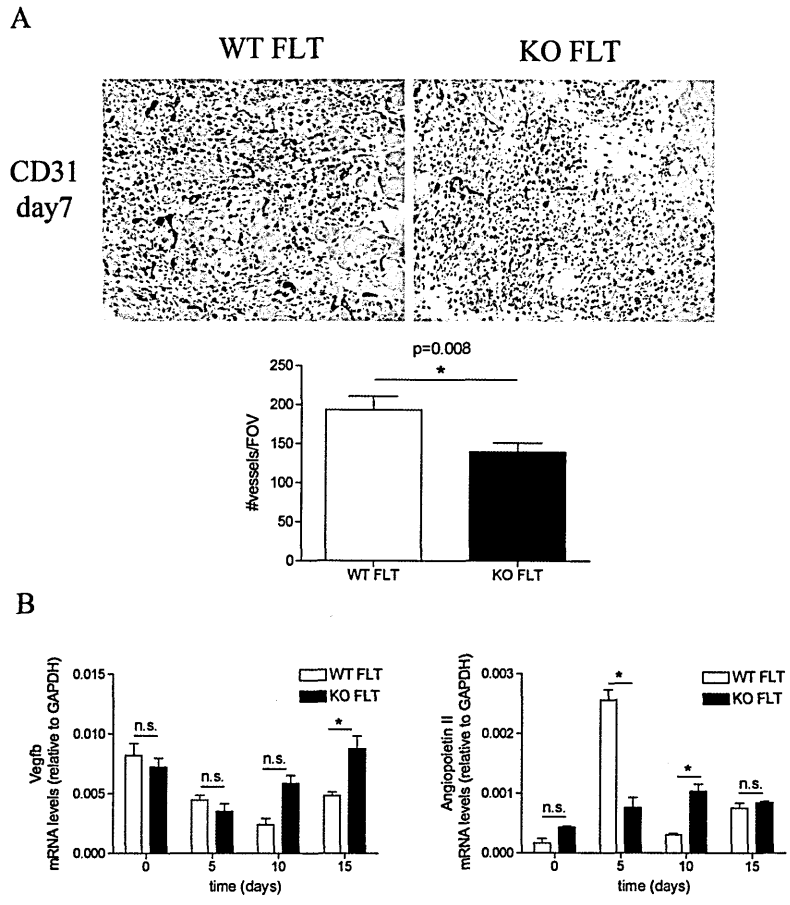

Figure 3.16 – Leukocyte Hmgb1 controls vessel remodelling in repairing muscle. **A.** Frozen sections from WT FLT (left panel) and KO FLT (right panel) TA at day7 after CTX damage are stained for CD31. Vessels are counted in at least 10 fields of view (FOV) at 20x magnification per mouse from 3 mice/group and analyzed by t-test for unpaired data. $p<0,05$ is considered as statistically significant. (*$p<0.05$) **B.** Genes involved in angiogenesis are analyzed by RT real time PCR in WT FLT and KO FLT mice before damage and at distinct time points after CTX injection. *Vegfβ* expression is shown in left panel, *Angiopoietin II* expression is shown in right panel. Data are compared using t-test for unpaired data. $p<0,05$ is considered as statistically significant. (*$p<0.05$)

Thus leukocyte Hmgb1 seems to control the correct kinetic and intensity of expression of AngII. The following question is how leukocyte Hmgb1 controls AngII expression. AngII levels are controlled by hypoxia (24). Therefore I have measured Hif1α mRNA on total muscle at distinct time points (Figure 3.17). In damaged muscles from Hmgb1 WT FLT mice Hif1α mRNA peaks at day5 after damage, while it is not upregulated in muscles from Hmgb1 KO FLT mice. Consistently with the previous

finding at day10 in KOFLT muscles there is a persistence of Hif1α expression that however never reaches the peak of WT FLT muscle at day5. The present data suggest that leukocyte Hmgb1 controls hypoxia sensing in damaged muscle. To further confirm this hypothesis I have measured mRNA levels of some Hif1α target genes, since Hif1α is modulated at post-translational level. According to Hif1α expression defect at day5, mRNA levels of carbonic anidrase IX (CAIX) and of Glut1 are dramatically reduced in Hmgb1 KO FLT compared with Hmgb1 WT FLT mice at day5. Our data support a role for leukocyte Hmgb1 in vessel remodelling, possibly licensing damaged tissue to sense hypoxia thus driving angiogenic factor expression.

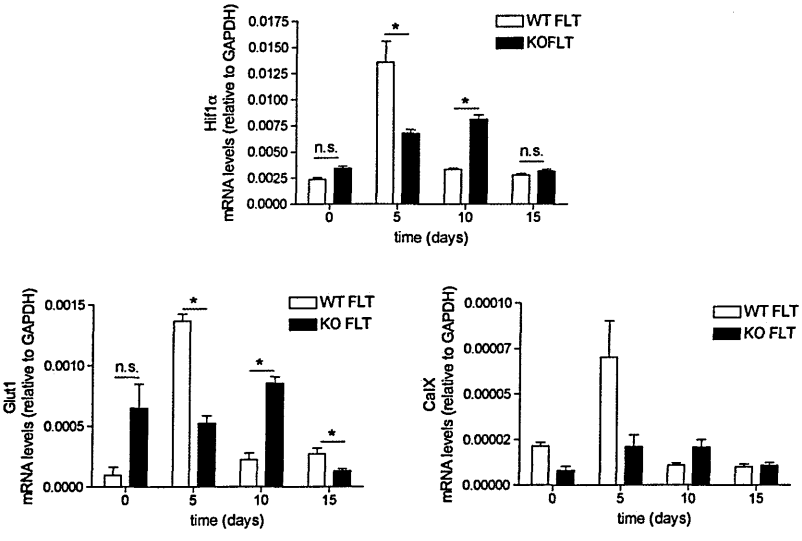

Figure 3.17 – Leukocyte Hmgb1 licenses damaged muscle to sense hypoxia in early phase of tissue repair. **C.** *Hif1α* mRNA expression is evaluated on total muscle before damage and at distinct time points after CTX injection (upper panel). HIF1α target genes are analyzed by RT real time PCR on the same samples. *Glut1* is reported in lower left panel and *CaIX* is reported in lower right panel. Data were analyzed by t-test for unpaired data. $p<0,05$ was considered as statistically significant (* = $p<0.05$, n.s. = not significant).

Owing to the pleiotropic effects of Hmgb1 (see INTRODUCTION) it has been so far unclear whether its role in wound healing depends on the Hmgb1 derived from infiltrating leukocytes or from damaged tissues. My experimental model allows solving this issue. Its main feature is the possibility of recreating a chimeric situation in which damaged muscle are Hmgb1

proficient and infiltrating leukocytes are either Hmgb1 proficient or deficient. In the discussion hints on results interpretation and limits of the chimeric model are provided.

DISCUSSION-2

In the present work we aimed at verifying a non-redundant role for leukocyte Hmgb1 in muscle healing, a prototype of the healing process in sterile injuries. The combined pharmacological blockade and an animal model that I have established ad hoc, in which leukocytes selectively lack Hmgb1. The set up of the foetal liver transplantation procedure is first discussed here. When a chimera is generated the main issue to address is the chimerism. Chimerism on peripheral blood is satisfactory being routinely >90% of donor cells in the WT into WT setting. White blood cells are generated in the bone marrow (145). The chimerism in the bone marrow is even higher than in peripheral blood being routinely >95%. I have also demonstrated that the total of the bone marrow myeloid population is of donor origin. The population of $CD45^-$ cells revealed in the bone marrow is likely to be composed by stromal and endothelial cells. In the spleen, lymph nodes and peritoneal liquid the chimerism is satisfactory as well. The population of $CD45^-$ cells in the spleen is possibly composed by stromal cells and red blood cells. It is intriguing to see a small percentage of cells that express both CD45.1 and CD45.2 markers. A fascinating hypothesis suggests that they are viable cells that have eaten dead counterparts and then they present on the surface the antigens of the dead counterparts (146, 147). In other words a viable $CD45.2^+$ cells could have eaten a dead $CD45.1^+$ cell and then it could have presented through MHC class I or class II molecule a fragment of the CD45.1 antigen, that is the epitope recognised by the antibody. Other explanation can be simply that the double positive cells are doublets that for some reasons elude the negative selection of doublets during acquisition of data, thus being merely the result of a technical bias. Another issue is the chimerism at muscle level after CTX injection. Residual host cells could have a selective advantage over donor cells and be preferentially recruited at the site of damage. Around 90% of infiltrating macrophages ($CD11b^+$ cells) is of donor origin, thus excluding this possibility. Finally the muscle of irradiated and transplanted mice heals with a kinetic

similar to untransplanted mice. This is confirmed both by histology and MRI. It seems that a slightly higher infiltrate is present at day3 and 7, probably as a consequence of the irradiation procedure that *per se* elicits inflammation. This can be seen both by histology and by MRI analysis. However the increase of inflammatory cells is minimal and does not hamper muscle repair.

The satisfactory results in the WT into WT setting do not imply an equal efficacy when Hmgb1$^{-/-}$ foetal liver cells are transplanted. Another member of the High Mobility Group superfamily of protein, Hmgb3, has been shown to be crucial in the balance between self-renewal and differentiation in haematopoiesis (148). It is not excluded that Hmgb1 could play a similar role. The chimerism on peripheral blood is good also in Hmgb1-/- FLT mice, being routinely >85% donor. However a higher percentage of residual host cells is detected. This result seems to indicate that Hmgb1$^{-/-}$ foetal liver cells have a lower ability to engraft. Haemochrome analysis reveals that erythropoiesis is conserved in Hmgb1$^{-/-}$ FLT mice. On the contrary platelet and white blood cells generation is impaired, since a lower number is detected. Since the number of white blood cells is reduced, the higher percentage of host cells results in a lower number of circulating host cells. In conclusion the chimerism is satisfactory and the number of circulating residual host cell is negligible. This is also confirmed by the fact that Hmgb1 in circulating white blood cells of Hmgb1$^{-/-}$ FLT mice is barely detectable. However the impaired generation of white blood cells opens a question about the composition of peripheral blood and bone marrow. Are all the populations equally represented in the two groups of mice? The analysis by flow cytometry unveils no differences. Hmgb3 deficiency is supposed to enlarge the production of precursors at the expenses of more mature cells. It is conceivable that Hmgb1 plays a similar role in managing the balance between precursors and mature cells. This remains just a speculation, since I have not analyzed precursors.

Keeping in mind the possible limitation coming from an aberrant number of circulating white blood cells I have analyzed the chimerism at muscle level after CTX damage. The chimerism analysis confirms that the chimerism is satisfactory both in $Hmgb1^{+/+}$ FLT and $Hmgb1^{-/-}$ FLT mice. Thus I continued analyzing the outcome of muscle repair in $Hmgb1^{-/-}$ FLT but also in mice treated intramuscularly (i.m.) with BoxA. Analyzing in parallel $Hmgb1^{-/-}$ FLT mice and mice treated with BoxA i.m. gives the possibility to dissect the role of extracellular Hmgb1 respect to leukocyte Hmgb1.

Through *in vivo* imaging and cytofluorimetric analysis we are able to demonstrate that the pharmacological block of extracellular Hmgb1 results in an impairment in the recruitment of inflammatory leukocytes. Interestingly, in our model in which leukocytes do not express Hmgb1 these results are not replicated suggesting that muscle (extracellular) Hmgb1 is primarily controlling leukocyte attraction.

Mice lacking leukocyte Hmgb1 have an impaired, but not absent, muscle healing. The healing defect points to a non-redundant role for leukocyte Hmgb1 in muscle repair, distinct from the role of total extracellular Hmgb1. In mice treated with BoxA the defect is limited to day15, when some residual necrotic fibers are revealed by histological analysis. However the defect is rapidly recovered and it is not as dramatic as in Hmgb1 KO FLT mice. The aberrant healing in this group of mice possibly involves a defective activation or differentiation of muscle stem cells. This does not seem to be the case: both *in vitro* and *in vivo* leukocyte Hmgb1 does not influence satellite cell differentiation and activation. Leukocyte Hmgb1 can be involved in the ability of satellite cells to replenish the quiescent satellite cell pool: TA from *Hmgb1* KO transplanted mice show a lower number of quiescent satellite cells. This is consistent with a recent report about the role of Hmgb1-RAGE axis in satellite cell quiescence (113). Quiescent satellite cell pool replenishment apparently does not justify the impaired muscle regeneration. Expression of myogenesis-related genes in muscles from *Hmgb1* KO transplanted mice is a consequence of the healing impairment rather

than a cause of the impairment itself. Leukocyte Hmgb1 results in a more effective regeneration, which is in turn dependent on the activation, proliferation and differentiation of satellite cells. When these events are jeopardized, such as in muscles from *Hmgb1* KO transplanted mice, expression of myogenesis related genes abates. As a result of a compensation effort of muscle to regenerate all myogenesis related genes experience a late peak of expression at day10 after CTX injection. Given the dramatic healing defect observed at day15 this compensatory reaction proves to be largely inefficient. It is possible that leukocyte Hmgb1 is crucial in orchestrating early events in the repair process. In the absence of these early events the healing of the tissue is compromised. The lack of expression of myogenic genes in Hmgb1 KO FLT mice may be a result of an overall decreased gene expression due to defective regeneration or a cause of the defect observed. The observation that at early times after injury the protein expression of myogenic factors such as Pax7 and MyoD is normal partially confirms the hypothesis of an overall reduced gene expression due to reduced myogenesis.

Leukocyte Hmgb1 controls angiogenesis in regenerating muscle: this is demonstrated by the lower number of vessels in muscles from *Hmgb1* KO transplanted mice. In physiological condition muscle repair depends on vascularization (48). We have thus monitored the expression of angiogenic signals such as Vegfβ and Ang2. Vegfβ is present at normal levels in mice lacking leukocyte Hmgb1 at any time point analyzed. In contrast Ang2 is dramatically reduced. Ang2 regulation is strictly required for vessel remodelling (24).

Collectively these data suggest that leukocyte Other signals, such as IL6 and TNFα may be also involved (16). Leukocyte Hmgb1 controls the expression of il6 and tnfα mRNA. The defect in il6 and tnfα mRNA production in Hmgb1 KO FLT mice can in part control angiogenesis even if macrophages secrete the protein in the absence of Hmgb1 when stimulated *in vitro*.

This does not necessarily reflect what happens *in vivo*. Macrophages *in vitro* are cultured at an oxygen partial pressure similar to room air. In the tissue, macrophages are found into a lower oxygen partial pressure (6, 18). It is well known that inflammatory reaction and O_2 tension are related (16, 24, 149). It has been proposed that damaged cells express and secrete molecules which modify key features of the extracellular environment, such as oxidoreductases and redox modifiers: in turn this signals cause structural and functional alterations in crucial pathways that mediate the cell response to environmental cues (150). Hypoxia is a major stimulus for the production of angiogenic factors such as Ang2, Tnfα and possibly IL6 (6, 16, 21). Hypoxia sensing *in vivo* passes mainly through HIF1α (6, 24). Leukocyte Hmgb1 is instrumental for the transcription of Hif1α. HIF1α activity is mainly controlled at post-translational level (6, 18). To verify whether HIF1α activity is also reduced we monitored the transcript of Hif1α target genes, such as carbonic anidrase 9 (CAIX) and the glucose transporter Glut1. The observation that both of them are reduced further strength the hypothesis that leukocyte Hmgb1 controls hypoxia sensing in regenerating muscle.

Besides CAIX and Glut1 the activation of other genes has been shown to depend on Hif1α. This is the case of VEGFβ (144). However I have failed to observe an effect of leukocyte Hmgb1 on VEGFβ production, suggesting that a hypoxia-independent pathway is involved, such as the EGFR/PI3K pathway recently proposed to be involved in VEGFβ secretion by tumour cells (151). Both endothelial cells and alternatively activated macrophages produce high amounts of VEGFβ (7). Previous data in the laboratory demonstrate that macrophages infiltrating the injured and regenerating muscle display an alternatively activated phenotype (42). They could be responsible for a hypoxia-independent VEGFβ production, which could involve the response to locally generated IL10. It has been recently described that stimulating monocytes with cancer cell supernatants containing IL10 results in monocyte production of pro-angiogenic

factor such as VEGF and bFGF in a hypoxia-independent manner (152). Further experiments would be required to confirm this hypothesis.

Collectively our data suggest that leukocyte Hmgb1 licenses damaged tissues to sense hypoxia. The hypoxia sensing allows the production of several angiogenic factors. The production of those factors mediates vessel remodelling, angiogenesis and ultimately effective healing (see cartoon below).

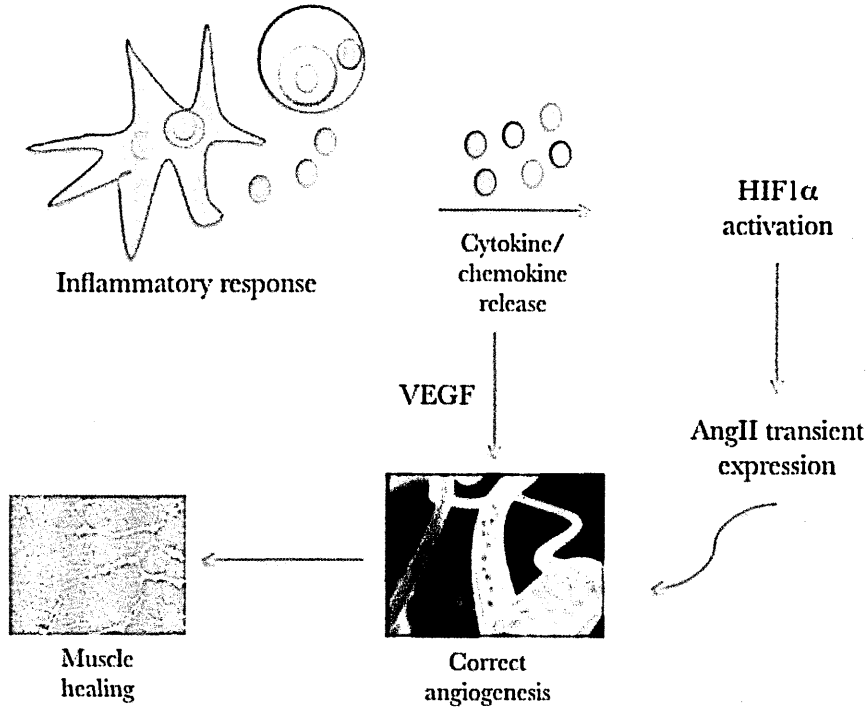

A model for angiogenesis regulation by leukocyte Hmgb1 in damaged tissues. During inflammatory response following damage hypoxia in a hallmark of the injured, inflamed tissues. Leukocyte Hmgb1 licenses the tissue to sense hypoxia. Hypoxia sensing prompts the production of angiogenic molecules (TNFα, IL6 and Ang2). The balance among these factors leads to reconstitution of the vascular bed and ultimately to tissue healing.

Our model may apply also to other fisiopathological conditions in which vascularization is jeopardized. This could apply to solid neoplasms in which HIF1α controls Ang2 expression (6, 18, 21). Generally the mechanisms underlying the regulation of HIF1α/Ang2 expression are poorly understood. It is tempting to further

investigate the role of leukocyte Hmgb1 in controlling hypoxia sensing and angiogenesis in damaged tissues.

In this model many points need further clarification. First it is not clear how leukocyte Hmgb1 could influence hypoxia sensing. It could be a direct effect of the secreted protein on neighbouring endothelial and muscle cells. It could be also an indirect effect: Hmgb1 is a nuclear factor deeply involved in transcriptional control. It could mediate the expression of one or more factors by leukocytes and the unknown factors are the responsible for the hypoxia sensing effect. It is also not clear how Hmgb1 control antigen presentation. I have evidenced some defects in the expression of molecules involved in this process that is of pivotal importance for the activation of adaptive responses, important as well to determine the correct reaction to tissue damage. The development of adaptive response needs further clarification and functional experiments to be substantiated. For example it would be interesting to perform an antigen presentation assay using dendritic cells and macrophages either Hmgb1 WT or KO and WT or KO syngeneic splenocytes. Another key point is whether the effect is directly on endothelial cell by enhancing their sprouting ability or whether leukocyte Hmgb1 controls the recruitment and the proliferation of pericytes and of endothelial precursors cells (79). Very recently a new mouse model that allows tracking of pericytes is available in the lab. It would be interesting to perform transplantation of Hmgb1 KO precursors in this model and then to verify the contribution to regeneration of pericytes.

In conclusion my animal model allows showing for the first time that leukocyte Hmgb1 controls muscle regeneration and possibly satellite cell turnover in damaged muscle. The control of muscle regeneration is likely to be mediated through the control of the vascularization of regenerating muscle. Our major hypothesis that needs to be further demonstrated states that leukocyte Hmgb1 controls muscle repair through the control of vascularization that is achieved by controlling hypoxia sensing at early

phases of healing. The main limitation of this study is the use of the chimera where a percentage, albeit negligible, of residual host cells is always present and could dilute some of the effects observed. Another limitation is the difficulty to mimic in vitro the complex relationship muscle-endothelium-leukocyte in order to dissect molecular events underlying this relationship. The main strength of the system is the unique opportunity to dissect the relative role of leukocyte and tissue Hmgb1, since up to now no animal model lacking only one of the two sources of Hmgb1 were present. It would be of importance to dissect the relative role of the two Hmgb1 also in other settings than muscle damage such as tumours or ischemic damage, where it has been demonstrated a general role for Hmgb1 but without dissecting the molecular basis of this event (103, 106, 124, 153, 154). That would be not only a biological speculation but would help in setting up therapies targeted to the dangerous component of the Hmgb1 response but sparing the useful one. For example in tumours it would be of importance to spare a possible role in antigen presentation and T cell activation while eliminating an angiogenic response useful for tumour growth.

BIBLIOGRAPHY

1. Bianchi, M.E. 2009. HMGB1 loves company. *J Leukoc Biol* 86:573-576.
2. Arnold, L., Henry, A., Poron, F., Baba-Amer, Y., van Rooijen, N., Plonquet, A., Gherardi, R.K., and Chazaud, B. 2007. Inflammatory monocytes recruited after skeletal muscle injury switch into antiinflammatory macrophages to support myogenesis. *J Exp Med* 204:1057-1069.
3. Straino, S., Di Carlo, A., Mangoni, A., De Mori, R., Guerra, L., Maurelli, R., Panacchia, L., Di Giacomo, F., Palumbo, R., Di Campli, C., et al. 2008. High-mobility group box 1 protein in human and murine skin: involvement in wound healing. *J Invest Dermatol* 128:1545-1553.
4. Chanson, M., Derouette, J.P., Roth, I., Foglia, B., Scerri, I., Dudez, T., and Kwak, B.R. 2005. Gap junctional communication in tissue inflammation and repair. *Biochim Biophys Acta* 1711:197-207.
5. Schmidt, E.P., Lee, W.L., Zemans, R.L., Yamashita, C., and Downey, G.P. On, around, and through: neutrophil-endothelial interactions in innate immunity. *Physiology (Bethesda)* 26:334-347.
6. Imtiyaz, H.Z., and Simon, M.C. Hypoxia-inducible factors as essential regulators of inflammation. *Curr Top Microbiol Immunol* 345:105-120.
7. Brancato, S.K., and Albina, J.E. Wound macrophages as key regulators of repair: origin, phenotype, and function. *Am J Pathol* 178:19-25.
8. Mosser, D.M., and Edwards, J.P. 2008. Exploring the full spectrum of macrophage activation. *Nat Rev Immunol* 8:958-969.
9. Lucas, T., Waisman, A., Ranjan, R., Roes, J., Krieg, T., Muller, W., Roers, A., and Eming, S.A. Differential roles of macrophages in diverse phases of skin repair. *J Immunol* 184:3964-3977.

10. Leibovich, S.J., and Ross, R. 1975. The role of the macrophage in wound repair. A study with hydrocortisone and antimacrophage serum. *Am J Pathol* 78:71-100.

11. Mirza, R., DiPietro, L.A., and Koh, T.J. 2009. Selective and specific macrophage ablation is detrimental to wound healing in mice. *Am J Pathol* 175:2454-2462.

12. Geissmann, F., Jung, S., and Littman, D.R. 2003. Blood monocytes consist of two principal subsets with distinct migratory properties. *Immunity* 19:71-82.

13. Cordeiro-da-Silva, A., Tavares, J., Araujo, N., Cerqueira, F., Tomas, A., Kong Thoo Lin, P., and Ouaissi, A. 2004. Immunological alterations induced by polyamine derivatives on murine splenocytes and human mononuclear cells. *Int Immunopharmacol* 4:547-556.

14. Fadok, V.A., Bratton, D.L., Konowal, A., Freed, P.W., Westcott, J.Y., and Henson, P.M. 1998. Macrophages that have ingested apoptotic cells in vitro inhibit proinflammatory cytokine production through autocrine/paracrine mechanisms involving TGF-beta, PGE2, and PAF. *J Clin Invest* 101:890-898.

15. Goren, I., Allmann, N., Yogev, N., Schurmann, C., Linke, A., Holdener, M., Waisman, A., Pfeilschifter, J., and Frank, S. 2009. A transgenic mouse model of inducible macrophage depletion: effects of diphtheria toxin-driven lysozyme M-specific cell lineage ablation on wound inflammatory, angiogenic, and contractive processes. *Am J Pathol* 175:132-147.

16. Arroyo, A.G., and Iruela-Arispe, M.L. Extracellular matrix, inflammation, and the angiogenic response. *Cardiovasc Res* 86:226-235.

17. De Smet, F., Segura, I., De Bock, K., Hohensinner, P.J., and Carmeliet, P. 2009. Mechanisms of vessel branching: filopodia on endothelial tip cells lead the way. *Arterioscler Thromb Vasc Biol* 29:639-649.

18. Denko, N.C. 2008. Hypoxia, HIF1 and glucose metabolism in the solid tumour. *Nat Rev Cancer* 8:705-713.

19. Germain, S., Monnot, C., Muller, L., and Eichmann, A. Hypoxia-driven angiogenesis: role of tip cells and extracellular matrix scaffolding. *Curr Opin Hematol* 17:245-251.

20. Liu, Q., Li, G., Li, R., Shen, J., He, Q., Deng, L., Zhang, C., and Zhang, J. IL-6 promotion of glioblastoma cell invasion and angiogenesis in U251 and T98G cell lines. *J Neurooncol* 100:165-176.

21. Anglesio, M.S., George, J., Kulbe, H., Friedlander, M., Rischin, D., Lemech, C., Power, J., Coward, J., Cowin, P.A., House, C.M., et al. IL6-STAT3-HIF signaling and therapeutic response to the angiogenesis inhibitor sunitinib in ovarian clear cell cancer. *Clin Cancer Res* 17:2538-2548.

22. Roberts, A.B., and Sporn, M.B. 1989. Regulation of endothelial cell growth, architecture, and matrix synthesis by TGF-beta. *Am Rev Respir Dis* 140:1126-1128.

23. Singh, H., Hansen, T.M., Patel, N., and Brindle, N.P. The molecular balance between receptor tyrosine kinases Tie1 and Tie2 is dynamically controlled by VEGF and TNFalpha and regulates angiopoietin signalling. *PLoS One* 7:e29319.

24. Fiedler, U., and Augustin, H.G. 2006. Angiopoietins: a link between angiogenesis and inflammation. *Trends Immunol* 27:552-558.

25. Kondo, T., and Ishida, Y. Molecular pathology of wound healing. *Forensic Sci Int* 203:93-98.

26. Crosby, L.M., and Waters, C.M. Epithelial repair mechanisms in the lung. *Am J Physiol Lung Cell Mol Physiol* 298:L715-731.

27. El Sabbahy, M., and Vaidya, V.S. Ischemic kidney injury and mechanisms of tissue repair. *Wiley Interdiscip Rev Syst Biol Med* 3:606-618.

28. Jiang, B., and Liao, R. The paradoxical role of inflammation in cardiac repair and regeneration. *J Cardiovasc Transl Res* 3:410-416.

29. Paylor, B., Natarajan, A., Zhang, R.H., and Rossi, F. Nonmyogenic cells in skeletal muscle regeneration. *Curr Top Dev Biol* 96:139-165.

30. Le Grand, F., and Rudnicki, M.A. 2007. Skeletal muscle satellite cells and adult myogenesis. *Curr Opin Cell Biol* 19:628-633.

31. Kerr, B.K. 2003. *Functiona Histology Atlas*: Casa Editrice Ambrosiana. 402 pp.

32. Le Gros Clark, W.E. 1946. An experimental study of the regeneration of mammalian striped muscle. *Journal of Anatomy* 80.

33. Godman, G.C. 1957. On the regeneration and redifferentiation of mammalian striated muscle. *Journal of Morphology* 100.

34. Mauro, A. 1961. Satellite cell of skeletal muscle fibers. *J Biophys Biochem Cytol* 9:493-495.

35. Wagers, A.J., and Conboy, I.M. 2005. Cellular and molecular signatures of muscle regeneration: current concepts and controversies in adult myogenesis. *Cell* 122:659-667.

36. Moss, F.P., and Leblond, C.P. 1970. Nature of dividing nuclei in skeletal muscle of growing rats. *J Cell Biol* 44:459-462.

37. Joe, A.W., Yi, L., Natarajan, A., Le Grand, F., So, L., Wang, J., Rudnicki, M.A., and Rossi, F.M. Muscle injury activates resident fibro/adipogenic progenitors that facilitate myogenesis. *Nat Cell Biol* 12:153-163.

38. Tidball, J.G., Berchenko, E., and Frenette, J. 1999. Macrophage invasion does not contribute to muscle membrane injury during inflammation. *J Leukoc Biol* 65:492-498.

39. Teixeira, C.F., Zamuner, S.R., Zuliani, J.P., Fernandes, C.M., Cruz-Hofling, M.A., Fernandes, I., Chaves, F., and Gutierrez, J.M. 2003. Neutrophils do not contribute to local tissue damage, but play a key role in skeletal muscle

regeneration, in mice injected with Bothrops asper snake venom. *Muscle Nerve* 28:449-459.

40. Nguyen, H.X., and Tidball, J.G. 2003. Null mutation of gp91phox reduces muscle membrane lysis during muscle inflammation in mice. *J Physiol* 553:833-841.

41. Honda, H., Kimura, H., and Rostami, A. 1990. Demonstration and phenotypic characterization of resident macrophages in rat skeletal muscle. *Immunology* 70:272-277.

42. Vezzoli, M., Castellani, P., Campana, L., Corna, G., Bosurgi, L., Manfredi, A.A., Bianchi, M.E., Rubartelli, A., and Rovere-Querini, P. Redox remodeling: a candidate regulator of HMGB1 function in injured skeletal muscle. *Ann N Y Acad Sci* 1209:83-90.

43. Tidball, J.G., and Villalta, S.A. Regulatory interactions between muscle and the immune system during muscle regeneration. *Am J Physiol Regul Integr Comp Physiol* 298:R1173-1187.

44. Husmann, I., Soulet, L., Gautron, J., Martelly, I., and Barritault, D. 1996. Growth factors in skeletal muscle regeneration. *Cytokine Growth Factor Rev* 7:249-258.

45. Olson, E.N., Sternberg, E., Hu, J.S., Spizz, G., and Wilcox, C. 1986. Regulation of myogenic differentiation by type beta transforming growth factor. *J Cell Biol* 103:1799-1805.

46. Allen, R.E., and Boxhorn, L.K. 1989. Regulation of skeletal muscle satellite cell proliferation and differentiation by transforming growth factor-beta, insulin-like growth factor I, and fibroblast growth factor. *J Cell Physiol* 138:311-315.

47. Charge, S.B., and Rudnicki, M.A. 2004. Cellular and molecular regulation of muscle regeneration. *Physiol Rev* 84:209-238.

48. Borselli, C., Storrie, H., Benesch-Lee, F., Shvartsman, D., Cezar, C., Lichtman, J.W., Vandenburgh, H.H., and Mooney, D.J. Functional muscle regeneration with combined delivery of angiogenesis and myogenesis factors. *Proc Natl Acad Sci U S A* 107:3287-3292.

49. Sorci, G., Riuzzi, F., Arcuri, C., Giambanco, I., and Donato, R. 2004. Amphoterin stimulates myogenesis and counteracts the antimyogenic factors basic fibroblast growth factor and S100B via RAGE binding. *Mol Cell Biol* 24:4880-4894.

50. Warren, G.L., O'Farrell, L., Summan, M., Hulderman, T., Mishra, D., Luster, M.I., Kuziel, W.A., and Simeonova, P.P. 2004. Role of CC chemokines in skeletal muscle functional restoration after injury. *Am J Physiol Cell Physiol* 286:C1031-1036.

51. Bianchi, M.E. 2007. DAMPs, PAMPs and alarmins: all we need to know about danger. *J Leukoc Biol* 81:1-5.

52. Matzinger, P. 1998. An innate sense of danger. *Semin Immunol* 10:399-415.

53. Bianchi, M.E., and Manfredi, A. 2004. Chromatin and cell death. *Biochim Biophys Acta* 1677:181-186.

54. Dumitriu, I.E., Baruah, P., Manfredi, A.A., Bianchi, M.E., and Rovere-Querini, P. 2005. HMGB1: guiding immunity from within. *Trends Immunol* 26:381-387.

55. Scaffidi, P., Misteli, T., and Bianchi, M.E. 2002. Release of chromatin protein HMGB1 by necrotic cells triggers inflammation. *Nature* 418:191-195.

56. Bell, C.W., Jiang, W., Reich, C.F., 3rd, and Pisetsky, D.S. 2006. The extracellular release of HMGB1 during apoptotic cell death. *Am J Physiol Cell Physiol* 291:C1318-1325.

57. Urbonaviciute, V., Furnrohr, B.G., Meister, S., Munoz, L., Heyder, P., De Marchis, F., Bianchi, M.E., Kirschning, C., Wagner, H., Manfredi, A.A., et al. 2008. Induction of inflammatory and immune responses by HMGB1-

nucleosome complexes: implications for the pathogenesis of SLE. *J Exp Med* 205:3007-3018.

58. Rovere-Querini, P., Capobianco, A., Scaffidi, P., Valentinis, B., Catalanotti, F., Giazzon, M., Dumitriu, I.E., Muller, S., Iannacone, M., Traversari, C., et al. 2004. HMGB1 is an endogenous immune adjuvant released by necrotic cells. *EMBO Rep* 5:825-830.

59. Wang, H., Bloom, O., Zhang, M., Vishnubhakat, J.M., Ombrellino, M., Che, J., Frazier, A., Yang, H., Ivanova, S., Borovikova, L., et al. 1999. HMG-1 as a late mediator of endotoxin lethality in mice. *Science* 285:248-251.

60. Abraham, E., Arcaroli, J., Carmody, A., Wang, H., and Tracey, K.J. 2000. HMG-1 as a mediator of acute lung inflammation. *J Immunol* 165:2950-2954.

61. Andersson, U., Wang, H., Palmblad, K., Aveberger, A.C., Bloom, O., Erlandsson-Harris, H., Janson, A., Kokkola, R., Zhang, M., Yang, H., et al. 2000. High mobility group 1 protein (HMG-1) stimulates proinflammatory cytokine synthesis in human monocytes. *J Exp Med* 192:565-570.

62. Zhang, X., Guo, L., Collage, R.D., Stripay, J.L., Tsung, A., Lee, J.S., and Rosengart, M.R. Calcium/calmodulin-dependent protein kinase (CaMK) Ialpha mediates the macrophage inflammatory response to sepsis. *J Leukoc Biol* 90:249-261.

63. Gardella, S., Andrei, C., Ferrera, D., Lotti, L.V., Torrisi, M.R., Bianchi, M.E., and Rubartelli, A. 2002. The nuclear protein HMGB1 is secreted by monocytes via a non-classical, vesicle-mediated secretory pathway. *EMBO Rep* 3:995-1001.

64. Bonaldi, T., Talamo, F., Scaffidi, P., Ferrera, D., Porto, A., Bachi, A., Rubartelli, A., Agresti, A., and Bianchi, M.E. 2003. Monocytic cells hyperacetylate chromatin protein HMGB1 to redirect it towards secretion. *EMBO J* 22:5551-5560.

65. Lamkanfi, M., Sarkar, A., Vande Walle, L., Vitari, A.C., Amer, A.O., Wewers, M.D., Tracey, K.J., Kanneganti, T.D., and Dixit, V.M. Inflammasome-dependent release of the alarmin HMGB1 in endotoxemia. *J Immunol* 185:4385-4392.

66. Dupont, N., Jiang, S., Pilli, M., Ornatowski, W., Bhattacharya, D., and Deretic, V. Autophagy-based unconventional secretory pathway for extracellular delivery of IL-1beta. *EMBO J* 30:4701-4711.

67. Hori, O., Brett, J., Slattery, T., Cao, R., Zhang, J., Chen, J.X., Nagashima, M., Lundh, E.R., Vijay, S., Nitecki, D., et al. 1995. The receptor for advanced glycation end products (RAGE) is a cellular binding site for amphoterin. Mediation of neurite outgrowth and co-expression of rage and amphoterin in the developing nervous system. *J Biol Chem* 270:25752-25761.

68. Rauvala, H., and Rouhiainen, A. Physiological and pathophysiological outcomes of the interactions of HMGB1 with cell surface receptors. *Biochim Biophys Acta* 1799:164-170.

69. Ling, Y., Yang, Z.Y., Yin, T., Li, L., Yuan, W.W., Wu, H.S., and Wang, C.Y. Heparin changes the conformation of high-mobility group protein 1 and decreases its affinity toward receptor for advanced glycation endproducts in vitro. *Int Immunopharmacol* 11:187-193.

70. van Beijnum, J.R., Buurman, W.A., and Griffioen, A.W. 2008. Convergence and amplification of toll-like receptor (TLR) and receptor for advanced glycation end products (RAGE) signaling pathways via high mobility group B1 (HMGB1). *Angiogenesis* 11:91-99.

71. Park, J.S., Svetkauskaite, D., He, Q., Kim, J.Y., Strassheim, D., Ishizaka, A., and Abraham, E. 2004. Involvement of toll-like receptors 2 and 4 in cellular activation by high mobility group box 1 protein. *J Biol Chem* 279:7370-7377.

72. Park, J.S., Gamboni-Robertson, F., He, Q., Svetkauskaite, D., Kim, J.Y., Strassheim, D., Sohn, J.W., Yamada, S., Maruyama, I., Banerjee, A., et al. 2006. High mobility group box 1 protein interacts with multiple Toll-like receptors. *Am J Physiol Cell Physiol* 290:C917-924.

73. Yang, J., Chen, L., Ding, J., Rong, H., Dong, W., and Li, X. High mobility group box-1 induces migration of vascular smooth muscle cells via TLR4-dependent PI3K/Akt pathway activation. *Mol Biol Rep* 39:3361-3367.

74. Degryse, B., Bonaldi, T., Scaffidi, P., Muller, S., Resnati, M., Sanvito, F., Arrigoni, G., and Bianchi, M.E. 2001. The high mobility group (HMG) boxes of the nuclear protein HMG1 induce chemotaxis and cytoskeleton reorganization in rat smooth muscle cells. *J Cell Biol* 152:1197-1206.

75. Vezzoli, M., Castellani, P., Corna, G., Castiglioni, A., Bosurgi, L., Monno, A., Brunelli, S., Manfredi, A.A., Rubartelli, A., and Rovere-Querini, P. High-mobility group box 1 release and redox regulation accompany regeneration and remodeling of skeletal muscle. *Antioxid Redox Signal* 15:2161-2174.

76. Lolmede, K., Campana, L., Vezzoli, M., Bosurgi, L., Tonlorenzi, R., Clementi, E., Bianchi, M.E., Cossu, G., Manfredi, A.A., Brunelli, S., et al. 2009. Inflammatory and alternatively activated human macrophages attract vessel-associated stem cells, relying on separate HMGB1- and MMP-9-dependent pathways. *J Leukoc Biol* 85:779-787.

77. Palumbo, R., Sampaolesi, M., De Marchis, F., Tonlorenzi, R., Colombetti, S., Mondino, A., Cossu, G., and Bianchi, M.E. 2004. Extracellular HMGB1, a signal of tissue damage, induces mesoangioblast migration and proliferation. *J Cell Biol* 164:441-449.

78. Riuzzi, F., Sorci, G., and Donato, R. 2006. The amphoterin (HMGB1)/receptor for advanced glycation end products (RAGE) pair modulates myoblast proliferation, apoptosis, adhesiveness, migration, and invasiveness. Functional

inactivation of RAGE in L6 myoblasts results in tumor formation in vivo. *J Biol Chem* 281:8242-8253.

79. Chavakis, E., Hain, A., Vinci, M., Carmona, G., Bianchi, M.E., Vajkoczy, P., Zeiher, A.M., Chavakis, T., and Dimmeler, S. 2007. High-mobility group box 1 activates integrin-dependent homing of endothelial progenitor cells. *Circ Res* 100:204-212.

80. Rouhiainen, A., Kuja-Panula, J., Wilkman, E., Pakkanen, J., Stenfors, J., Tuominen, R.K., Lepantalo, M., Carpen, O., Parkkinen, J., and Rauvala, H. 2004. Regulation of monocyte migration by amphoterin (HMGB1). *Blood* 104:1174-1182.

81. Campana, L., Bosurgi, L., Bianchi, M.E., Manfredi, A.A., and Rovere-Querini, P. 2009. Requirement of HMGB1 for stromal cell-derived factor-1/CXCL12-dependent migration of macrophages and dendritic cells. *J Leukoc Biol* 86:609-615.

82. Schiraldi, M., Raucci, A., Munoz, L.M., Livoti, E., Celona, B., Venereau, E., Apuzzo, T., De Marchis, F., Pedotti, M., Bachi, A., et al. HMGB1 promotes recruitment of inflammatory cells to damaged tissues by forming a complex with CXCL12 and signaling via CXCR4. *J Exp Med.*

83. Dumitriu, I.E., Bianchi, M.E., Bacci, M., Manfredi, A.A., and Rovere-Querini, P. 2007. The secretion of HMGB1 is required for the migration of maturing dendritic cells. *J Leukoc Biol* 81:84-91.

84. Dai, S., Sodhi, C., Cetin, S., Richardson, W., Branca, M., Neal, M.D., Prindle, T., Ma, C., Shapiro, R.A., Li, B., et al. Extracellular high mobility group box-1 (HMGB1) inhibits enterocyte migration via activation of Toll-like receptor-4 and increased cell-matrix adhesiveness. *J Biol Chem* 285:4995-5002.

85. Andersson, U., and Rauvala, H. Introduction: HMGB1 in inflammation and innate immunity. *J Intern Med* 270:296-300.

86. Yanai, H., Ban, T., and Taniguchi, T. Essential role of high-mobility group box proteins in nucleic acid-mediated innate immune responses. *J Intern Med* 270:301-308.

87. Yanai, H., Ban, T., Wang, Z., Choi, M.K., Kawamura, T., Negishi, H., Nakasato, M., Lu, Y., Hangai, S., Koshiba, R., et al. 2009. HMGB proteins function as universal sentinels for nucleic-acid-mediated innate immune responses. *Nature* 462:99-103.

88. Maroso, M., Balosso, S., Ravizza, T., Liu, J., Aronica, E., Iyer, A.M., Rossetti, C., Molteni, M., Casalgrandi, M., Manfredi, A.A., et al. Toll-like receptor 4 and high-mobility group box-1 are involved in ictogenesis and can be targeted to reduce seizures. *Nat Med* 16:413-419.

89. Yang, H., et al. 2012. Redox modification of cysteine residues regulates the cytokine activity of HMGB1. *Molecular Medicine.*

90. Yang, H., Hreggvidsdottir, H.S., Palmblad, K., Wang, H., Ochani, M., Li, J., Lu, B., Chavan, S., Rosas-Ballina, M., Al-Abed, Y., et al. A critical cysteine is required for HMGB1 binding to Toll-like receptor 4 and activation of macrophage cytokine release. *Proc Natl Acad Sci U S A* 107:11942-11947.

91. Hreggvidsdòttir, H.S.e.a. 2012. HMGB1-partner molecule complexes enhance cytokine production by signalling through the partner molecule receptor. *Molecular Medicine.*

92. Sha, Y., Zmijewski, J., Xu, Z., and Abraham, E. 2008. HMGB1 develops enhanced proinflammatory activity by binding to cytokines. *J Immunol* 180:2531-2537.

93. Bianchi, M.E., and Manfredi, A.A. 2007. High-mobility group box 1 (HMGB1) protein at the crossroads between innate and adaptive immunity. *Immunol Rev* 220:35-46.

94. Manfredi, A.A., Capobianco, A., Bianchi, M.E., and Rovere-Querini, P. 2009. Regulation of dendritic- and T-cell fate by injury-associated endogenous signals. *Crit Rev Immunol* 29:69-86.

95. Dumitriu, I.E., Baruah, P., Valentinis, B., Voll, R.E., Herrmann, M., Nawroth, P.P., Arnold, B., Bianchi, M.E., Manfredi, A.A., and Rovere-Querini, P. 2005. Release of high mobility group box 1 by dendritic cells controls T cell activation via the receptor for advanced glycation end products. *J Immunol* 174:7506-7515.

96. Sundberg, E., Fasth, A.E., Palmblad, K., Harris, H.E., and Andersson, U. 2009. High mobility group box chromosomal protein 1 acts as a proliferation signal for activated T lymphocytes. *Immunobiology* 214:303-309.

97. Manfredi, A.A., Capobianco, A., Esposito, A., De Cobelli, F., Canu, T., Monno, A., Raucci, A., Sanvito, F., Doglioni, C., Nawroth, P.P., et al. 2008. Maturing dendritic cells depend on RAGE for in vivo homing to lymph nodes. *J Immunol* 180:2270-2275.

98. Semino, C., Angelini, G., Poggi, A., and Rubartelli, A. 2005. NK/iDC interaction results in IL-18 secretion by DCs at the synaptic cleft followed by NK cell activation and release of the DC maturation factor HMGB1. *Blood* 106:609-616.

99. Chen, G.Y., Tang, J., Zheng, P., and Liu, Y. 2009. CD24 and Siglec-10 selectively repress tissue damage-induced immune responses. *Science* 323:1722-1725.

100. Zhu, X.M., Yao, Y.M., Liang, H.P., Xu, C.T., Dong, N., Yu, Y., and Sheng, Z.Y. High mobility group box-1 protein regulate immunosuppression of regulatory T cells through toll-like receptor 4. *Cytokine* 54:296-304.

101. Zhang, Q., O'Hearn, S., Kavalukas, S.L., and Barbul, A. Role of High Mobility Group Box 1 (HMGB1) in Wound Healing. *J Surg Res*.

102. Germani, A., Limana, F., and Capogrossi, M.C. 2007. Pivotal advances: high-mobility group box 1 protein--a cytokine with a role in cardiac repair. *J Leukoc Biol* 81:41-45.

103. Abarbanell, A.M., Hartley, J.A., Herrmann, J.L., Weil, B.R., Wang, Y., Manukyan, M.C., Poynter, J.A., and Meldrum, D.R. Exogenous high-mobility group box 1 improves myocardial recovery after acute global ischemia/reperfusion injury. *Surgery* 149:329-335.

104. Limana, F., Germani, A., Zacheo, A., Kajstura, J., Di Carlo, A., Borsellino, G., Leoni, O., Palumbo, R., Battistini, L., Rastaldo, R., et al. 2005. Exogenous high-mobility group box 1 protein induces myocardial regeneration after infarction via enhanced cardiac C-kit+ cell proliferation and differentiation. *Circ Res* 97:e73-83.

105. Rossini, A., Zacheo, A., Mocini, D., Totta, P., Facchiano, A., Castoldi, R., Sordini, P., Pompilio, G., Abeni, D., Capogrossi, M.C., et al. 2008. HMGB1-stimulated human primary cardiac fibroblasts exert a paracrine action on human and murine cardiac stem cells. *J Mol Cell Cardiol* 44:683-693.

106. Biscetti, F., Straface, G., De Cristofaro, R., Lancellotti, S., Rizzo, P., Arena, V., Stigliano, E., Pecorini, G., Egashira, K., De Angelis, G., et al. 2010. High-mobility group box-1 protein promotes angiogenesis after peripheral ischemia in diabetic mice through a VEGF-dependent mechanism. *Diabetes* 59:1496-1505.

107. Mitola, S., Belleri, M., Urbinati, C., Coltrini, D., Sparatore, B., Pedrazzi, M., Melloni, E., and Presta, M. 2006. Cutting edge: extracellular high mobility group box-1 protein is a proangiogenic cytokine. *J Immunol* 176:12-15.

108. Wake, H., Mori, S., Liu, K., Takahashi, H.K., and Nishibori, M. 2009. High mobility group box 1 complexed with heparin induced angiogenesis in a matrigel plug assay. *Acta Med Okayama* 63:249-262.

109. Lin, Q., Yang, X.P., Fang, D., Ren, X., Zhou, H., Fang, J., Liu, X., Zhou, S., Wen, F., Yao, X., et al. High-mobility group box-1 mediates toll-like receptor 4-dependent angiogenesis. *Arterioscler Thromb Vasc Biol* 31:1024-1032.

110. Qiu, Y., Chen, Y., Fu, X., Zhang, L., Tian, J., and Hao, Q. HMGB1 promotes lymphangiogenesis of human lymphatic endothelial cells in vitro. *Med Oncol* 29:358-363.

111. Schlueter, C., Weber, H., Meyer, B., Rogalla, P., Roser, K., Hauke, S., and Bullerdiek, J. 2005. Angiogenetic signaling through hypoxia: HMGB1: an angiogenetic switch molecule. *Am J Pathol* 166:1259-1263.

112. He, M., Kubo, H., Ishizawa, K., Hegab, A.E., Yamamoto, Y., Yamamoto, H., and Yamaya, M. 2007. The role of the receptor for advanced glycation end-products in lung fibrosis. *Am J Physiol Lung Cell Mol Physiol* 293:L1427-1436.

113. Riuzzi, F., Sorci, G., Sagheddu, R., and Donato, R. 2012. HMGB1/RAGE regulates muscle satellite cell homeostasis via p38 MAPK/myogenin-dependent repression of Pax7 transcription. *J Cell Sci.*

114. Grundtman, C., Bruton, J., Yamada, T., Ostberg, T., Pisetsky, D.S., Harris, H.E., Andersson, U., Lundberg, I.E., and Westerblad, H. Effects of HMGB1 on in vitro responses of isolated muscle fibers and functional aspects in skeletal muscles of idiopathic inflammatory myopathies. *FASEB J* 24:570-578.

115. Calogero, S., Grassi, F., Aguzzi, A., Voigtlander, T., Ferrier, P., Ferrari, S., and Bianchi, M.E. 1999. The lack of chromosomal protein Hmg1 does not disrupt cell growth but causes lethal hypoglycaemia in newborn mice. *Nat Genet* 22:276-280.

116. Orkin, S.H., and Zon, L.I. 2008. Hematopoiesis: an evolving paradigm for stem cell biology. *Cell* 132:631-644.

117. Carter, G.T., Abresch, R.T., and Fowler, W.M., Jr. 2002. Adaptations to exercise training and contraction-induced muscle injury in animal models of muscular dystrophy. *Am J Phys Med Rehabil* 81:S151-161.

118. Clarkson, P.M. 1992. Exercise-induced muscle damage--animal and human models. *Med Sci Sports Exerc* 24:510-511.

119. Clarkson, P.M., Nosaka, K., and Braun, B. 1992. Muscle function after exercise-induced muscle damage and rapid adaptation. *Med Sci Sports Exerc* 24:512-520.

120. McNeil, P.L., and Khakee, R. 1992. Disruptions of muscle fiber plasma membranes. Role in exercise-induced damage. *Am J Pathol* 140:1097-1109.

121. Pisani, D.F., Bottema, C.D., Butori, C., Dani, C., and Dechesne, C.A. 2010. Mouse model of skeletal muscle adiposity: a glycerol treatment approach. *Biochem Biophys Res Commun* 396:767-773.

122. Brunelli, S., and Rovere-Querini, P. 2008. The immune system and the repair of skeletal muscle. *Pharmacol Res* 58:117-121.

123. Chan, R.K., Austen, W.G., Jr., Ibrahim, S., Ding, G.Y., Verna, N., Hechtman, H.B., and Moore, F.D., Jr. 2004. Reperfusion injury to skeletal muscle affects primarily type II muscle fibers. *J Surg Res* 122:54-60.

124. Blaisdell, F.W. 2002. The pathophysiology of skeletal muscle ischemia and the reperfusion syndrome: a review. *Cardiovasc Surg* 10:620-630.

125. Gutierrez, J.M., Chaves, F., Gene, J.A., Lomonte, B., Camacho, Z., and Schosinsky, K. 1989. Myonecrosis induced in mice by a basic myotoxin isolated from the venom of the snake Bothrops nummifer (jumping viper) from Costa Rica. *Toxicon* 27:735-745.

126. Lomonte, B., and Gutierrez, J.M. 1989. A new muscle damaging toxin, myotoxin II, from the venom of the snake Bothrops asper (terciopelo). *Toxicon* 27:725-733.

127. Bacci, M., Capobianco, A., Monno, A., Cottone, L., Di Puppo, F., Camisa, B., Mariani, M., Brignole, C., Ponzoni, M., Ferrari, S., et al. 2009. Macrophages are alternatively activated in patients with endometriosis and required for growth and vascularization of lesions in a mouse model of disease. *Am J Pathol* 175:547-556.

128. Bosurgi, L., Corna, G., Vezzoli, M., Touvier, T., Cossu, G., Manfredi, A.A., Brunelli, S., and Rovere-Querini, P. 2012

. Transplanted Mesoangioblasts Require Macrophage IL-10 for Survival in a Mouse Model of Muscle Injury. *J Immunol.*

129. Heemskerk, A.M., Strijkers, G.J., Vilanova, A., Drost, M.R., and Nicolay, K. 2005. Determination of mouse skeletal muscle architecture using three-dimensional diffusion tensor imaging. *Magn Reson Med* 53:1333-1340.

130. Heemskerk, A.M., Sinha, T.K., Wilson, K.J., Ding, Z., and Damon, B.M. 2009. Quantitative assessment of DTI-based muscle fiber tracking and optimal tracking parameters. *Magn Reson Med* 61:467-472.

131. Heemskerk, A.M., Strijkers, G.J., Drost, M.R., van Bochove, G.S., and Nicolay, K. 2007. Skeletal muscle degeneration and regeneration after femoral artery ligation in mice: monitoring with diffusion MR imaging. *Radiology* 243:413-421.

132. Loerakker, S., Oomens, C.W., Manders, E., Schakel, T., Bader, D.L., Baaijens, F.P., Nicolay, K., and Strijkers, G.J. 2011. Ischemia-reperfusion injury in rat skeletal muscle assessed with T2-weighted and dynamic contrast-enhanced MRI. *Magn Reson Med* 66:528-537.

133. Marqueste, T., Giannesini, B., Fur, Y.L., Cozzone, P.J., and Bendahan, D. 2008. Comparative MRI analysis of T2 changes associated with single and repeated bouts of downhill running leading to eccentric-induced muscle damage. *J Appl Physiol* 105:299-307.

134. Mathur, S., Vohra, R.S., Germain, S.A., Forbes, S., Bryant, N.D., Vandenborne, K., and Walter, G.A. 2011. Changes in muscle T2 and tissue damage after downhill running in mdx mice. *Muscle Nerve* 43:878-886.

135. Su, S.H., Su, S.J., Lin, S.R., and Chang, K.L. 2003. Cardiotoxin-III selectively enhances activation-induced apoptosis of human CD8+ T lymphocytes. *Toxicol Appl Pharmacol* 193:97-105.

136. Griffith, T.S., and Ferguson, T.A. 2011. Cell death in the maintenance and abrogation of tolerance: the five Ws of dying cells. *Immunity* 35:456-466.

137. Carlson, B.M., and Faulkner, J.A. 1983. The regeneration of skeletal muscle fibers following injury: a review. *Med Sci Sports Exerc* 15:187-198.

138. Schwenzer, N.F., Steidle, G., Martirosian, P., Schraml, C., Springer, F., Claussen, C.D., and Schick, F. 2009. Diffusion tensor imaging of the human calf muscle: distinct changes in fractional anisotropy and mean diffusion due to passive muscle shortening and stretching. *NMR Biomed* 22:1047-1053.

139. Saupe, N., White, L.M., Sussman, M.S., Kassner, A., Tomlinson, G., and Noseworthy, M.D. 2008. Diffusion tensor magnetic resonance imaging of the human calf: comparison between 1.5 T and 3.0 T-preliminary results. *Invest Radiol* 43:612-618.

140. Palazzolo, I., Stack, C., Kong, L., Musaro, A., Adachi, H., Katsuno, M., Sobue, G., Taylor, J.P., Sumner, C.J., Fischbeck, K.H., et al. 2009. Overexpression of IGF-1 in muscle attenuates disease in a mouse model of spinal and bulbar muscular atrophy. *Neuron* 63:316-328.

141. Philippou, A., Papageorgiou, E., Bogdanis, G., Halapas, A., Sourla, A., Maridaki, M., Pissimissis, N., and Koutsilieris, M. 2009. Expression of IGF-1 isoforms after exercise-induced muscle damage in humans: characterization of the MGF E peptide actions in vitro. *In Vivo* 23:567-575.

142. McKay, B.R., O'Reilly, C.E., Phillips, S.M., Tarnopolsky, M.A., and Parise, G. 2008. Co-expression of IGF-1 family members with myogenic regulatory factors following acute damaging muscle-lengthening contractions in humans. *J Physiol* 586:5549-5560.

143. Chazaud, B., Sonnet, C., Lafuste, P., Bassez, G., Rimaniol, A.C., Poron, F., Authier, F.J., Dreyfus, P.A., and Gherardi, R.K. 2003. Satellite cells attract monocytes and use macrophages as a support to escape apoptosis and enhance muscle growth. *J Cell Biol* 163:1133-1143.

144. Andrikopoulou, E., Zhang, X., Sebastian, R., Marti, G., Liu, L., Milner, S.M., and Harmon, J.W. 2011. Current Insights into the role of HIF-1 in cutaneous wound healing. *Curr Mol Med* 11:218-235.

145. Shen, Y., and Nilsson, S.K. 2012. Bone, microenvironment and hematopoiesis. *Curr Opin Hematol.*

146. Russo, V., Tanzarella, S., Dalerba, P., Rigatti, D., Rovere, P., Villa, A., Bordignon, C., and Traversari, C. 2000. Dendritic cells acquire the MAGE-3 human tumor antigen from apoptotic cells and induce a class I-restricted T cell response. *Proc Natl Acad Sci U S A* 97:2185-2190.

147. Russo, V., Zhou, D., Sartirana, C., Rovere, P., Villa, A., Rossini, S., Traversari, C., and Bordignon, C. 2000. Acquisition of intact allogeneic human leukocyte antigen molecules by human dendritic cells. *Blood* 95:3473-3477.

148. Nemeth, M.J., Kirby, M.R., and Bodine, D.M. 2006. Hmgb3 regulates the balance between hematopoietic stem cell self-renewal and differentiation. *Proc Natl Acad Sci U S A* 103:13783-13788.

149. Eltzschig, H.K., and Carmeliet, P. 2011. Hypoxia and inflammation. *N Engl J Med* 364:656-665.

150. Rubartelli, A., and Sitia, R. 2009. Stress as an intercellular signal: the emergence of stress-associated molecular patterns (SAMP). *Antioxid Redox Signal* 11:2621-2629.

151. Karar, J., and Maity, A. PI3K/AKT/mTOR Pathway in Angiogenesis. *Front Mol Neurosci* 4:51.

152. Diaz-Valdes, N., Basagoiti, M., Dotor, J., Aranda, F., Monreal, I., Riezu-Boj, J.I., Borras-Cuesta, F., Sarobe, P., and Feijoo, E. Induction of monocyte chemoattractant protein-1 and interleukin-10 by TGFbeta1 in melanoma enhances tumor infiltration and immunosuppression. *Cancer Res* 71:812-821.

153. Tang, D., Kang, R., Zeh, H.J., 3rd, and Lotze, M.T. 2010. High-mobility group box 1 and cancer. *Biochim Biophys Acta* 1799:131-140.

154. Sims, G.P., Rowe, D.C., Rietdijk, S.T., Herbst, R., and Coyle, A.J. 2010. HMGB1 and RAGE in inflammation and cancer. *Annu Rev Immunol* 28:367-388.

LIST OF FIGURES

RESULTS – 1

Figure 1.1 - Kinetic of the response of skeletal muscle to a sterile injury.....69

Figure 1.2 – The injection of CTX does not perturb the general composition of peripheral blood..... 70

Figure 1.3 – Local and systemic Hmgb1 expression in injured and regenerating muscle.....72

Figure 2.1 - Establishment of an MRI imaging approach to the study of muscle damage and repair in vivo.....75

Figure 2.2 - T2 map sequence can be used to follow muscle oedema.....77

Figure 2.3 - Fractional anisotropy and diffusion constant can be used to quantitatively assess and prospectically follow variations of the muscle architecture.....79

RESULTS – 2

Figure 1.1 - Effects of Hmgb1 in injured and regenerating muscle damage.....85

Figure 1.2 - Hmgb1 has an effect on muscle weight.....86

Figure 1.3 - Hmgb1 partially controls the size of oedema but not the number of infiltrating cell.....88

Figure 1.4 - Hmgb1 influences the recruitment of macrophages at day7 after acute damage.....90

Figure 1.5 - Hmgb1 influences macrophage and lymphocyte recruitment in damaged muscle at day15.....91

Figure 1.6 - Hmgb1 blockade delays muscle repair.....92

Figure 2.1 - A good chimerism is reached in peripheral blood and bone marrow of transplanted mice.....95

Figure 2.2 - Efficacy of foetal liver as a source of haematopoietic precursors.....96

Figure 2.3 - Cells of donor origin are effectively recruited at sites of muscle injury...97

Figure 3.1 – Hmgb1-/- FLT mice express negligible amount of Hmgb1 in circulating leukocytes but have altered haemochromes.....100

Figure 3.2 – Hmgb1-/- FLT mice have normal leukocyte lineage distribution in PB and BM.....101

Figure 3.3 – F.A. is not different in TA from WT and KO FLT mice.....103

Figure 3.4 – Hmgb1 is important for correct repair at day7.....104

Figure 3.5 – Leukocyte Hmgb1 controls muscle repair at day15.....105

Figure 3.6 – Leukocyte Hmgb1 does not affect the extent of the oedema in damaged muscle.....106

Figure 3.7 – Leukocyte Hmgb1 does not control inflammatory cell recruitment at the site of damage at day7 after CTX injection.....109

Figure 3.8 – Leukocyte Hmgb1 does not control the expression of specific polarization cell surface marker of macrophages.....112

Figure 3.9 – Leukocyte Hmgb1 does not control the expression of cytokines specific for pro (M1) or anti-inflammatory (M2) macrophage phenotypes.....113

Figure 3.10 – Leukocyte Hmgb1 partially controls cytokine mRNA expression on total muscle.....114

Figure 3.11 – Leukocyte Hmgb1 possibly controls the coming back to a quiescent state of satellite cells.....115

Figure 3.12 – BoxA does not impair satellite cells differentiation.....117

Figure 3.13 – Extracellular Hmgb1 does not control satellite cell differentiation.....118

Figure 3.14 – Macrophage Hmgb1 does not influence satellite cell differentiation....119

Figure 3.15 – Macrophage Hmgb1 does not influence satellite cell differentiation....120

Figure 3.16 – Leukocyte Hmgb1 controls vessel remodelling in repairing muscle.....122

Figure 3.17 – Leukocyte Hmgb1 licenses damaged muscle to sense hypoxia in early phase of tissue repair.....123

LIST OF TABLES

Table 1 - Sum up of results obtained with pharmacological blockade of Hmgb1...93

Table 2 - Transplantation does not influence T2rt trend during muscle damage and repair.....98

Table 3 - Transplantation does not influence F.A. trend after tissue injury.....98

ACKNOWLEDGEMENTS

I would like to dedicate this thesis to Chiara

First I thank my director of studies, Patrizia Rovere-Querini for giving me the opportunity to work on this exciting project and my supervisor Prof. Angelo Manfredi for his continuous help and support.

Many thanks to my collaborators at the experimental Imaging Centre, Tamara Canu, Antonio Esposito and to the Head of Radiology Department Prof. Alessandro Del Maschio for the great help they gaxve me in analyzing mice by MRI.

I also would like to thank all my colleagues, especially Elena Rigamonti, Francesco Santarella, Antonella Monno, Michela Vezzoli, Gianfranca Corna for the precious help and useful scientific discussion. Francesco, thank you especially for being a tolerant student with this crazy teacher and a good fellow for the "outside lab" life.

I cannot forget my family that continuously supported me during my PhD course. Special thanks to my parents that have always believed in me, even more than what I have done. Also big thanks to my long-lasting friends Lorenzo, Alice, Elena, Paola, Lucia(s), Francesca, Elisa(s), Dimitrios, Marco, Sara, Bea, Giorgia and Yle, for sharing with me problems, crazy moments but also for the fun we always have when we are together.

An enormous thanks to my flatmate Silvia, that have been sharing with me scientific and personal success and disasters all throughout my PhD project. Thank you especially for sharing with me your friendship that I know is really precious.

Finally a big "Thank you!" to my second family, the great volleyball team GSO Vimodrone, that allowed me to survive the thesis writing period without getting crazy and let me discover how beautiful your love is!